Perception, recording and reproduction of physical invariants during bare fingertip exploration of tactile textures

Séréna Bochereau

Doctoral Thesis
Université Pierre et Marie Curie
Paris VI

Speciality: Mechanics, Acoustics, Electronics and Robotics

Perception, Recording and Reproduction of Physical Invariants during Bare Fingertip Exploration of Tactile Textures.

SÉRÉNA BOCHEREAU

INSTITUT DES SYSTÈMES INTELLIGENTS ET DE ROBOTIQUE (UMR 7222)

Defended on the 23^{rd} of January 2017 before the committee:

Prof. Karon MacLean	University of British Columbia	Reviewer
Prof. Hannes Bleuler	EPFL	Reviewer
Prof. Mike Adams	University of Birmingham	Examiner
Prof. Romain Brette	Institut de la Vision	Jury President
Prof. Sinan Haliyo	UPMC	Examiner
Prof. Vincent Hayward	UPMC	Advisor

This thesis was carried out as part of a EU funded FP7 Marie Curie Initial Training Network called PROTOTOUCH. Its main research goal was to exploit multiscale multiphysics simulation software, supported by neurophysiological measurements, for the virtual prototyping and optimisation of tactile displays. I am grateful for the collaboration opportunities that have contributed to the interdisciplinary nature of my thesis work. It shows in chapters 2 and 5 where work was carried out in bio-tribology with the University of Birmingham and in microneurography with the University of Göteborg.

Ackowledgements

First and foremost I want to thank my advisor Prof. Vincent Hayward for being a fantastic mentor. I would like to thank him for encouraging my research and allowing me to grow as a research scientist. His advice and support have been invaluable during my PhD experience. The passion and enthusiasm Vincent has for research was contagious and extremely motivating.

I would also like to thank all my committee members. My reviewers Prof. Karon MacLean and Prof. Hannes Bleuler provided brilliant comments and suggestions which really improved the manuscript. With Prof. Mike Adams, Prof. Romain Brette and Prof. Sinan Haliyo, they all contributed to make my defence an enjoyable and stimulating moment by providing interesting discussions and perspectives.

The members of the Hayward group at ISIR have been a great source of friendships as well as advice and collaboration. Camille Fradet has been a great fellow PhD student. I would also like to acknowledge Dr. Bernard Javot, Ramakanth Singal, Amir Berrezag and Rafał Pijewski from whom I learned a lot while building my device. Finally, I would especially like to thank Prof. Jess Hartcher-O'Brien and Dr. Steve Sinclair who both gave me tremendous advice and support on all levels throughout my PhD.

I would like to acknowledge my funding agency, the EU FP7 Marie Curie PROTOTOUCH project. I've learned a lot from my PROTOTOUCH peers with whom I've developed friendships and I am grateful for the collaboration and travel opportunities the project fostered.

Lastly, I would like to thank my family for all their love and encouragement as well as most especially the other Vincent for all his support, motivation, and patience throughout this experience. Thank you.

Contents

List of Figures

List of Tables

Summary

This thesis investigates tactile perceptual constancy with the view to better understand and reproduce virtual tactile interactions. It entailed developing a new tactile device capable of measuring interaction forces between a fingertip and a texture, and recreating that sensation by vibrating a glass plate. Several studies were elaborated to search for percepts that maintain constancy over different exploration conditions showing with increasing certainty that the tangential force integral is a promising candidate. Evidence is shown that for brief tactile stimuli such as when a fingertip slips over an asperity, there are strong connections between the tangential force integral in the mechanical domain, the perceived intensity in the cognitive domain and the spike response in the neural domain.

Context. My work fits in the wider aim of virtually creating the sensation of sliding over asperities or textures in a simple but effective manner. Since 2007 several devices have been developed relying on sophisticated technologies such as for example piezoelectric actuators, voice-coil motors, ultrasonic waves or electrostatic vibrations. These methods are powerful however only currently successfully render large periodic spatial features. This is largely due to our lack of knowledge of what cues are behind tactile percepts and what part of the signal is perceptually relevant to characterise different textures. In fact, understanding the mechanical characteristics of tactile interactions is key to identifying what information from a fingertip deformation event is perceived by our somatosensory system to recognise a specific texture. If we are made aware of this information, haptic rendering is guaranteed to vastly improve. Therefore, in this thesis I took a step in this direction by investigated the existence of such cues in the mechanical signal generated during asperity exploration, by drawing on two hypothesis:

Hypothesis 1: The essential relevant information for our somatosensory system is contained in the friction forces in the form of tangential micro-fluctuations perceived by the finger. When a finger interacts with a surface, slip is always accompanied by fluctuations caused by a combination of effects particular to the finger and the surface in contact. These effects, which result from bio-tribological properties, depend on many factors including the surface micro-geometry, the nature of the constituent materials, their structure, the presence of water exuded physiologically and the fingerprint characteristics. There is increasing certainty that the tangential component of these friction fluctuations is the most informative. It has also been demonstrated that this complex physics is processed by the brain to perform motor and perceptual tasks, such as gripping or identifying the surface's constituent material and topology.

Hypothesis 2: Our somatosensory system relies on invariants to make sense of a haptic scene. These processes by which our brain makes sense of a mechanical interaction, mostly unconscious, allow us to effortlessly discriminate plastic from wood and to manipulate extraordinarily diverse objects without realizing the huge variations in the physics of contact due to our exploration manner never being the same. This perceptual independence to different sensing

conditions means that either the nervous system does a complicated computation for each exploration or that the nervous system has a mechanism able to recognize certain physical quantities specific to the object and that remain unchanged regardless of exploration conditions. Our hypothesis is that these processes are effortless because the brain is capable of extracting the invariant characteristics of a surface from the noisy signal. In fact, it was shown that in vision and audition, sensory neurons have adapted to efficiently code the signals that occur most frequently. In touch, there is no formal efficient coding mechanism that has been formally elaborated. It is however known that the tactile perception of texture is relatively insensitive to changes in exploration speed and methods, which may be viewed as an instance of perceptual constancy.
Conjecture: If invariants exist, there is a high chance they are contained in the tangential force. The work herein involved designing a device capable of recording and reproducing the tangential force in order to investigate the existence of invariants in the tangential force.

The Scientific Instrument. The instrument performance was built to match the known capabilities of the somatosensory system: a bandwidth of 5 to 500 Hz in sensing as well as in reproduction because the mechanoreceptors are mostly sensitive to this frequency band. In order to record and replay the interaction in identical conditions, the same sensors and sliding interaction were used for both functionalities and the stimulator was designed to mirror the bulk fingertip mechanics. These mechanical constraints help ensure that all the information required for realism is transposable and included in the raw measurement on which the virtual stimulations is based. The device (Chapter 2) includes a tribometer for measuring perpendicular forces independently from each other in order to estimate the local and instantaneous friction coefficient. The tangential component of the measured friction can then be reproduced by vibrating a glass plate under the controlled action of a critically damped electrodynamic actuator. Under the vibrating glass plate, there is a high-speed camera to measure the deformations of the fingerprint ridges during sliding over the vibration glass. These measurements complement the force data collected by the tribometer allowing us to witness the deformations of a fingertip when stimulated by texture-specific vibrations of non-transparent materials, which we can normally not see neither study.

Empirical and theoretical studies investigating invariance. The starting point (Chapter 3) was a pilot based on a phenomenon observed in other modalities. I investigated the relationship between duration and amplitude in tactile stimuli. The experiment shows that when a stimulus is temporally longer but has a smaller amplitude, it can be felt as intense as a stimulus that is temporally shorter and that has a larger amplitude. Our hypothesis is that the instantaneous mechanical perturbation is different in varying exploration conditions (speed and normal force), meaning that it occurs at different timescales but that the overall deformation is the same. Chapter 4 involves understanding what was the perceptual constancy that allowed us to recognise two wavelet stimuli of different profiles as the same. We looked at the mechanical response of a finger sliding over several braille dots in different conditions, and found that it is the integral of the tangential force which informs on the height of the dots regardless of the exploration profile. Chapter 5 checks whether the invariant was perceptually relevant. An experiment was carried out to see if participants could tell, based on the tangential force integral, which virtual dot they actively explored was higher. During the task, the dot profile was constantly changing in response to speed and the only value that remained the same for a given dot across the trials was the tangential force integral. These studies suggest that the integral of the local tangential forces is a robust invariant that should

be provided to the somatosensory system in asperity height reproduction instead of the set of all the instantaneous values. Chapter 6 extends this observation to textures. Participants were asked to identify which stimulus amongst three (1 reference and 2 comparisons) was different. These stimuli only varied in their exploration speed. Poor performance shows that the overall deformation is more relevant than the speed characteristics for a large range of speeds. These encouraging findings suggest that considerable liberties can be taken in terms of the speed when reproducing virtual textures.

Contributions.

Theoretical

- We showed that amplitude and duration of the tangential force are relevant to encode short tactile signals.
- In fact, an invariant that englobes both amplitude and duration, the tangential force integral, was found in the interaction mechanics of a finger sliding over a braille dot.
- This invariant proved to be perceptually relevant since it was likely used as basis in a discrimination task therefore a strong connection was found between the mechanical (tangential force integral) and the cognitive domain (perceived intensity).

Applied

- To enable these studies, a device was developed to record, reproduce and image finger/texture-elicited vibrations and has also the potential to support many studies thanks to all three functionalities.
- Finally, some conjectures were made with respects to our insensitivity to speed meaning more liberties can be taken in terms of speed control requirements for texture reproduction as compared to what was previously believed.

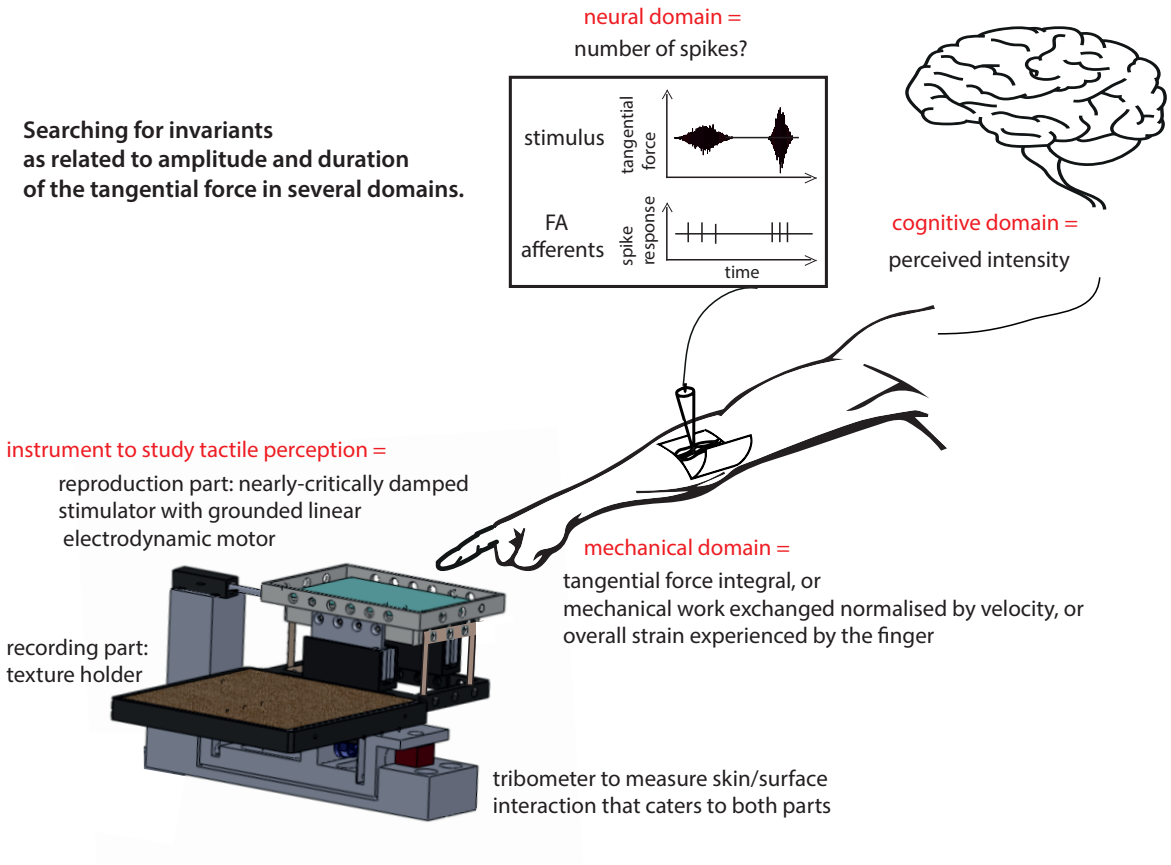

Figure 1 – Thesis Overview: Designing a device capable of recording and reproducing the tangential force in order to investigate the existence of invariance in short events such as asperity exploration in the mechanical (tangential force integral), neural (spike response) and cognitive (perceived intensity) domains.

Chapter 1

State of the Art

Contents

This chapter serves as a literature review to provide context to the work described in the thesis. The background in each domain (mechanical, neural and cognitive) that allowed me to understand our tactile system are detailed and comments are given on how these were used and built on.

1.1 The Mechanics of Touch

1.1.1 Finger Anatomy

Bone. The human finger is mainly a bony structure. Each finger has between two (the thumb) and three phalanges (all other fingers) that are each separated by joints. These allow for flexibility, strength and many manipulation possibilities.

Subcutaneous Tissue. The hypodermis or subcutaneous tissue is a fat layer [42] composed of loose connective tissue and elastin. Its role is to connect the bones and muscles [223] with the dermis as well as to supply the epidermis with blood vessels and nerves.

Glabrous Skin. Most of the human skin is hairy skin. On inner hand, we have glabrous skin instead. It is thicker than hairy skin and has no hair follicles. 1) The dermis comprises the first layers of the glabrous skin. It consists of connective tissue in a semi-liquid phase, allowing to take the impact when stressed or strained but still giving strength and elasticity to the skin through an extracellular matrix composed of collagen and elastic fibers. 2) The thinner epidermis lies on top of the dermis. It forms a protective barrier over the body's surface, keeping water in our body and preventing germs from entering. The epidermis contains no blood vessels, and cells in the deepest layers are nourished by the upper layers of the dermis. There are about 17 000 mechanoreceptive units in the epidermis of the glabrous skin of the human hand [115], much more than in the hairy skin that is less tactually sensitive. 3) The stratum corneum is the outer layer of the epidermis (of which the keratin is the last layer) and has a thickness of around 10 μm [96, 210]. It is composed of dead cell tissue, making it relatively hard and tough.

Fingernail. Composed of compacted, dead keratinized cells, the fingernail is a hard but deformable structure bound to the bone that prevents the skin from being pushed around [68]. The mechanical forces applied to the nail are transmitted to the mechanoreceptors present in the nail bed [169, 189]. Actually, the fingernail is relatively sensitive and can transmit estimates of material roughness and hardness. Using a two point discrimination task, Seah et al. [216] showed that the discrimination threshold between two probes was quite good on the nail (6.7 mm statically and 2.2 mm dynamically) giving similar results to those of the finger pulp ($\approx$ 2.4 mm).

Muscles. Two types of muscles control finger movements. First, intrinsic muscles are located in the hand and allow for the precise movements of the hand. Second, extrinsic muscles are located in the forearm and allow for the hand to flex and extend.

Nerves. Nerves send signals 1) from the brain to the muscles (motor nerves), or 2) from mechanoreceptors to the brain (sensory nerves). Motor nerves allow us to contract our muscle while sensory nerves enable the feel of different sensations. The skin of the fingers is supplied by three different nerves: a) the median nerve on the palmar surface, the tips and nail beds of the thumb, index, middle and half of the ring fingers, b) the ulnar nerve mostly on the back of the hand and on the other half of the ring finger and the little finger and c) the radial nerve for the rest.

Fingerprint Ridges. The epidermis is not a smooth layer, and instead is made of fingerprint ridges and valleys. These ridges form rough ellipsoids around the centre of the finger pad, giving a loop, a whorl or an arch pattern that is unique to each individual. They compress, decompress and stretch during finger pad interactions, by changing their width, height, and length [259] to accommodate the deformation undergone by the finger pad. The stratum corneum is soft on the ridges and hard in the grooves [37], allowing the skin to stretch more and be more compliant at right angles to the ridges than parallel to them [259]. This enables the skin of the finger pad to deform extensively without damage when stressed in shear. In fact, we can easily indent the skin around an asperity, creating 200% deformation at the tip, with full recovery.

The surface of the fingerprint ridges aren't smooth and, instead, are made of small asperities that have varying shapes, sizes and heights [250, 61]. These multiple micro features on the surface in contact could explain the complexity of the signal and the occurrence of the decaying harmonics observed in [271].

Warman and Ennos [261] argued that one of main uses of the fingertip ridges was to improve grip by a number of ways (allowing excess water to escape, maximising the contact area at small forces, allowing large normal forces to be applied without damaging the skin). Others [204, 215] found that, when fingerprint ridges are oriented perpendicular to the scanning direction, they enhanced the vibrations in the range where the mechanorecptors are the most sensitive (scanning velocity/fingerprint period $\approx$ 250 Hz).

1.1.2 Fingertip Mechanical Properties

The frictional interaction of the fingertip with an arbitrary surface often exhibits chaotic characteristics. This complexity is attributed to the multi-scale, nonlinear physics that occur during sliding [271]. Fingertip hydration, applied pressure, contaminants, and exploration velocity are also constantly varying during sliding, influencing the contact dynamics [4]. The fingertip itself is a bi-phasic multilayer composite structure that has different mechanical behaviours at the different time and length scales of its deformation. Here, the three main characteristics of the fingertip mechanical properties are described.

Viscoelastic. In both normal [219, 194, 112] and lateral [193] uniaxial loading, the finger tip mechanical behaviour can be represented by an exponential nonlinear model: the finger pad responds in a linearly viscoelastic manner during loading, but exhibits a nonlinear behavior during unloading, with a hysteresis varying between 32% and 47% and a relaxation time around 10 s [219, 259, 194]. During a normal collision at high velocity, the finger pad is capable of dissipating 80 % of energy [112]. Actually, the skin and tissues that hand-hold a stylus can be modelled for small displacements with mass-, damper- and spring-like elements [107].

Cohen et al. [43] found that, when vibrated at high frequencies, the skin started to decouple above 100, 120 or 150 Hz depending on how high the amplitude was. This decoupling mechanism could be explained by the dual behaviour of the fingertip skin: the fibrils of the skin collagen fibres have a randomly coiled structure when relaxed, giving this soft and elastic behaviour under small stresses. However under higher constraints, the fibres are straightened out and oriented in the direction of the stress resulting in them becoming stiffer [47].

Highly Deformable. The finger pad can experience large deformations under even small loads. A normal deformation of 2 mm was reported for normal loads of 1 N [219], and a

tangential deformation of 3.5 mm for tangential loads of 2 N [180]. Almost all of the pulp displacement (82%) actually occurs before the load reaches 1 N even if it eventually reaches 5.2 N [218]. Shearing loads can lead to gross deformations of 100% without damage [259], collision with one small bump representing a deformation of around 30% [150].

Anisotropy. Jones and Hunter [122] noticed that tangential forces directed proximally experiences greater friction than if the force were directed distally. Wang and Hayward [259] found that these directional effect of the finger pad skin are not related to the finger geometry but to the orientation of the ridges: the skin is locally ten times stiffer along the fingerprints than across them. Actually, the young's modulus is slightly lower in the media-lateral direction (114.9 kPa) than in the proximal-distal direction (137.5 kPa) [270].

Delhaye et al. [51] found that the evolution of the contact area, the orientation, the length and the position of the stuck area all depend on the direction of the motion. When the movement was in the ulnar and radial directions rather than in the proximal or distal directions, almost all of the micro-slips occurred at the periphery of the contact area, progressing to the centre of the contact area much later, resulting in it being systematically off-centered proximally. They later found that depending on the stimulus direction, either the compressive part (ulnar, proximal and radial directions) or the tensile part (distal direction) was dominant [49]. Additionally, the fingertip's distribution of compressive strains was aligned with the stimulus direction. This builds on the observation that stiffness usually showed a dependency on direction of stimulation (the average is between 1.6 and 2 N) while damping and inertia did not [180].

1.1.3 Fingertip Tribology.

Our knowledge of friction has supported the claim that a lot of information is generated through the vibrations elicited when we slide over a texture. This section explains the extent to which the signal is perturbed by speed, moisture, applied pressure, fingertip angle, direction, etc., which results in the mechanical signal for the same finger exploring the same texture to vary significantly. Characterizing this interaction with the most amount of precision is important in order to understand the mechanics and what details are sensed by our mechanoreceptors. To this end, i developed a device which is able to record the fingertip dynamics during sliding over textures and then witness their reproduction with a vibrating glass plate. Devices that measure forces and image fingertip dynamics with static surfaces exist however none can image fingerprint dynamics during the active exploration of a vibrating surface (that which approximates what occurs when we slide over a texture). Being able to understand the behaviour of fingerpad deformation with this much accuracy in terms of forces (10 mN sensitivity, 500 Hz bandwidth) and images (2000 Hz for an area of a few mm^2) can help understand how using different vibrations relating to texture interaction affects the fingerpad dynamics.

1.1.3.1 Friction and Load.

In the condition of Coulombic slip, the friction coefficient is simply the tangential load divided by the normal load : $F = kW$, where F is the tangential of frictional force, k is the friction coefficient or the frictional load index and W the normal load. Cartmill [35] showed that the frictional force F of the fingers of small clawless primates depends on the fractional power of the normal load, termed the load index n, which is constant and equal to one in Coulombic slip. Actually, the basic model $F = kW^n$ [8] is a good representation of the friction evolution for the human finger pad [261, 258] which exhibits a non-linear behaviour after sustained

contact. Indeed, during a single swipe, Coulombic slip occurs at the beginning of the contact (the load index n is about one during the transient when we have short occlusion times) which evolves into non-coulombic slip (n tends to 0.75) during steady state sliding (transition from multiple to single asperity contact) [4].

The coefficients k and n have been shown to obey a first-order kinetic relationship:

$$n = n_\infty + (n_0 - n_\infty) \exp^{-t/\lambda} .$$

$$k = k_\infty + (k_0 - k_\infty) \exp^{-t/\lambda} .$$

with λ the characteristic time, which is of the order of 20 s, and t the time of the event.

There is evidence that, contrary to classic contact mechanics theory [116], two different coefficients of friction contribute to the net friction: the static (before the transient) and the dynamic friction (steady state sliding). Since they influence the dynamics of contact, this multiplies the possible stick-slip evolutions of the contact area.

1.1.3.2 Contact Area.

When two surfaces (the finger and the explored surface) move relative to each other tangentially under load, the adhesion between the surface asperities creates a frictional force. This adhesion mechanism relates the frictional force F to the contact area A by $F = \tau A$ where τ is the interfacial shear strength associated with the rupture of the intermolecular junctions.

Since τ and the normal load W are linearly proportional, the gross contact area A is proportional to the normal load, such as $A = cW$ where c is a material constant [116]. Actually, since 2000, several groups [225, 132] showed that A decreases with normal load following a negative power law, reflecting a relationship more of the form $A = cW^n$.

These relationships between A and F, and A and W show that the real contact area is perhaps the most important influence on finger friction [247]. Delhaye et al. [51] found that the average initial contact is 1.9 ± 1.4 mm^2 and the average slipping contact is 1.2 ± 1.0 mm^2.

The irregularities on the fingerprint surface actually cause the area of intimate contact to be much less than the apparent area [28]. According to Persson [195], a rubber sliding on relatively smooth surfaces (for example a tire on a road surface) only makes apparent contact with about 5% of the smooth surface. Our recent findings [61] demonstrated that it is the micro-asperities on the fingerprint ridges that make up the real area of contact, the value now being much smaller than previously assumed. With increasing load, the number, the size, and the connectivity of the junctions between the micro-asperities in contact grows simultaneously. We will see that the contact area at a given normal load depends on several variables such as the hydration state of the finger, its displacement, and the sliding time [4].

Static Friction. Static friction can be measured during uniaxial compression tests where the finger is immobile. After the force increases past 1 or 2 N [218], the contact area reaches a plateau and the main friction mechanism is adhesion.

Another case of static friction is during the initial phase of a sliding event. The normal forces used to strike a surface range between 0.2 and 1.0 N during discrimination tasks [135, 173, 197]. Compliance of the index finger skin indicated that the skin is mostly compliant in this range of forces (above which it becomes stiff). The static friction occurs at the first instant of contact so the force applied by the finger is, in this condition, very low.

Transient Phase. The partial slip or transient phase can be defined between the onset of finger displacement and the first instant of full slip. During this phase, the finger is stuck to the surface and requires a certain level of applied force before pealing off and begin sliding, giving this phase the particularity of being a mix of adhesion and slip. Its duration, which depends on the direction of movement, the normal force and the speed, can range between 90 and 980 ms. Typically, an annulus of failure grows from the periphery of the contact region to eventually invade the whole contact [7]. It was shown that above a threshold tangential force, the stuck ratio (region of the contact with sticking/ total region of contact) decreases linearly with the tangential force to zero [7, 4, 51]. Terekhov and Hayward [242] found that, under increasing load, not all stuck surfaces continuously diminish down to a vanishing surface area. Specifically, if the static coefficient of friction is greater than the kinetic coefficient of friction, then there exists a minimal stick surface area. The presence of this threshold tangential force was previously explained by the existence of an intrinsic value of interfacial shear strength at zero contact pressure [249].

Gueorguiev et al. [84] found that the difference in the magnitude of the interfacial force variations responsible for the ability to discriminate between glass and PMMA, was most significant during the partial slip phase, showing that it is a perceptually decisive moment of the sliding event.

Dynamic Friction. The first instant of full slip is defined as the moment when the stuck ratio falls to zero [7]. Steady-state slip is defined as the state achieved when a finger is in complete sliding and the contact area stabilizes to a constant value. The friction coefficient also remains constant for a characteristic sliding time of 20 s and is usually about an order of magnitude higher as compared to the onset phase [192]. During this phase, the average surface roughness is in fact proportional to the dry frictional noise that is generated when a medium travels over the surface [188].

Tomlinson et al. [246] found that for fine surfaces, the roughness of the finger dominates over that of the material's surface; there are only small difference between the coefficient of friction for different materials. However, as the surface roughness increases so does the coefficient of friction. Later [245], they found that at low ridge height and width, the friction was dominated by adhesion, above a ridge height of about 40 μm, interlocking friction contributes greatly to the overall friction and finally above a height of 250 μm, hysteresis contributes to up to 20% of the total friction.

Moisture. Skin moisture dramatically affects the contact dynamics during the transient phase [4] since the stratum corneum is very sensitive to water [192]. During the initial sliding phase, capillary adhesion occurs at small normal loads and short time scales [56]. At longer contact times, the moisture secreted by the many sweat pores in the fingerprint ridge start softening the ridges by plasticisation [4, 54, 3]. This water absorption mechanism is the principal mechanism responsible for the increase in friction due to moisture, capillary adhesion being second [247]. Initially, the stratum corneum is in a glassy state so that each junction forms a Coulombic multiple-asperity contact. With the onset of plasticisation due to the trapping of moisture in the junctions, the asperities become softer, more rubbery. This change explains why friction transitions to non-Coulombic in the steady state sliding.

A moist, softer skin provides a larger effective contact area than dry skin [196]. This increase in the contact area (rather than the reduction in the interfacial shear strength) is the main factor responsible for the increase of net friction of slight moist skin [3]. When interacting with a smooth nonporous surface, the sweat accumulates between the ridges rather than within

them leading to bridging between them which increases the friction [192, 4]. However, with exceeding moisture (wet contact), the friction will decrease. Moist skin is more flexible than dry skin [3]. As a result, the bulk dynamics of deformation are slower with dry skin, making it easier for the nervous system to sense them. We can stipulate that humans with dryer skin on average have a higher discrimination ability.

Excess hydration reduces the tendency of the contact to slip, regardless of the variations in the coefficient of friction [7]. In such cases, different parts of the skin can be in a stick or slip state at the same time. Actually, André et al. [7] observed a moisture regulation mechanism where the fingertip moisture level, often at one extreme or the other, actively stabilises towards an optimal moisture level that requires and allows minimal friction (U-shape type curve). They stipulated that this moisture regulation could be purely passive, with the increase in moisture arising from occlusion when the skin is dry and the decrease in moisture resulting from reabsorption when skin is moist.

Speed. Increasing the speed accelerates the evolution of the contact area. Tada et al. [236] hypothesized that the indentation depth and sliding speed affected the propagation rate of the slip region. When the sliding speed exceeds a critical value, detachment waves were seen in the contact zone [11]. Pasumarty et al. [192] showed that the friction coefficient increases with speed within the range of 5 to 20 mm/s on smooth glass. An increase in the sliding speed decreased the shear strength produced since it affected the critical temperature of the stratum corneum polymer composition [30].

1.2 The Neurology of Touch

This section describes the characteristics of the human sensory apparatus.
After a fingertip interaction, certain details are picked up by our skin mechanoreceptors and eventually reach our somatosensory cortex. Looking into afferent response using microneurography gives us a sense of what information is recuperated and how the mechanical information is coded before arriving to the cognitive domain. This is extremely important information when searching for the validity of an invariant or to understand how the information is transmitted to the higher levels, and know if at the peripheral level the constancy is coded. Hence, our colleagues at the University of Göteborg performed recordings of fast adapting mechanoreceptors to measure the firing response to signals that contained invariant parameters.

1.2.1 Mechanoreceptors

Mechanoreceptors are the sensors in our glabrous skin which convert the mechanical stimuli experienced by our finger pad into tactile sensations. They are known for being the most populated on the finger pad but are actually all over the body (and often located where stress is concentrated [157]). Mechanoreceptors have different forms and characteristics [117] but they can be physiologically categorised according to their adaptation and receptive field properties [124].

Receptive field. Type I mechanoreceptors respond at threshold to stimulation from a limited territory ($\approx 2\ mm^2$), are located in superficial skin and have sharp borders, while Type II can cover a much wider territory (up to 10 mm^2), have vague border and are usually located in deep skin.

Rate of Adaptation. When a slowly adapting (SA) receptor is deformed, it responds for the whole duration of the stimulus and is rather insensitive to the transient part. When a rapidly or fast adapting (RA or FA) receptor is deformed, it fires action potentials for a duration and a density directly related to the rate of change of the stimulus, only firing during the transitions.

Some groups believe that the mechanoreceptive afferent systems each serve a distinctly different perceptual function [117] and that these channels partially overlap in their absolute sensitivities, making it likely that supra-threshold stimuli may activate two or more channels at the same time [124]. While this is under debate, most research groups agree that most tactile perceptual qualities are determined by combined inputs from the different channels.

1.2.1.1 SA Afferents

The slowly adapting afferents are very sensitive to spatial discontinuities such as edges and their responses are suppressed by surrounding stimuli [198]. Even though they are specialized in signals from static contact, their signal also contains information about tactile motion [62]

Merkel cell neurites or SA type I The Merkel's disks consist of large, pale cells with lobulated nuclei forming synapse-like contacts with enlarged terminal endings [85]. These form long chains that run down the ridge [190], and have a distinctive tree-like structure which terminates in the Merkel cells at the dermal-epidermal interface. The SA type I mechanoreceptors have a receptive field diameter of 3-4 mm [114] and an approximate density of 70 sensors per cm^2 [115]. Their vibration sensitivity was found to be between 2 and 32 Hz [114].

Neurophysiological studies suggest that the SA type I mechanoreceptors are most important in small-scale perception [139]. Spatial resolution tests performed by static stimulation of the skin showed that the 75% thresholds is 0.87 mm for gap detection and 1.0 mm for grating detection [120]. Indeed, they are at least four times more sensitive to stimulus height than RA afferents over the range from 280 to 620 μm. 20-50% of the SA type I in a study by Blake and colleagues [23] responded more vigorously to corners than to edges.

Rufini's Endings or SA type II The vibration range of Ruffini's ending is between 10 Hz and 300 Hz [114]. They respond to vertical displacement of the skin over an area of 20-50 mm^2 and to directional stretching of the skin over an area up to 250 cm^2, however their region of maximum sensitivity is smaller than 2 mm^2.

They provides information for the perception of hand conformation and for the perception of forces acting on the hand [121]. They are sensitive to skin stretch [189], slip [231] and vertical displacement [38]. Additionally, SA type II mechanoreceptors near the nail convey vectorial information about the forces acting on the fingertip arising in everyday manipulation [22]. Recently, it has been suggested that their role in skin mediated touch is minor, if not inexistant, since glabrous skin seems to contain very few of them [189]. Actually, the Rufini's endings are very hard to identify [38, 86].

1.2.1.2 RA or FA Afferents

The rapidly adapting afferents are responsible for the detection of slip, tactile motion [117], local lateral deformation as well as for surface form and texture when surface variations are too small to effectively activate the SA type I afferents [118]. Their firing correlates with structural patterns [263] and an increased roughness correlates with increased firing [44].

The RA afferents detect surfaces micro-features such as very small surface depressions (squares 800 μm wide) [23] and barely detectable micrometer-sized protrusions or very small single raised dot (4 μm high, 550 μm of diameter) on smooth surfaces [231].

Meisner's Corpuscles or RA type I Many of the Meisner's Corpuscles live inside the surperficial regions of the dermis but are still mechanically connected to the epidermis. The RA type I were first seen to be sensitive in the range of 2-40 Hz [175] but since Johansson et al. [114] found their sensibility to be between 8 and 64 Hz.

The RA type I system provides information about minute skin motion and, thereby, plays a central role in grip control [121]. It is also sensitive to skin temperature, where changes of sensitivity in function of temperature between 15° and 40° were clearly detected [255].

Pacinian's Corpuscles or RA type II The largest receptors are the Pacinian's corpuscles, large enough to be seen with a naked eye in a preparation. There are about 300 in the whole hand [232]. They are barely present in the superficial subcutaneous regions [248] and, instead, live in the deeper underlying tissue, often surrounding joints and bone [33].

Their vibration sensitivity starts at 64 Hz [114] and according to various studies goes up to 300 Hz [16], 400Hz [175] and even 1000 Hz [137, 175]. They are specifically aimed at detecting vibrations, with a maximum sensitivity around 250 Hz after which the sensitivity decreases continually.

The RA type II system can detect and perceive distant events by vibrations transmitted through objects [121], probes, and tools [118] held in the hand. They are known to be primarily responsible for detecting the roughness of a surface. It has been shown that their adaptation reduces the discrimination of perceived roughness [77], especially when sliding over surfaces with spatial periods below 100 μm [100]. The Pacinians can detect vibrations with peaks as small as 0.1 mm [251].

1.2.2 Neural Correlates

The mechanoreceptor response travels through the peripheral nerve fibres into the spinal cord, the thalamus and finally to the primary somatosensory cortex. Neural codes are still mysterious. Most receptors exhibit a behaviour in which the rate of discharge is related to the intensity of the stimulation. However, evaluation of the total number of spikes instead of its rate is sometimes applicable.

Measurements at the Periphery. Neurographic recordings (electrophysiology), where the action potential (the signals transmitted by the neurons) of nervous cells are measured by inserting electrodes in peripheral nerves, are possible in humans in certain peripheral nerves that are accessible without surgery (usually the median nerve). This allows the study of the peripheral nervous system response to different stimuli. The validity of this practice was confirmed when it was noticed that the firing patterns are highly repeatable and that population activity can be estimated from serial recordings of single afferents.

Measurements in the Central Nervous System. The most common methods to study neural correlates in the human brain are electroencelphalography or EEG (low precision but fast), functional magnetic resonance imaging or FMRI (better resolution but slow), position emission tomography or PET (low resolution, slow, but specific) and magnetoencephaloraphy or MEG (very fast but low resolution). These techniques are non-invasive.

1.3 The Cognition of Touch

The knowledge of human thresholds has clinical applications since significant deviations from the norm can be used as a cue for the diagnosis of a patient [32, 153]. In addition, these thresholds roughly indicate the performance specification of a device designed to stimulate the haptic system. Also, good ergonomics rely on understanding adequate dimensions and other physical characteristics of objects and machines that people interact with. Finally, the knowledge of thresholds is also necessary when planning any scientific experiment intended to study the perceptual system since adequate stimuli must be chosen.

There are several methods of evaluating the response to a physical stimulus. In the present thesis, these limitations and thresholds were investigated further.

1.3.1 Perceptual Limitations and Thresholds

Looking at past work on human sensitivity to these different signal quantities (high acuity to amplitude and duration, low acuity to speed and frequency) reinforced the choice of beginning our investigations by looking into amplitude and duration as important cues for tactile perception. It also supported our observation that the details of the deformation at a given time (which can be seen as the frequency of the deformation) are less important than the overall experience. That, with our relative insensitivity to detecting exploration speed, led to investigating design liberties in terms of speed.

1.3.1.1 Perception of Amplitude

Nefs et al. [182] found that amplitude differences as small as 2 μm can be detected for sinusoidal gratings of spatial periods between 0.25 and 1cm during active sliding. LaMotte and Mountcastle [137] found that in the range 17-30 dB above detection threshold, two signals need to vary by 10% in amplitude to be felt different. Additionally, the minimum level of amplitude required for differences in frequency to be experienced is 8 dB above detection threshold. Indeed, the relationship between vibration frequency and perceived intensity of the stimuli was investigated by Verrillo [256] who showed that it obeys a power law function with an exponent of 0.89 for frequencies under 350 Hz.

Verrillo [254] also noticed that the amplitude detection threshold decreased as the length of the stimuli increases. In the case of multi-pulse stimuli, he showed that the skin actually feels an amplitude equivalent to the sum of the individual energies resulting from each pulse [253]. Later, Gescheider et al. [76] found that the amplitude detection threshold increases as the number of pulses increases and as the interpulse interval decreases. Contactor size affects perception amplitude [251]. Brisben et al. [29] showed that while the contact force (between 0.05 and 1N) has no effect on vibration amplitude perception, the amplitude threshold decreased by 60% on average when subjects held a vibrating cylinder of 32 mm diameter rather than a 1 mm diameter probe for frequencies around 300 Hz. Interestingly, they also found that the threshold with vibration parallel to the skin surface was, on average, 30% lower than thresholds with vibration perpendicular to the skin at 300 Hz. The same was observed by [107] when a finger was holding a vibrating stylus.

1.3.1.2 Perception of Size

The human tactile ability to detect the presence of small asperities on surfaces is extremely high. In optimal conditions, the finger can easily detect asperities of a few μm high [154, 140]. The height detection threshold increased with decreasing dot diameter: 1 μm for a diameter

of about 600 μm, 3 μm for a diameter of about 200μm and 6 μm for diameters of about 40 μm [113]. The mean detection threshold was found to be overall lowest for straight edges than for raised circular dots.

Since textures may be seen like assemblies of asperities, surfaces which are randomly (sandpaper) or periodically (gratings) made of asperities are used to evaluate discrimination thresholds. For random surfaces, the Weber fraction (perceived change compared to actual stimuli changes) varies from 28% for large grains to 80% for fine grains [167]. For periodic textures, grating estimation is excellent [173]. When participants were asked to discriminate between Gaussian profile whose width varied between 150 μm and 240 μm, the thresholds ran from 1 μm for the narrowest Gaussian profiles to 8 mm for the widest profile. The detection threshold depended on the spatial width of the Gaussian profile with a power function exponent of about 1.3 [154]. Johnson and Phillips [120] carried out a task in which subjects could not discriminate grating orientation until the gaps were larger than 0.5 mm and higher than 0.8 mm. Recently, Skedung et al. [226] found a limit of detection of 13 nm of amplitude for sinusoidal gratings of 760 nm of wavelength.

1.3.1.3 Perception of Distance

There are two different mechanisms for distance perception. The first is when the distance between the two features is smaller than the space between two fingers. In this case, the haptic system does not seem to obey Weber-Fechner's law and can estimate the width of a object up to 1.5 mm in width using a pinch movement [59]. This value is slightly below 2.5 mm, the standardised distance between two braille dots.

However, when the distances involved are larger than the finger span or when a grasp in not possible, another strategy for estimating distances is used. In this case, we speak of 'distance travelled' and tactile detection is combined with proprioception, exploration speed and the shape of the path taken to make a distance judgement [146, 102]. Whitsel et al. [266] found that when brushing stimuli was applied at different speeds (20 to 250 cm/s) but on the same length of the forearm, the faster stimuli resulted in the impression of smaller distance travelled. Actually, spatial acuity depends on many factors including the temporal frequency and adaptation of the stimulation [20].

1.3.1.4 Perception of Duration

Human tactile discrimination is more sensitive to duration than to frequency [73, 81, 158]. Essick et al. [66] found that a simple power function, with an exponent of 0.6, describes the psychophysical relation between perceived and actual duration. When participants were asked to reproduce the duration of visuo-tactile stimuli they experienced, the apparent duration of the stimulus strongly increased with stimulus speed for values between 3 and 150 mm/s and for stimuli under 1 s [244].

Pleasant and painful somatosensory stimulation have opposing effects on time perception. Pleasant touch results in shorter estimates of duration than reality while unpleasant or painful touch results in an overestimation of the length of the perceived duration [183].

1.3.1.5 Perception of Frequency

In the frequency range between 25 and 640 Hz, the absolute threshold as a function of frequency has a U shaped curve that reaches a maximum sensitivity around 250 Hz [252]. Hu-

mans are able to discriminate the frequency of vibrations with a differential threshold that varies from 4 to 10% depending on the conditions [176], and to resolve temporal separations of 10 ms [191]. It was found that the low-frequency (10-30Hz) complex vibrotactile waveforms were discriminable from one another while discrimination of the high-frequency (100Hz and more) vibrations was poor [17].

The sensitivity was reported to decrease when the temperature of the skin decreases (10 dB loss when temperature drops from 30° to 15°) [255].

1.3.1.6 Perception of Speed and Slip

The effects of speed of relative motion on perceived roughness is multiple and complex. Dépeault et al. [52] found that the speed magnitude perception increased linearly with the speed of the moving platform (33 to 110 mm/s), but that the nature of the surface had an effect on the perceived speed. The roughest surfaces (8 mm dot spacing) were estimated to move 15% slower than the smoother, textured surfaces (2-3 mm dot spacing), for both periodic and quasi-randomly dot distributions. While all subjects were able to scale the speed of the textured surfaces, some were unable to do so for the smooth surface. The same is true for slip. When small features on smooth surfaces are detected by humans, slip can even be detected before fully developed slip is achieved [264], but when the texture is too smooth, slip is not detected [231]. Essick et al. [66] disproved the hypothesis that the subjects compute estimates of mean velocity from the ratio of perceived distance to perceived duration. Lederman [147] found that the smaller the range of speeds used, the larger the influence of speed on perceived roughness.

Roughness perception is lighlty affected by the variations in the exploration speeds [136]. However, increasing speeds tended to make surfaces feel 'smoother' [141, 142]. This effect tends to reverse itself as the inter-element spacing increased. Beyond this point, surfaces often feel rougher with increasing speed. Interestingly, the passive condition produced larger effects of speed on perceived roughness than active touch did [141, 142, 147].

Multiple regression analyses indicate that tactile motion explained 70 to 82% of the variance in the magnitude estimates of speed in Depeault et al's experiments [52], as compared with only 14 to 19% attributed to dot spacing. Human ability to detect the speed of relative motion in passive exploration was reported to be much poorer than in active exploration. This phenomenon is called tactile suppression [257].

Heaviness perception is correlated with slip perception and influences grip force scaling [70]. If a hand-held object is very slippery, the mechanoreceptors detect a low friction slip event and instigate the increase of grip force [277].

After digital anaesthesia, subjects apply significantly greater grip force to prevent slip since they can not detect slip properly and the coordination between grip and load forces is disrupted [171].

1.3.1.7 Perceptual Constancy

The nervous system tends to 'conserve' certain quantities like nature conserves energy. Perceptual cues are linked to invariants that have mathematical, physical, and biological origins [89]. There are different types of invariants, and they are often separated into three main categories. 1) Static invariants are related to the size and shape of the contact surface, 2) Kinematic invariants are related to rolling, moving and sliding and 3) Generic invariant are based on the laws of physics and relate to the how exploration parameters stay constant during a particular movement.

One question of great interest is whether the nervous system senses distance, elasticity, and viscosity independently, or does it sense them through other related quantities independently estimated. In touch, several studies concluded that human tactile roughness scaling is relatively independent of scanning speed [142, 136, 282], indicating that information about surface roughness is potentially extracted from these complex signals [45].

This perceptual constancy could potentially be elucidated based on the results of neurophysiological correlates. With such a technique, an invariant central representation of surface roughness could be extracted from the ambiguous peripheral signals that vary with roughness and the stimulating conditions (e.g. speed) by potentially using simple subtraction process [165]. However, such a mechanism is still unclear today.

General invariants have not yet been found in touch even though there is increasing evidence for their existence. My approach was to search for invariant quantities in the tangential component of the mechanical signal and look for their representation in the cognitive and neural domains.

1.3.2 Consequences for Object and Texture Perception

1.3.2.1 Illusions

The scientific study of illusions can help understand how to optimise the presentation of stimuli and the development of tactile devices. These devices can in turn to provide insight into how people process tactile, haptic and multisensory cues [143].

Priors are necessary for perception since our assumption is for them to hold. According to Hayward [88], an illusion is perceived when the discrepancy between our prior experience and our percept is surprising and even amusing when we become aware of it. Another reason for the existence of illusion is the existence of invariants. For example, different deformation conditions can be perceptually equivalent if their strain fields are similar and indistinguishable by the sensory system [129], resulting in one percept being confused with another.

The funnelling illusion [15] delivers short and simultaneous vibratory signals (around 5 ms) at two locations on the forearm however only one pulse half way between the two contact locations is felt. A variant of the funnelling illusion is the cutaneous rabbit where a progression of many pulses on the forearm are felt when in reality only a few pulses were displayed on that path [24].

Kahrimanovic et al. [126] found that when two shapes of the same physical volume are explored, a tetrahedron is perceived to be bigger in volume than a cube and a cube is perceived to be bigger than a sphere. Sherrick et al. [221] noted that cold objects feel heavier. Additionally, when lifting two boxes of equal weight but of different sizes, most people are convinced that the smaller box is heavier than the bigger one [57, 177]. This is because the brain anticipates and assumes that materials who look similar have the same density [39]. Reid described the vertical-horizontal illusion occurring where estimating the length of identical objects at different orientation results in vertically-placed objects feeling larger than horizontally-placed ones [206].

Recently much attention has been given to illusions during bare finger surface exploration. When holding a comb under their index and moving a pen across it, most people report that they experience the sensation of a raised object moving under the finger [88]. The basis of this illusion is related to the observation that normal loading and tangential loading can create similar strain distribution, meaning that the brain extracts the lateral stretching of the skin with the sensation of feeling a raised object [179]. Nakatani et al. [178] described a related phenomenon produced when scanning surfaces divided into strips made of different materials

or textures. If a smooth strip with orthogonal ridges is placed on either side of a flat line, a fishbone texture is experienced. Another example is a simple device made of a slider traversing over attractive (illusory bump) or repulsive (illusory bump) magnet combinations [88].

1.3.2.2 Texture Dimensions

When evaluating textures attributes for seven surfaces, Ekman et al. [65] found that roughness was approximately a power function of the coefficient of friction and smoothness was approximately the inverse of roughness. Additionally, preference and smoothness were directly proportional to each other.

Hollins et al. [101] used a different methodology; they obtained similarity data between 17 stimuli by asking participants to group them in 3-7 arbitrary categories to avoid the subjectiveness in the choice of adjectives. From multidimensional scaling (MDS) analysis, two robust and orthogonal dimensions were identified, smooth/rough and hard/soft, as well as a third dimension that did not correspond closely with any of the rating scales used, but that could be associated to springiness. Later [98], they asked five subjects to directly estimate the dissimilarity of all pairs of these 17 stimuli. By fitting the ratings on five adjective scales in the MDS space, they identified the first two dimensions as rough/smooth and soft/hard as previously, however the third less dominant dimension was labelled as sticky/slippery. Another study involved MDS and correspondence analysis of 24 different car seat materials resulting in the perceptual dimensions to be soft/harsh, thin/thick, relief and hardness [199].

Bergmann Tiest and Kappers [243] argued that in experiments with a number of stimuli in the order of 20, the stimuli cannot reliably 'fill up' a space of more than 3 dimensions. Therefore, they conducted a free sorting task of 124 different material samples analysed using multidimensional scaling. They estimated the number of dimensions for haptic perception of materials to be 4. Rough/smooth and hard/soft lines were plotted in both 2D space giving varying relationships with the dimensions: in one case they were almost orthogonal and in the other they were almost smashed together. They found that the relation between objective and perceived compressibility and roughness are both described by an exponential function.

Since then, Okamoto et al. [186] reviewed the many studies on texture dimensions that often disagreed and aimed to find a commonality. They concluded that the four main dimensions are rough/smooth, warm/hot, hard/soft and lastly friction which regroups both moist/dry and sticky/slippery.

1.3.2.3 Perception of Roughness

As we just saw, roughness is the most prominent texture attribute. Stevens and Harris [235] found that the roughness judgments of 12 abrasive emory cloths were related to their grit number by a power law with an exponent of 1.5. Indeed, the sensation of roughness is strongly influenced by friction and tangential force amplitude, whereas the spatial period of simulated texture alone makes a negligible contribution [227]. When evaluating grit values of abrasive papers with average fine particle sizes between 1 and 40 μm, the discrimination increased with particle size since it was based on the amplitude information presented in surface unevenness [167]. Magnitude estimates of perceived roughness in these cases increased almost linearly as the longitudinal spatial period increased up to 8.5 mm [165]. Additionally, among the considerable number of perceptual studies concerned with surfaces made of isolated asperities, Lamb found that subjects could correctly distinguish 75% of surfaces in which the period of the dots differed by only 2 % [135].

Lederman et al. [149] showed that for engraved linear metal gratings with rectangular waveforms, the groove width between the ridges had the strongest influence on perceived roughness. While the ridge height decreased roughness perception, neither the groove-to-ridge ratio nor the spatial period of the gratings affected it. The depth to which the finger penetrates the groove, the cross-sectional area of the finger within the groove, and the cross-sectional area of the deviation of the skin from its resting position, all predicted the roughness well as a function of finger force and groove width [241] since roughness is a little higher for higher forces and higher speeds. When the spatial frequencies are low, roughness perception was found to depend on geometrical characteristics of the texture [97, 228].

Mechanical oscillations are the main perceptual information for asperities at micrometer scales [271, 258] and even higher [161]. In the case of periodic textures, the vibration signal contains a fundamental frequency component corresponding to the finger velocity divided by the spatial period of the stimulus. The fundamental frequency is driven by the periodicity of the gratings and harmonics follow a non-integer power-law decay that suggests strong nonlinearities in the fingertip interaction [271]. This regularity was found for a wide range of textural length scales and scanning velocities [50]. However, often subjects' judgments is unaffected by the spatial period of stimulus gratings, even if spatial period partly determines the fundamental frequency of vibrations created during skin-surface contact.

1.3.2.4 Duplex Theory of Tactile Texture Perception

Fine surfaces that are easily discriminated when moved across the skin are indistinguishable in the absence of movement. Coarse surfaces, however, are equally discriminable in both the moving and stationary conditions. For textures composed of particles smaller than 100 μm, eliminating movement reduces the range in which subjective roughness magnitude are reported. In contrast, the logarithmic range over which magnitude estimates of coarse textures are distributed slightly increases [103, 127].

These observation suggest that two mechanisms contribute to texture perception. This phenomenon is called the duplex theory of tactile texture perception and is defined as follows. For fine surfaces (below 100 μm), vibration is the main cue to texture, and it indicates increasing roughness with increasing particle size. Above 100 μm, spatial mechanisms are progressively used, gradually becoming the dominant contributor to texture perception [103].

Several groups have found explanations for this duplex theory in the response of the mechanoreceptors. Johnson and Hsiao [118] speculated that the smallest distance allowed for two dots to be perceived distinctly, an inter-element spacings of about 2 mm, is in line with the centre-to-centre spacing of SA type I units on the fingertip. On the other end, LaMotte and Srinivasan [138] and later Bensmaïa and Hollins [19] suggested that the RA type II units encode very fine surfaces. Actually, Lederman et al. [148] found that adaptation of vibrotactile channels reduced the perceived roughness of fine texture but did not for coarse gratings. Similarly, Johnson and Lamb [119] found that vibrating coarse gratings on the fingertip did not show any substantial effect on perceived roughness. Taylor and Lederman [241] showed that friction makes little contribution to the roughness perception of coarse surfaces while it does for fine surfaces. Adding supplementary vibrations can modify the perception of a fine texture, showing that vibrotaction is important for fine texture discrimination [99]. Additionally, when exploring smooth textures, subjects maintain a relatively constant normal force and instead vary the tangential force suggesting that receptors sensitive to these tangential forces are important in the perception of smooth surface friction [229]. These observations suggest that two different types of mechanoreceptors are used for each texture scale, SA type I are sensitive to coarse texture and RA type II are sensitive to friction and vibrations of fine textures.

Instead of looking for invariants in texture perception, I began by simplifying the problem by looking at invariants in asperity perception, which can be viewed as a coarse texture with defined spatial features. The invariant I found for asperities was hard to extrapolate to fine textures because fine textured surfaces have no detectable individual features with a clear "beginning" and "end". For this reason, when I looked at expanding my results from coarse asperities to finer textures in chapter 6, I chose a grainy texture that had a roughness linked to the periodicity of distinctive features: a metal mesh of medium coarseness. If my conjecture had a chance of being applicable to textures, a good place to start was periodic surfaces at the limit between the definition of fine and coarse textures.

1.4 Design Strategies for Haptic Devices

Display technologies should aim at recreating the perceptual system of the user. Therefore the knowledge of perceptual cues can help design devices which can economically create a desired percept [88]. However, designing tactile devices that can provide these cues, the mechanical signals described in the previous sections, is usually a compelling engineering challenge.

There are two main types of haptic devices [155]. The first is force feedback devices which act on proprioception by providing forces that react to our movements in space. The second is tactile displays which usually act on the highly sensitive fingertip.

Force feedback devices operate in the low range of frequencies (under 10Hz) and do not produce textural effects that resemble what is required to reproduce texture. Their main uses are in surgical simulations, games, robots and teleoperation. While they are not the subject of the current work, we can learn from looking at their well-documented design guidelines. Later, I will focus on the actuators of tactile displays which use lateral entrainment to stimulate the fingertip during slip.

My primary aim was not to produce a haptic device to stimulate textures like the ones described in section 1.4.5. Instead, it was to design a scientific instrument capable of conducting studies that could improve the rendering of virtual stimulation for all these types of devices by further understanding the cues used by our somatosensory system. This section is useful in understanding other aspects of haptic device design. Since the instrument I developed is a haptic device participants would interact with, it still had to fill the requirements laid out for haptic devices as well as have dynamic properties in the range sensitive to fingerpad mechanics and sensing.

1.4.1 Behavioural Implications

In these sections, I explain the choices for the instrument, those allowing the procedure best adapted to surface exploration: bare fingertip active lateral exploration by sliding over a surface.

1.4.1.1 Active vs. Passive

Many years ago, Katz [127] observed that movement between the skin and its surrounding is as important to touch as light is to vision. The information available from static interaction of fingers and hands with objects is perceptually weak [79]. Instead, active exploration of surfaces gives cues about the material and the topography of the object [133, 145, 101, 97]. Meenes and Zigley [164] found that participants could only report unevenness of pressure between 12 different types of papers during static passive touch exploration, while with dynamic passive touch, roughness and smoothness could also be assessed.

Another study by Morley and colleagues [173] showed that tactile roughness discrimination thresholds were approximately halved with movement as compared to without; the difference between the roughness of textures discriminated at 75% correct levels increased from 5% to 10%. Similarly, when participants were asked to match cookie cutters that they could only explore tactually with their graphical representations, the results were much better in the active condition than in the passive one [93].

1.4.1.2 Exploratory Procedures

The exploratory movements used varies with the intent of the explorer [144]: lateral slip for texture (rubbing back and forth across a small homogeneous area), indentation for material stiffness (pressure applied by torque or normal force on stable object), static contact for thermal properties (passive rest without holding), unilateral support for weight (lifted and gently maintained in hand), two-handed grasp for size (contact with as much of the object as possible) and contour following for shape (smooth single movement, turning when an edge is reached). The reason for the choice of these specific procedures for different tasks in free exploration is that they are optimal to acquire the information related to the different object properties.

Davidson et al. [48] found that movements could be reliably classified into categories such as global search (simultaneous exploration of several object attributes), detailed search, palm search, tracing, gripping, pinching, and top sweeping.

1.4.1.3 Bare Finger vs. Rigid Probe

While we usually interact with objects manually, we also use intermediary links such as gloves and tools. Klatzky and Lederman [130] found that glove and seath & glove exploration conditions produced above-chance roughness discrimination, resulting in much less accuracy than with the bare finger. The smaller probe (2 mm vs. 4 mm contact diameter) provided better discrimination performance. Actually, when textures are felt through a tool, discrimination and detection become more much complicated because many factors (often related to the finger/tool and tool/texture interaction mechanics) interfere with the final percept [131]. Indeed, the doubling effect of increasing speed on the perceived roughness is twice as strong when using a probe (30% on average) as compared to the bare finger (10% on average) [147]. The rigid link scales up the roughness discrimination of fine textures [130].

Conversely, Yoshioka et al. [281] found that roughness ratings were similar between indirect and direct touch, and instead, that hardness and stickiness ratings tended to differ. They hypothesised that compliance and friction, which are used to discriminate hardness and stickiness information, are processed by separate groups of neurons for direct and indirect touch.

1.4.2 Design Principles and Guidelines

To stimulate the human tactile sense, devices must be technically able to program mechanical phenomena of perceptual relevance and functional importance. The main difference between tactile and force feedback device requirement is the proprioception and motor control that should be taken into account in the case of force feedback devices [213].

The quality of the haptic rendering is often judged by the discrepancy between the technical specifications of the tactile display and the user's perceptual system [213]. The specifications to look out for are dynamic range, resolution, and adequacy of the signals used. By

studying our tactile system, we can get closer to the most pertinent methods to stimulate appropriately our tactile sense to obtain the desired effect. As layed out by Gault et al. [74], our understanding of the sense of touch is limited however we should aim for several requirements. First, a latency of the order of 10 ms (minimal time in which humans can detect two consecutive tactile stimuli) is required. Okamoto et al. [185] found that in force feedback devices, a time delay higher than 40 ms is noticed. Second, a wide frequency bandwidth is necessary since humans can sense frequencies between 1 Hz and 1000 Hz, and short events (taps or pulses) are felt differently than high-frequency texture vibrations.

Proper ergonomics to allow for user comfort (no mechanical noises) and adequate magnitudes [213] are crucial to a realistic interaction. MacLean and Hayward [156] explained that if the dynamic range and refresh rate scatter, 'jitter' or 'activeness' can be experienced and if the rendering is too weak, too compliant or too slow, the forces feel 'spongy'. They also stated that some interactions feel wrong because the virtual model is unrealistic (usually oversimplified) or the rendering technique and handle geometry are inadequate. To avoid these issues, a thorough planning, experience and re-iterations of each specific functionality is advised.

Furthermore, a good haptic interface has a 'read and write' ability, meaning it can measure the user's action and can react to it [91], either by sending a stimulus in line with, say, the force applied or by completing the task requested by the user. This ensures that the generated movements obey strict correlations with the motor effort exerted by the user on the object. Both of the 'read' and 'write' tasks require a simultaneous exchange of information between the user and the device. Hence sensors and fast communication is a necessity. Since users are constantly interacting with the device to experience it, the device's physical interface must allow for large variability in terms of the space, speeds, effort, acceleration etc. that it can measure and displayed. Having an adequate range, resolution, and bandwidth of position sensing and force rendering is crucial. Actually, Salisbury et al. [213] insisted that most of these properties (inertia, friction, stiffness, and resonate frequency) be symmetric between the device and the user. This allows the device to be at the right scale for the user.

It is in general very difficult to produce perfectly 'realistic' haptic interaction due to the current technical limitations and the complexity of the different texture dimensions that make up at texture (roughness, stickiness, temperature, softness etc.). These all probably require their own technology to create a complete and convincing experience. However, the haptic rendering can already easily be improved by combining the stimulation with other sensory modalities. Indeed, when used in combination with a graphic display, the haptic stimulation is easily associated to the graphically displayed object, even if they occur in different spatial locations. Auditory feedback can also greatly increase the tactile experience. Multi-sensory integrations offer many possibility to improve the overall experience, even if the quality and accuracy of the other modality isn't excellent. Actually, the audio-tactile minimum synchrony necessary is about 80 ms [184] and the visual-tactile minimum synchrony is around 50 ms [128].

1.4.3 Tactile Signals

Once the device has most of the functionalities discussed in the later section, the next step is to use a pertinent signal that can readily recreate the desired mechanical phenomena. In some cases, we can use a simplified physical model to render haptic objects [71, 208]. This requires a robust model for the objet that is being reproduced. An example of this is the rolling ball illusion, where the motor vibrates according to the physical equation of a rolling ball, and the user mistakes the hollow tube for a tube containing a rolling ball [278]. A more direct approach is to record the raw data of the interaction we want to reproduce and then replay it as a function of state variables or time [187]. To explore a surface properly, the finger

moves, as observed by Katz [127], therefore the most pertinent is to record force data when a finger is actively exploring a surface. This can be done with a biomimetic finger in which an array of sensors measures the contact and slip while exploring surfaces [104].

Other methods involve glueing a force sensor or an accelerometer on the fingertip nail and measuring the fluctuations due to finger movements [19, 108, 238, 220]. However, these sensors add a small mass to the fingertip which perturbs the measurement. Other non-contact methods include acoustics [67] or velocimetry [161]. Lastly, tribometers can measure the interaction forces in tangential and normal directions separately. Some tribometers measure a passive interaction [192, 163, 53, 3, 60] but in other cases the bare finger can slide over the tribometer platform, where a tactile sample such as a texture or an asperity can be mounted [162, 273, 69, 201].

Between all of the options, the chosen method should be based on the type of display and the way (sliding, holding, tapping, passing contact, passive or active exploration) the user will interact with it. The best practice is to make measurements at the location where the device is touched by the user [92]. For a fingertip interaction device which can be actively explored (the aim of the current thesis), the most appropriate method would be to record the forces when a bare finger explores the texture to be reproduced.

Aside from reproducing textures, there are many exciting projects that aim at designing haptic icons and haptic metaphors [156] in digital media which can inform on tasks and navigation by providing feedback. These don't require such thorough data collection and can instead benefit from content artists. These often get inspiration from the audio signals which are already used as specific informants.

Actually, open-source tactile libraries are starting to emerge and are available for haptic designers to use. For example, VibViz is an interactive tool with a 120-item library of haptic textures, icons and metaphors that have diverse functional and affective characteristics [217].

1.4.4 Sensing Requirements

There are a number of ways in which the haptic display can be programmed in order to respect the laws of physics and create sensations that respond to the user's action.

The controlled parameters can include the following: the fingertip load, force sensors, position sensors, speed sensors and accelerometers. In the case of hand-held devices, the participant is most likely moving and exploring the device in different directions. In this case, precise additional (motion) sensors will need to be incorporated in the control loop to make sure a complete picture of the way the fingertip or the hand explores the device can be made. In the case of haptic displays, the main desired technical requirements for these sensors are that they should be stationery or grounded and have sufficient resolution (based on the human perceptual limits described earlier).

Ideally, several of these parameters are reliably and constantly estimated. They are then accounted for during the synthesis, usually by replaying the tactile signal as a function of these variables. While a fast response is often required to avoid large lags, some design liberties can be taken while still creating a very satisfactory rendering. For example, Wiertleweki et al. [273] reproduced sensations of virtual gratings with different spatial frequencies and amplitudes without using low-frequency and normal skin movements. They however concluded that textures should be displayed spatially even if they are sensed through time, since participants found it difficult to discriminate textures based on the temporal information only.

These requirements may be put into questions as our understanding of our tactile perception evolves. For example, a design liberty in terms of speed sensing was investigated in Chapter 6.

1.4.5 Reproduction Techniques

So far, there are no tactile devices that satisfy all the requirements mentioned in the previous sections. Actually, instead of featuring all the requirements for every type and quality of rendering (textures, objects, haptic icons and metaphors), most actuators are designed to create a single type of tactile feeling for a narrow application. In very few cases however, the same actuator is used for different interactive properties, such as exoskeletons and small vibrators in mobile phones [203].

Controlled Friction 'Surface displays' refer to electromechanical devices that can create artificially produced haptic sensations [94]. They move a real glass-like surface by sensing the interacting finger's position and applying very high frequencies ($>$ kHz). A large amount of surface displays rely on ultrasonic vibrations [275, 181] to reduce friction by lifting up the finger aerodynamically, also known as the squeeze film effect. It was first developed by Watanabe and Fukui [262] and since has been implemented in the STIMTAC [21] and in the T-PaD [276, 40] which can create the sensation of virtual edges. Recent advances have rendered features 25 μm high at an update rate of 5 kHz [272]. The other main technique for surface display involves using electrostatic attraction between the finger and the plate to enhance the friction [240, 5, 166] (and repulsion to reduce the friction). However, the range of forces and frequencies they can render is smaller. This was implemented by TeslaTouch [12] and Senseg [159]. Recently, efforts have gone into merging both electrostatic and ultrasonics stimulation principles [80, 41].

Vibrations Vibrotactile devices do not produce low-frequency forces like force-feedback devices and supra-threshold frequencies that vary the fingertip/surface physics like surface displays. Instead, they focus on the fact that the human perceptual system is most sensitive to frequency signals between 30 and 800 Hz, and therefore vibrate the finger in that range. Vibrations are an efficient way of eliciting tactile sensations and this is what the thesis has aimed at. The configuration chosen was that of a finger exploring a flat glass surface actuated by a motor. The following technologies are examples of the types of actuators that could be used.

– **Piezoelectric Transducers** Piezoelectricity is the property of certain materials to convert applied mechanical deformation into electric charges and conversely, to convert electrostatic fields into strain. Metec Inc. uses piezoelectric motors to move the Braille pins up and down by changing the electric current in the structure supporting the pins. These transducers can also directly vibrate the screen of a portable device. Wiertlewski and Hayward [274] created a device able to record and replay tactual textures using a bidirectional piezoelectric transducer which could successfully display five differentiable and matchable virtual textures that varied in roughness and spatial frequency.

– **Eccentric Mass Motors** Vibration D.C. motors or Eccentrically Rotation Motors (ERMs) rotate an unbalanced shaft eccentrically creating a wobbling force that translates into vibrations. Their main purpose is to alert the user of a cell phone, pager, gaming controllers but they are also used in personal massagers. Therefore it is not important that there is a significant lag and that they can only display sinusoidal patterns with small amplitudes and frequencies. These limitations, however, make them impossible to use to create any sophisticated tactile feelings or to use in an interactive device where a low latency is essential.

– **Voice-coil Motors** Aside from these piezoelectric actuators or ERMs, voice-coil transducers and speakers can create rich vibrotactile sensations [75]. The older models provided low displacement and forces. For example, Fukamoto [72] embedded a voice coil type actuator that provided sufficient force when driven at the resonant frequency but only a single frequency and amplitude of vibration could be produced. Later, Yao et al. [278] designed a more performant voice-coil motor, the 'Haptuator', which could reproduce acceleration over a large bandwidth (typically 50 Hz to several kHz). Its principle is based on Lorentz forces which linearly move a magnet suspended in a membrane. They are however limited in the low frequency range by the suspension elasticity, the maximum displacement (usually a few mm), and the mass of the magnet. The elasticity can be slightly reduced by removing the membrane of the motor and placing the two moving parts of the motor in perfect alignment. The maximum displacement can be slightly increased by adding a larger coil region compared to the magnet. It is also advantageous to dampen the resonance by adding a damper in the dynamic set-up, and this often extends the flat bandwidth. This was the approach taken in this thesis.

1.4.6 Applications

I've limited the description of tactile device to our particular case: 1) that of a grounded device that the finger explores actively 2) where the vibrations are delivered to move a glass plate. This particular scenario can lead to a large amount of applications. Flat touch screens are used everywhere: phones, tablets, the entertainment monitor in a plane, the control monitor of a car, a 3D printer, to name a few. Tactile feedback can become an important feature of interfaces for future devices by providing more effective, comfortable, and enjoyable interactions. Gemperle et al. [75] pointed out that the fundamental requirements for mobile actuators are small, miniature size, lightweight, low voltage ($\approx$ 5V), low power consumption and customization ability so that it can fit to devices of different sizes and forms.

Indeed, a good use of haptic feedback [155] is to support the graphics or to create expressive control and notifications. This requires a good understanding of haptic metaphors and ergonomics. We can imagine interfaces where users can feel and recognize incoming information without interrupting their activity. An interesting illusion was described by Amemiya and Gomi [6] where a motor transmits asymmetric oscillations to the fingerpad giving a very vivid the sensation of directional pulling. This could be integrated into displays to help with directional cueing during navigation in a car for example. The study of the sensation of keyclick to be reproduced was investigated by Monnoyer et al. [170] and it was found that a falling friction induces the sensation of a click. This was rendered using an ultrasonic device but the same principle could be implemented using a vibrating motor to assist the action of pressing on an icon or a touch pad key.

Aside from warning messages (pagers) or informational signals (directional cueing, metaphors for different length of signal types), the recreation of a texture can add new functionalities, and new methods of communication. One can easily imagine the endless applications of having textures displayed on interactive displays. First, we can have tangible e-commerce where users can touch the texture of the product the want to buy. They can sense the difference in softness between different textiles as opposed to having to visiting a store. Another exciting possibility would be to allow product designers to feel the effect of their creations without having to build them. Finally, there are many opportunities for sensory augmentation. We can imagine interactive tactile games which will allow stroke patient to practice recognising textures of varying difficulty, providing them with sessions they can do outside of the contact time with the doctor and allowing for a greater variety than what is currently offered for their

rehabilitation. Additionally, there are options where the doctors can feel from a distance and could do a diagnostics on a skin disease if coupled with a sensing apparatus. Also, for visually impaired patients, we can image compensation techniques that will help guide the patient when interacting with a touch screen for tasks that are hard to visualize.

Chapter 2

Characterizing and imaging gross and real finger contacts under dynamic loading.

Contents

This work was submitted by S. Bochereau, B. Dzidek, M. Adams and V. Hayward as 'Characterizing and imaging gross and real finger contacts under dynamic loading' to *IEEE Transaction on Haptics*.

Preface to Chapter 2

This chapter presents the tactile device that was designed, realised and used to carry out the experiments described in this thesis. The recording apparatus was used in Chapter 4. A simplified version of the reproduction apparatus was used in Chapter 3. The current reproduction apparatus was used in Chapter 5 and 6.

Abstract

We describe an instrument intended to study finger contacts under tangential dynamic loading. This type of loading is relevant to the natural conditions when touch is used to discriminate and identify the properties of the surfaces of objects — it is also crucial during object manipulation. The system comprises a high performance tribometer able to accurately record *in vivo* the components of the interfacial forces when a finger interacts with arbitrary surfaces which is combined with a high-speed, high-definition imaging apparatus. Broadband skin excitation reproducing the dynamic contact loads previously identified can be effected while imaging the contact through a transparent window, thus closely approximating the condition when the skin interacts with a non-transparent surface during sliding. As a preliminary example of the type of phenomenon that can be identified with this apparatus, we show that traction in the range from 10 to 1000 Hz tends to decrease faster with excitation frequency for dry fingers than for moist fingers.

2.1 Introduction

For almost a century it has been observed that our tactile system mostly extracts information about the substance and the surface details of objects during the sliding movements of the fingers [133, 145, 101, 97]. Unless a finger contact is nearly perfectly lubricated, the slip of a finger against most surfaces elicits complex oscillations. Steady sliding may occasionally be induced by lubrication from surfactants in aqueous solutions [207, 31], something that happens when we clean dishes with soapy water and experience difficulties feeling them. The more common case of the dry or moderately wet surfaces, however, is invariably associated with slip-induced oscillations.

These perceptually significant mechanical oscillations arise even if the counter-surfaces have roughnesses down to nanometer scales [84]. They are evident for asperities at micrometer scales [271, 258] and higher [161]. These observations justify the need to develop methods to characterise finger contacts under dynamic loading conditions, since such dynamic contacts are the rule rather than the exception during the tactile interaction with objects.

Since the observations of Gibson regarding human perceptual behaviour [79], it has been widely recognised that the information available from statically loading fingers and hands with objects has little perceptual value. There are three main types of informative finger contacts: when a finger interacts with an object causing a quasi-static evolution of its mechanical state, when a finger collides with a surface, and during sliding on a surface or at the onset of slip [90]. Only the latter two cases qualify as dynamic contacts.

The apparatus that was developed in the current work specifically addresses the study of dynamics contacts. The evolution of these contacts can be divided into three parts [219, 194, 7, 242, 84] which typically can be identified through two approaches. A first approach is through the bulk measurement of frictional forces. Such measurements require special instruments owing to the need to obtain a reliable response over a large frequency range, to viz., 500 Hz. A second approach is to image the contact of the finger through a transparent surface. While the bulk frictional response of a finger to movement is relatively easy to obtain in the quasi-static case, the evaluation of the mechanical consequences of the friction associated with a dynamic finger is more difficult. Thus far such characterisation was either obtained indirectly, either acoustically [67], through acceleration signals [108, 238, 220], remote velocimetry [161], or directly by imaging through transparent surfaces.

When a person explores a surface, skin tribology depends crucially on the spontaneous motor programs that are called upon for each type of surface and perceptual task. For example, seeking to detect a small asperity on a smooth surface, such as a micro-crack, will involve a very low tonic output, but the identification of the essence of a wood from its grain might evoke much greater activation. Replacing a complex surface with which the skin interacts by a rigid surface that oscillates in a complex manner, [273], is arguably a reasonable approximation to sliding on a complex surface. Consider that the propagation of mechanical waves in the skin is of the order of 10 m/s, [202], which at 10 Hz corresponds to a wavelength of 1 m. At 1 kHz, the wavelength reduces to 10 mm but at such frequencies viscous forces dominate, [260], and the skin may then be considered a rigid solid. It can be further observed through behavioural studies that the tangential component of the interaction force with an object is particularly rich in information concerning the texture roughness and shape of the surface topographical features making up the texture [228].

From the above observations we constructed an apparatus that can excite the skin tangentially with arbitrarily complex displacements in a wide frequency range, while simultaneously imaging the contact at high spatial and temporal resolutions. The apparatus can also measure the tribology of a finger sliding on arbitrary natural surfaces and can further ascertain that

interfacial forces, which arise during exploration and during testing, are indeed equivalent. We present preliminary results and discuss their implications. Before doing so, we briefly review relevant contact imaging and tribological measurement techniques.

2.2 Related Work

2.2.1 Imaging Finger Contacts

A prism-based Frustrated Total Internal Reflection principle (Frustrated TIR), see Fig. 2.1, was adopted by Levesque and Hayward to image finger contacts with flat, raised, or indented surfaces [150]. This technique can produce high contrast images of the intimate contact of a finger with a transparent surface. It was possible to image the temporal evolution of the skin strain patterns in the contact region area during rotation and lateral movements. By examining changes in the triangulation of tracked skin features, they found that patterns of skin compression and expansion resulted from a combination of gross movements and surface features.

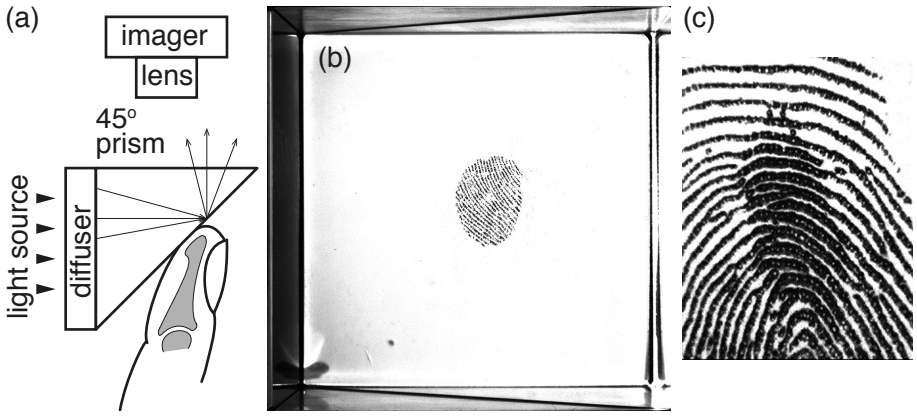

Figure 2.1 – (a) Prism-based Frustrated Total Internal Reflection principle. With a correctly designed diffuser, light entering the prism is completely reflected, yielding a bright background. Any object in intimate contact (or up to a few tens of nanometers) with the face of the prism at distances smaller than the wavelength of the light disrupts reflection locally. (b) High contrast images of the 'real' contact since objects distant from the surface by more than a few tens of nanometers will leave reflected light intact. (c) Transitions from sticking to sliding, see [4], can be directly observed since sliding ridges exhibit smaller contact areas than sticking ridges.

Using the same device, André et al. [7] found that the skin hydration level reduced the tendency of a contact to slip, irrespective of the variations of the coefficient of friction. Delhaye et al. [51], employing a similar technique, but with coaxial illumination to facilitate the movement of the counter-surface, observed the contact area evolution during the stick to slip transition in distal, proximal, radial and ulnar directions. This study examined the differences in the stick ratio and the contact area displacement with time or tangential force using an optical flow algorithm. Coaxial illumination, however, produces lower contrast images than prism-based frustrated reflection since the background inter-ridge surfaces reflect significant light, but it has the advantage of giving images that do not required aspect-ratio correction.

Another very popular approach to take advantage of the Frustrated Total Internal Reflection principle is in a direct manner [63, Sec. 12.3], as shown in Fig. 2.2(a). Here, light is

injected in a slab of glass acting as a light trap, giving a dark background when no object is in contact with it. When there is an intimate contact, reflection is also frustrated, but here some of the light escaping from the contact scatters and diffuses inside the finger tissues. Another portion escapes the trap, giving rise to an intensity graded image on a black background Fig. 2.2(b). Some of this light also reflects from the surfaces that are in close vicinity. In the image shown in Fig. 2.2(b), the bright spots visible inside the sweat ducts are probably the result of specular reflections of this light against menisci of exuding sweat, see Fig. 2.2(c). Wiertlewski et al. recently took advantage of this technique for imaging finger contacts at ultrasonic frequencies [268], which to our knowledge is the first example of *in vivo* finger contact imaging under dynamic loading, albeit in the normal direction.

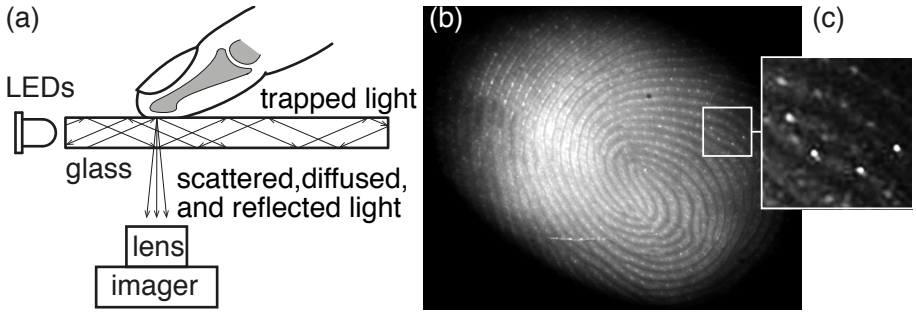

Figure 2.2 – (a) Imaging finger contacts using frustrated total reflection to scatter light at the points of contact. Illumination can be conveniently provided by LED devices. (b) The resulting image combines scattered, tissue-diffused, and reflected light. (c) Contrast enhanced area of detail shows specularities from sweat menisci.

Lastly, using direct illumination and image processing techniques to compensate for low contrast, Tada and Kanade showed that as the normal force increases, a large overall area is created, and that the stick region disappears faster as speed increases [237].

2.2.2 Finger Tribometry Against Natural Textures

Several tribometers exist that are capable of measuring finger tribology *in vivo* [192, 163, 53, 3, 60]. Some of these devices are capable of measuring the interaction of a bare finger with a wide range of natural textures [162, 273, 69]. The particular design adopted herein, Fig. 2.3., was developed by Wiertlweski et al. [267] and adapted by Platkiewicz et al. [201] to record natural textures. Recently, Janko et al. [111] described a high performance tribometer that was employed to identify a range of physical effects arising from the nonlinear nature of friction.

The present design, Fig.2.3, features a very high ratio of interfacial forces component separation to ensure that normal loading and frictional forces are accurately measured. The leaf springs transmitting normal loads to the load cells have the feature of being 1000 times stiffer in the normal direction than in the tangential direction. The normal force components was computed using two load cells (9313AA1, Kistler AG, Switzerland) and the tangential force component using one load cell (9217A, Kistler AG, Switzerland).

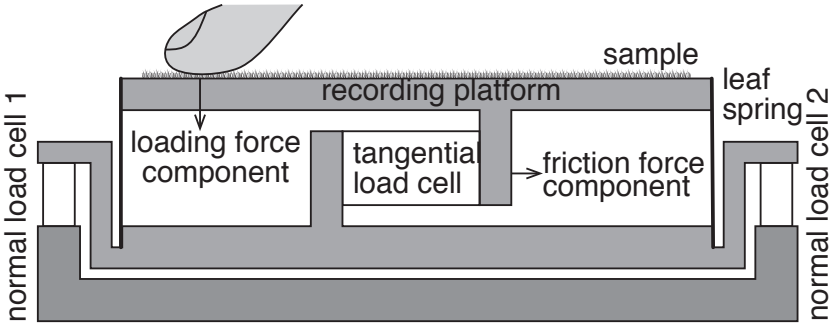

Figure 2.3 – Tribometer measuring tangential and normal components independently, catering to both the recording (seen here) and the reproduction, seen Fig.2.6, apparatuses.

2.3 Device Overview

The device, Fig.2.4, consists of (a) a tribometer that allows us to precisely measure friction forces catering to both:
- the recording apparatus : a sample holder (b) on which you can place a sample of textured material, slide a finger over it and measure the vibrations resulting, and
- the reproduction apparatus : a glass-plate stimulator (c) with an imaging display (d) where you can apply vibrations to a glass plate, measure the interaction forces, and look at them through the glass plate.

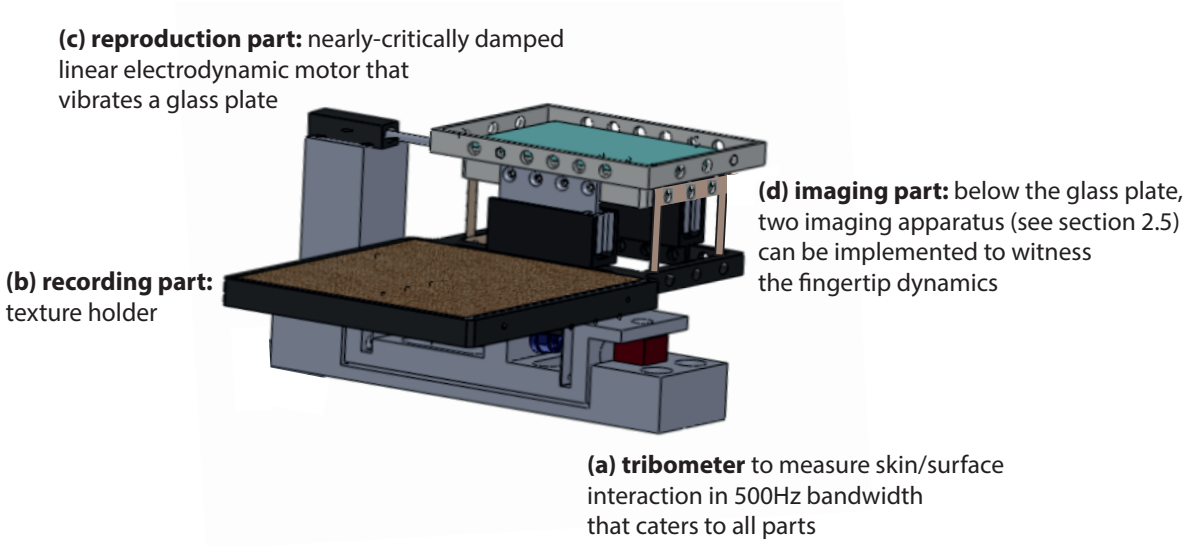

Figure 2.4 – Device able to record, reproduce and image the fingertip friction elicited when sliding over textures or asperities.

The ultimate goal of having these functionality is to first use (a-b) to record finger dynamics between any texture and a finger pad during sliding then replay the measured vibrations using (c) and measure the virtual interaction in terms of forces with (a) and images with (d).

2.4 Apparatus

2.4.1 Requirements

The main challenge was to achieve force sensing with sufficient bandwidth, at least up to 500 Hz but ideally up to 1 kHz, in order to cover the temporal frequencies associated with scanning textures [82, 34]. In practice, this requirement reduces down to eliminating any sharply undamped modes from the mechanical structure at frequencies in the desired operating band that would be difficult to compensate by inverse filtering.

In terms of skin excitation, the requirements involved ensuring a stable and robust signal causality relationship between a transducer and a finger over a wide frequency band. One approach, the isotonic approach, is to arrange for the transducer to have a mechanical impedance that is much smaller than that of the finger and to measure displacements resulting from a known applied force. Such an approach is possible, [269], but difficult to implement here owing to the mass of the plate used to image the finger contact. The converse approach, the isometric approach, which is adopted here, is to arrange for the transducer to have an impedance that dominates that of the finger and to measure the force resulting from the finger's displacement.

2.4.2 Design and Construction

The tribometer design, Fig.2.3, was optimised by constructing it from three single-block mechanical parts connecting the load sensors, achieving high rigidity. The load cells were designed so that they screwed into the single-block mechanical parts ensuring little mechanical loss. Next, the sample holder platform was designed to be light and rigid. It was machined out of a single block of grade 2017 aluminium as depicted by Fig 2.5.

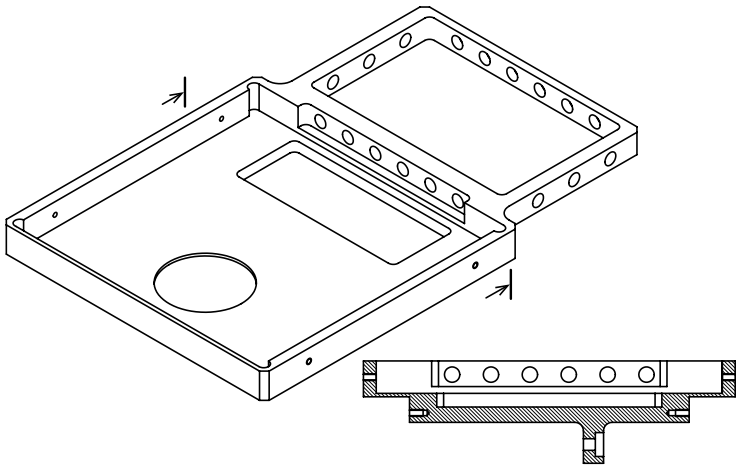

Figure 2.5 – Sample holder platform. In the recording part, textures samples (10cmx10cm) can be placed (left) and in the reproduction part, a glass plate (5cmx8cm) is suspended using leaf springs (right).

In the reproduction apparatus, the lateral glass frame supported the skin excitation transducer, which was connected to it by a set of compliant leaf springs. The transducer was actuated by a contact-less electrodynamic voice-coil motor (Model NCC01-07-001-1R, H2W, Santa Clarita, CA). It is represented schematically in Fig. 2.6. The plate in contact with the

finger serves as a transparent imaging window. The imaging system is described in the next section.

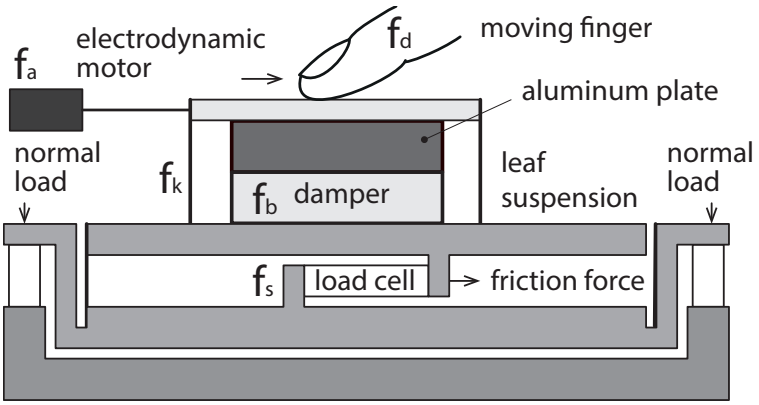

Figure 2.6 – Reproduction apparatus with the tribometer that measures the finger-vibrating glass interaction.

The modal response of the sample holder platform was evaluated using an impact hammer to excite the structure (Low impact hammer type 086E80, PCB Piezotronics). The results revealed that the response was satisfactory with a first peak at 550 Hz due to the platform's cantilevered design, see Fig. 2.7. The tribometer's performance was reported in [84].

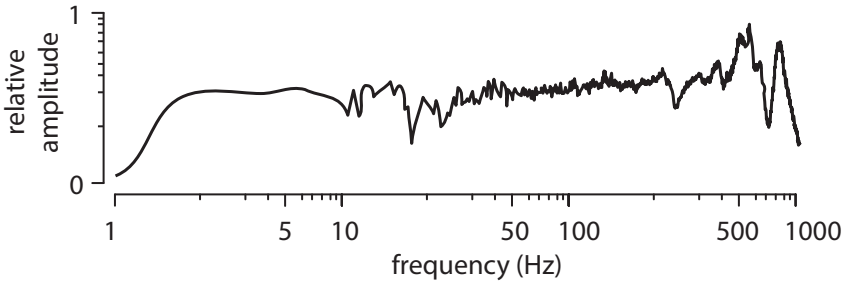

Figure 2.7 – Mechanical impulse response of the platform over 20 tests.

We adopted the guideline that the stiffness of the plate suspension and the damping coefficient should be of the same order as that of a fingertip while the moving mass should be many times greater in order to achieve the required signal causality. This way, any force applied by the motor to the plate will be converted into an acceleration in a consistent manner (i.e. independent of finger force). In the lateral-medial direction, the mean bulk elasticity of human fingers is known to be about 1.0 N/mm and the damping coefficient of the order of 1.0 Ns/mm [269]. These target figures were thus adopted. As a result of the mechanical properties of the finger, the amplitudes of the bulk oscillations during exploration can reach one or two millimetres, thus the transducer was designed to achieve these values when oscillating a mass of approximately 100g at different frequencies (10 to 1000 Hz).

The springs were made from copper beryllium beams that were cut to give the required stiffness. The frame holding the moving glass plate was machined from magnesium for rigidity and low mass. To achieve the required damping, we designed a Foucault-current damper of a design similar to that described in [168]. The armature was made of two aluminium plates that moved without contact between pairs of magnets, as seen in Fig. 2.8.

The damping viscosity obtained is a function of several parameters [168]. The size, spacing,

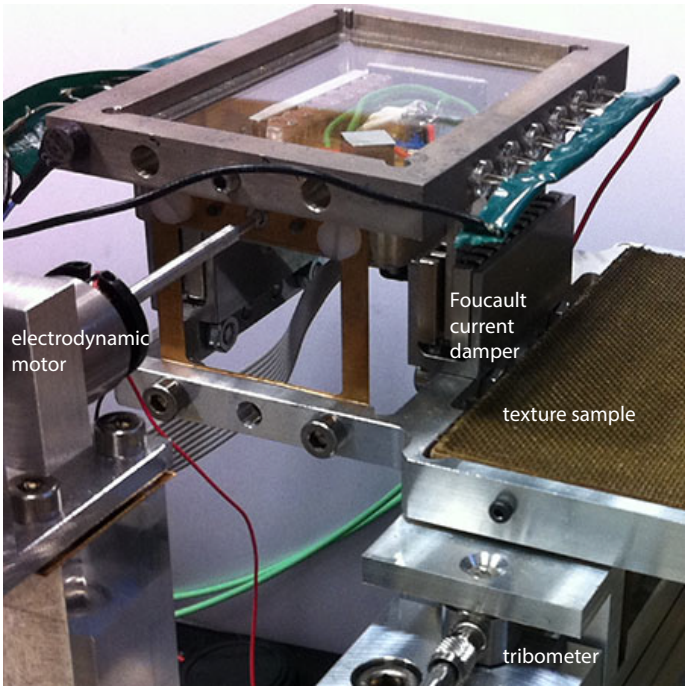

Figure 2.8 – Reproduction apparatus with the transparent plate mounted on the tribometer (left) alongside the recording apparatus where a texture sample is placed (right).

and number of magnets are important ones. We employed twelve pairs positioned every 2 mm using plastic spacers on either side of the moving plate. The material with which the armature was made was non-alloyed aluminium (99% pure) to maximise conductivity and minimise mass. The air gap between the magnet and the armature was set to 0.1 mm. The magnets were 5 x 3.5 x 2 mm and made of Neodymium (NdFeB) with nickel coating giving a flux density 1.4 T.

2.4.3 Identification

Sending a step impulse to the motor, Fig. 2.9, allowed us to identify the parameters of the system by minimising $|\hat{f}(t) - f(t)|$ where $\hat{f}(t) = Ae^{-\xi F_0 t}cos(F_0 t + \phi)$ and $f(t)$ are the mathematical model and the measured ground reaction forces respectively. Table 2.1 lists the theoretical parameters of the fitted mathematical model, m is an identified parameter.

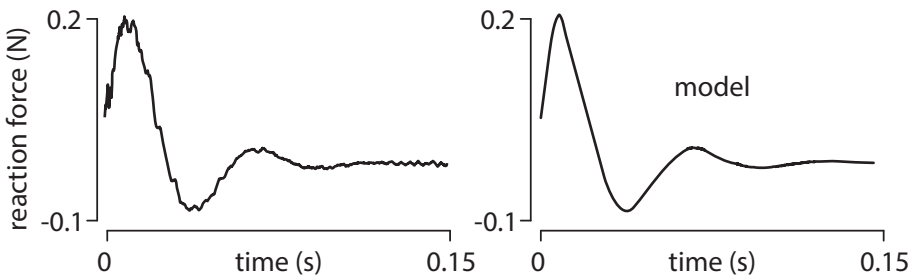

Figure 2.9 – Damped response to a step function.

Table 2.1 – Transducer parameters.

mass m	81 g
resonance frequency F_0	17 Hz
spring constant k	0.93 N/mm
damping ratio ξ	0.35

2.4.4 Interfacial Force Measurement during Excitation

From the system's free body diagram, Fig. 2.6, the forces acting on the plate are: the force of elasticity, f_k, the force of viscosity, f_b, the interfacial force of finger friction, f_d, and the force of the actuators, f_a, giving $-m\ddot{x} = f_k + f_b + f_\mathrm{d} + f_\mathrm{a}$. However, the reaction force sensed by the tribometer's lateral sensor is, $f_\mathrm{s} = f_k + f_b$, thus if the acceleration of the plate, $\ddot{x}$, is measured, then the interfacial force of the finger friction can be evaluated from $f_\mathrm{d} = -m\ddot{x} - f_\mathrm{s} - f_a$, where all the terms are known and where m is the only parameter to be precisely determined.

2.5 Two Imaging Apparatuses

A high-speed camera (Model Mikrotron MotionBLITZ EoSens mini2) was employed to image a fingerpad contact under dynamic loading in the two modes described earlier. To achieve high spatial resolution in addition to the high temporal resolution, it was fitted with a Navitar 6000 zoom having a 12 mm fine focus augmented with a telescopic adapter and a 0.75x lens attachement. This set-up allowed focus from a whole fingertip contact down to just five fingerprint ridges at high resolution. Obtaining a sufficient level of illumination was a challenge in order to serve the needs of the two total internal reflection methods that were available.
Please note that the two imaging techniques used here cannot be used simultaneously and switching them requires some re-arrangement and calibration.

2.5.1 Prism-based Frustrated Total Internal Reflection

A right-angle prism was positioned below the vibrating glass plate using a 3-axis micropositioner, and adjusted to leave a 0.1 mm gap between the prism and the glass plate. Index-matching immersion oil was then used to fill the gap and the oil was retained there by capillarity, thus realising a continuous, yet deformable, optical milieu, see Fig. 2.10. A bright cold light source (KL 2500 LED, Schott, Germany) was employed for illumination. An opal diffuser ensured that the light was transmitted onto the camera by illuminating the prism volume without being reflected back by the smooth air-glass interface and without escaping the prism from internal surfaces.

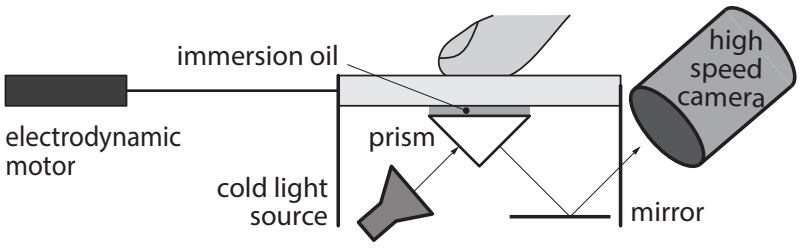

Figure 2.10 – Dynamically loaded fingertip imaged though prism-based Frustrated Total Internal Reflection set-up.

The prism was immobile, did not add mass to the moving parts and allowed for high-speed imaging. In this mode, the natural damping introduced by the liquid interfaces eliminated the need for eddy-current damping. With this technique, images at high spatial resolution and high temporal resolution could be obtained. One example of an image acquired in a static condition is shown in Fig. 2.11.

Figure 2.11 – Occluded real finger contact imaged under static conditions at 24 Hz frame rate showing the degree of detail that can be obtained at 2 N and 2 s of contact time.

Contrast was sufficient to enable excitation at imaging frequencies as high as 1 kHz. One example can be seen in Fig. 2.12 where a 'real' contact area could easily be imaged at such high frequencies[1].

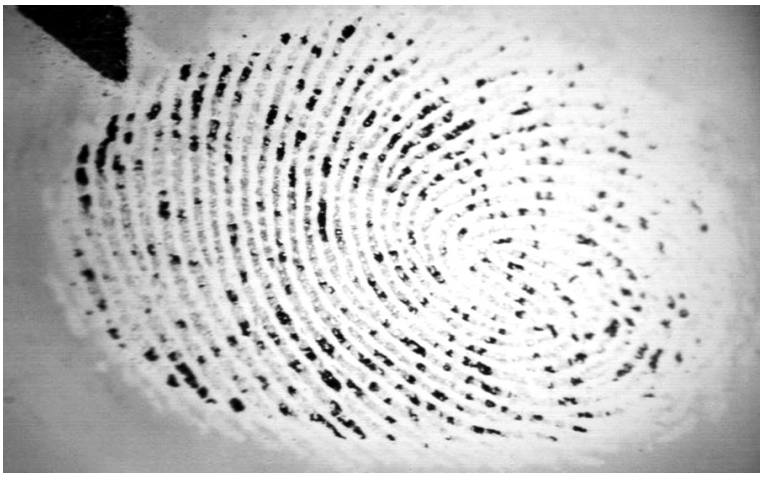

Figure 2.12 – Real finger contact area under static conditions at a 1 kHz frame rate after 2 s of contact time and for a 2 N normal load.

[1]The literature also refers frequently to the notion of 'true' contact. Here the terms 'real' and 'true' are considered to be equivalent.

2.5.2 Direct Illumination Total Internal Reflection

Green coloured light was transmitted into the glass plate by a set of laterally-placed light emitting diodes (LED), creating total internal reflection, and allowing for the fingerprint in contact with the plate to be visible. To increase light incidence, the four edges of the glass plate were polished to an optical quality finish. The green coloured light minimised the fraction of light diffused by the skin tissue, which acted as a filter for the complementary colour.

The frame was designed to house twelve green LEDs (HLMP-CM1A-560DD, Avago, 59000 mcd each with 15° dispertion giving 26 lm of illumination in total. They shine through 2 mm diaphragms to guide as much light as possible into the 2 mm-thick glass plate to reduce the reflections on the edges of the glass that could escape the light trap, see Fig. 2.13. Optionally to increase the light intensity even further, we also used a cold light source (KL 2500 LED, Schott, Germany) with a green filter transmitting the light into the glass frame. With this configuration, it was possible to reach 100 Hz image sampling capability.

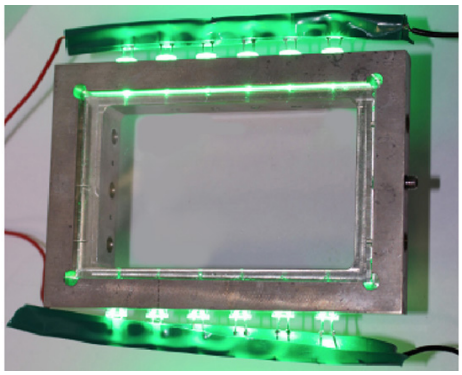

Figure 2.13 – Illuminated vibrating plate.

A 45° angle mirror was used to enhance the optical stability of the set-up and facilitate the horizontal camera mounting, see Fig. 2.14. The light path from the green LEDs around the set up was frustrated until light reflected off a fingerprint ridge in contact with the glass.

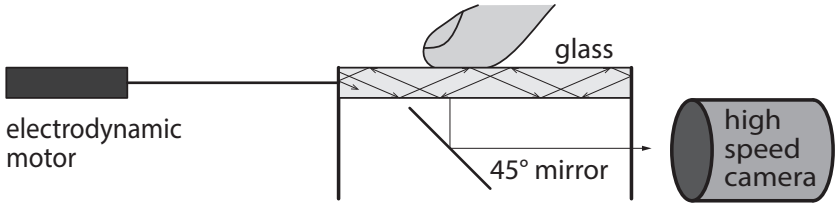

Figure 2.14 – Direct Frustrated Total Internal Reflection set-up.

Figure 2.15 illustrates the type of image that can be obtained with this method. It is a combination of light arising from the real contact, light reflected by the fingerpad surface, and light diffused in the tissue. This image should be contrasted with that seen in Fig. 2.12 as they each deliver very different types of information.

2.6 Preliminary Bio-tribology Measurements

In this section we show some examples of the stimulation and characterisation capabilities of the apparatus described previously. It is made evident without elaborative quantitatification

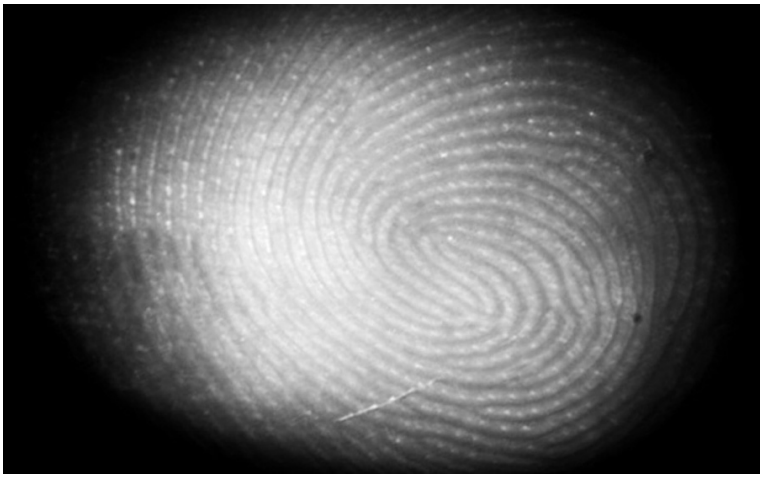

Figure 2.15 – Fingerpad image mode at 100 Hz for 2 N normal load.

that the establishment of the real contact area by a finger is a multifactorial phenomenon. For brevity, the physics behind these observations will be discussed in future publications.

2.6.1 Real Contact Area Dynamics during Static Loading

The imaging apparatus was able to precisely visualise the way in which the real contact area evolves with occlusion time and with applied load, see [4] and [60], for a definition of these terms. Briefly, occlusion occurs when a fingerpad is in contact with a smooth impermeable surface so that the secretion of moisture from the sweat pores in the fingerprint ridges is trapped at the interface and is absorbed by the *stratum corneum*. The ridges and their surface topographical features become more compliant over a period of tens of seconds due to the plasticisation by the moisture and hence the real area of contact increases with the time of contact until an asymptotic value is reached.

A static test was performed while the real finger contact area was imaged in a time-lapsed manner using the prism-based Frustrated TIR method, (1, 1.5, 3, 5, 8, and 20 s). A flat glass prism was pressed down onto the fingerpad in order to induce total internal reflection, with the applied load gradually increased until the required maximum value is achieved. We observed this phenomenon previously using a different apparatus configuration [60]. Before a set of measurements, the index finger was washed with commercial soap, rinsed with distilled water and allowed to dry for 10 min until an equilibrated clean skin state was achieved. The result can be seen in Fig. 2.16.

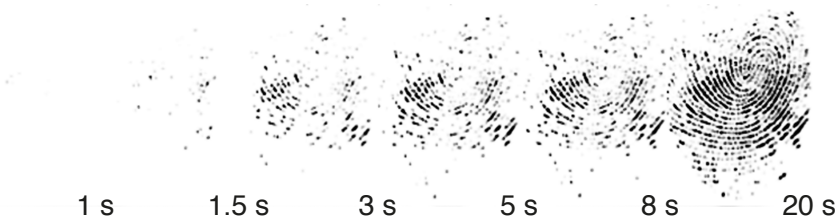

Figure 2.16 – Time-lapse real contact imaging as the normal load increases according to the time dependent normal loading indicated by Fig. 2.17.

It can be observed how the real contact area increases gradually owing to occlusion dy-

namics while the gross contact area reaches its ultimate value very rapidly, see Fig. 2.17. This phenomenon wad discussed and analysed elsewhere in greater detail where the methods are also described [61].

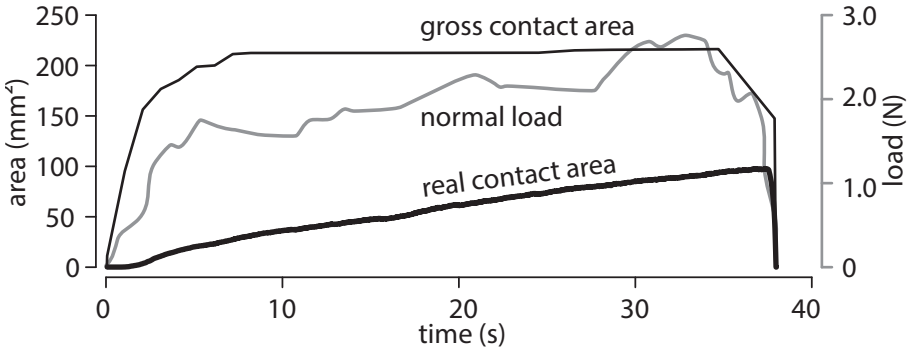

Figure 2.17 – Result of the analysis of the images of Fig. 2.16.

2.6.2 Real Contact Area Under Dynamic Conditions

Exploring textures always corresponds to dynamic contacts since fingertips constantly make and break multiple contacts as the skin ridges interact with the relatively moving asperities. It is these rapid mechanical fluctuations that contain the texture perceptual information.

During steady sliding, the resulting broadband, complex oscillations that can be readily observed and converted to the frequency domain and thus viewed as a sum of a large number of sinusoidal signals. It is thus informative to investigate how dynamic contacts behave as a function of frequency. The formation of the real contact area as the origin of friction between a fingertip and a surface is a multifactorial phenomenon. To investigate these factors, dynamic tests were performed where the participant pressed a finger on the glass plate, and then maintained it at around 1 N while the plate was vibrated at different frequencies. Absence of slip between the fingerpad and the glass plate could be visually ascertained. The same fingerpad skin state preparation was carried out for the dynamic conditions as for the static ones. Figure 2.18 illustrates the complex influcence of the different factor that were varied: tangential loading rate, contact duration, and skin hydration.

Several trends can be observed by simple inspection. Skin hydration has a significant impact at the onset of a contact and during its evolution, as can be observed by comparing images (row pairs) taken for the same loading conditions but at different times after contact onset. Dry and moist refer to different natural states of the finger; the clean index finger of one of the authors was dabbed with a dry or moist tissue before each measurement to induce the appropriate state. The effects of dynamic lateral loading are also different according to normal loading rate as can be seen by inspection of the columns of Fig. 2.18.

Notably, a moist finger tended to become less sensitive to loading rate than a dry finger. Another trend is that dynamic normal loading does not seem to disrupt the occlusion process and hence the increase in the real area of contact with time. Since finger hydration could not be controlled with accuracy, monotonicity is not always present in the images sequences taken under different conditions. Taking advantage of the simultaneous tribological measurement, we could nevertheless conduct a preliminary quantification of the creation of traction for different hydration states under dynamic loading.

Figure 2.19 reports the resulting traction measured under the above conditions and at frequencies of 10, 20, 50, 100, 200, 500, and 1000 Hz. Recall that traction, or interfacial shear

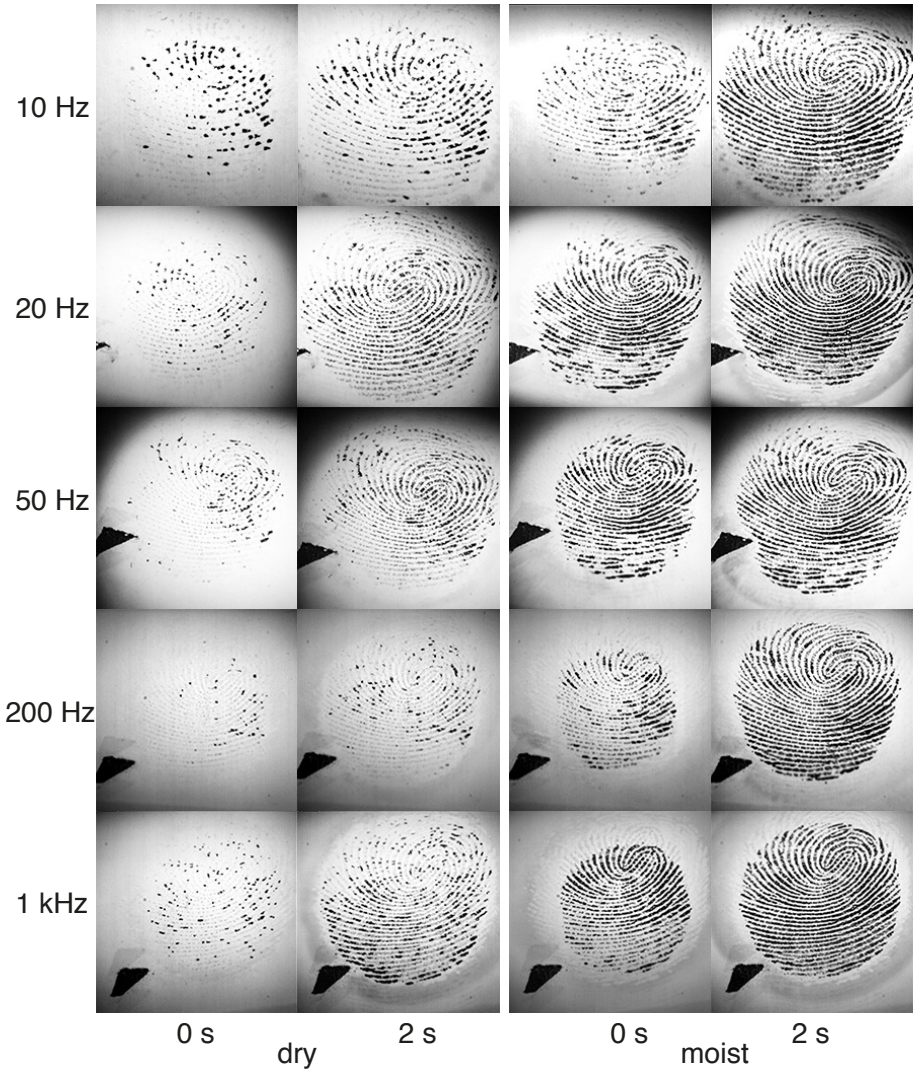

Figure 2.18 – Real contact imaging as a function of tangential loading rate, contact duration, and skin hydration.

stress, is defined as the force per unit of real contact area [4]. In this preliminary analysis we averaged the tangential traction force component and the real contact area over three trials per condition of duration 2 s. The normal load was 0.94±0.6 N for the dry condition and 0.75±0.3 N for the moist condition. To minimise the estimation error of the real contact area due to the variations in the initial moisture contents, the value employed in the analysis was based on the difference between the final and initial values.

It can be observed that while the formation of the real contact area is relatively insensitive to loading rate, shear stress tends to decrease with this parameter. This effect is less pronounced for moist fingers than for dry fingers. A possible explanation for this phenomenon can be found in the acceleration of the occlusion mechanism at the low frequencies. Thus the effect is weaker at higher frequencies for dry fingers since moisture results in a contact with a significant initial occlusion [61]. Note that the estimation of interfacial shear stress accounted only for the increment of real contact area over a period of two seconds. The observation that the growth of real contact area for dry fingers is more sensitive to the effect of time — and here to loading rate — than it is for moist fingers may contribute to explaining the previously

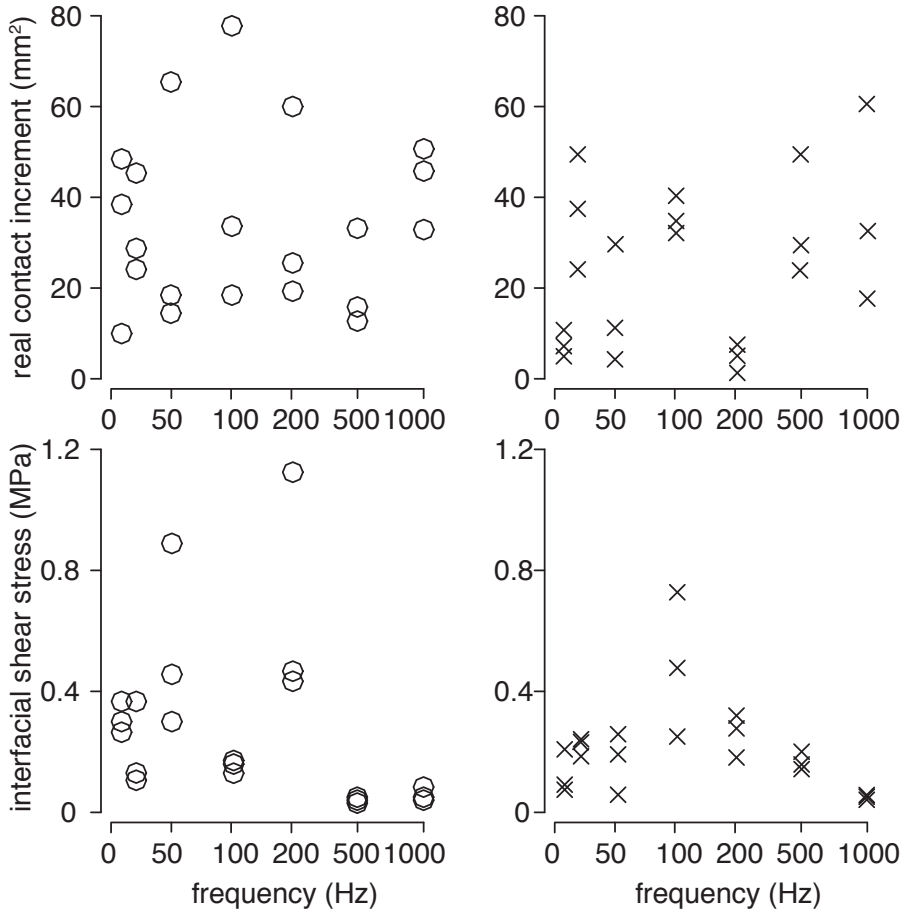

Figure 2.19 – Real contact growth over 2 s and interfacial shear stress as a function of tangential loading frequency (∘ dry, × moist).

observed phenomenon that the dryness of fingers may not necessarily impact significantly the coefficient of friction but rather the propensity of a finger contact to fail rapidly under load [7].

2.6.3 Images obtained with direct Frustrated TIR

Images taken under direct Frustrated TIR were acquired in conditions similar to that of the previous section but for lower frequencies and longer durations owing to the limitations of this approach in obtaining contrasted images. Unlike those of Fig. 2.18, the frames shown in Fig. 2.20 were heavily processed to compensate for the lack of illumination dynamics by normalising them to the darkest and brightest pixels. This means that the images obtained at the onset of a contact have very few brightness levels.

The comparison of the images in Fig. 2.18 and in Fig. 2.20 strongly corroborates the assumption adopted in [268] that the brightness level strongly correlates with friction, which is turn is correlated with the real contact area. In effect its real contact is likely to increase the portion of light being scattered while the other contributors to brighness, diffusion and reflection, would remain by and large unchanged. On the other hand, the notion that brightness correlates with the mean contact pressure is not well supported by the present results since correlating brightness, and hence real contact, with gross pressure would depend on an analysis of the contact mechanics at the ridge length-scale and more importantly at the

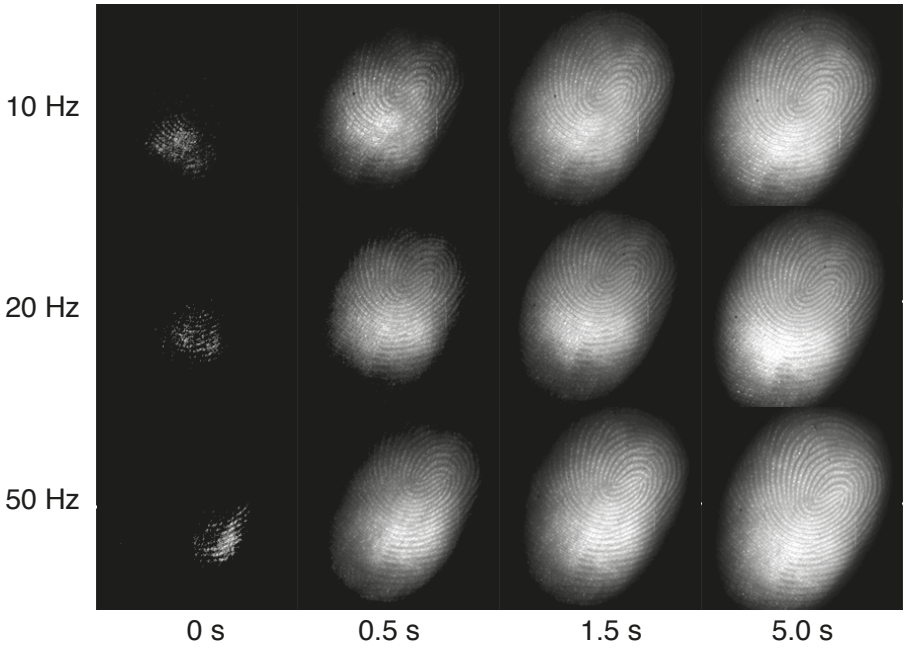

Figure 2.20 – Images acquired using direct Frustrated TIR.

asperity length-scale [61].

2.7 Conclusion

We described an apparatus capable of recording the dynamics of finger interaction with natural textures and to excite fingers with the same dynamics but with the added benefit of imaging with high spatial and temporal resolutions the evolution of both the gross behaviour of the finger through direct Frustrated TIR as well as the microscopic details of the real contact area. This will allow us to gain information of how a fingerpad deforms under load while sliding on otherwise non-transparent materials.

The apparatus enables a wide range of studies related to physical underpinning of tactile material discrimination and identification in perceptual tasks. It could also lead to a better understanding of the grip regulation mechanisms on arbitrary surfaces.

Standardised loading patterns such as sharp transients or step loadings can also be examined in order to visualise the transient phenomena that most certainly take place during natural discriminative or prehensile behaviours. The role of the fingerprint in tactile perception may also potentially be clarified since our newly introduced technique will allow us to investigate the behaviour of ridges at frequencies that are relevant to natural conditions. Future work may also involve evaluating the effects of dynamic loading on fingertip ridge deformation.

Acknowledgment

This work was supported by the FP7 Marie Curie Initial Training Network PROTOTOUCH, (No. 317100) and the European Research Council (FP7) ERC Advanced Grant (PATCH) to V.H. (No. 247300). The authors would like to thank Bernard Javot and Rafał Pijewski for their excellent engineering advice, Ramakanth Singal for building the motor's current

amplifier, Stephen Sinclair for help with the signal acquisition software, and Simon Johnson for invaluable advice regarding the imaging apparatus.

Contributions

The tribometer was designed by Michael Wiertlewski and adapted to measure finger/texture interaction using a plastic texture holder by Jonathan Platkiewick before I began my PhD. I adapted the tribometer's excellent design to three single-blocks, hence removing the noise generated by the screws and attachments. I designed the sample holder platform, the magnesium glass holder, the leaf springs and the magnet holders. The leaf springs I cut myself with the Charly Robot but the other parts were manufactures by professionals (the SAP for the sample holder platform and the tribometer single-blocks, and an in-house engineer Sylvain Pledel for the rest). I ordered the camera, zoom, filters, LEDs, prism, screws, magnets ect. that were needed to complete the set-up. The Prism-based Frustrated TIR apparatus was put together by Brygida Dzidek and myself. The motor's current amplifier was built by Ramakanth Signal.

Chapter 3

Amplitude-duration Interdependence in Complex Tactile Signals

Contents

This work was published in S. Bochereau, A. V. Terekhov and V. Hayward. Amplitude and Duration Interdependence in the Perceived Intensity of Complex Tactile Signals. In *Haptics: Neuroscience, Devices, Modeling, and Applications, Part-I*, Auvray, M. and Duriez, C. (Eds). pp. 93-100, 2014 *(Best Oral Paper Honorable Mention)*

Preface to Chapter 3

Exploring perceptual constancies in the tactile modality is worthwhile because it allows a better understanding of the perceptual effects of different physical characteristics of the stimuli. Moreover, it may have implications in creating shortcuts when generating virtual stimuli. Here, we investigated the presence of an amplitude-duration interdependence phenomenon in the intensity perception of a tactile stimulus.

Abstract

The dependency of the perceived intensity of a short stimulus on its duration is well established in vision and audition. No such phenomenon in terms of the amplitude has been reported for the tactile modality. In this study, naive observers were presented with pink noise vibrations enveloped in a Gabor wavelet. Characteristic durations ranging between 0.1 and 0.7 s and intensities ranging from 0.3 and 3.0 10^{-3} m/s^2 were presented to the fingertip. Using a two alternative forced choice staircase procedure, the points of subjective equivalence were estimated for the 0.4 s long reference stimulus. Similarly to vision and audition, lower intensities were consistently reported for shorter stimuli. The observed relationship could be interpreted as reflecting a mechanism of haptic constancy with respect to exploration speed.

3.1 Introduction

For many sensory modalities, the perceived intensity of a stimulus tends to depend on the time of exposure to the stimulus. In audition, the perceived intensity, termed loudness, grows approximately as a power function of the duration of a stimulus if it is shorter than 0.15 s [134, 234]. Similarly, the sensation of pain evoked by electrical stimulation of teeth is more intense if the stimulation is presented for a longer time [222]. In vision, a positive and approximate power law relationship is also seen between the perceived brightness of a light source and the exposure time [13, 64]. This law holds for different aspects of our visual perception [125] suggesting that it reflects the overall response dynamics of the photoreceptors responsible for vision. These findings question whether the approximately proportional relationship between the duration of the stimuli and its perceived intensity could represent a general law of perception, a property that was dear to the Gestalt psychologists, like the laws of motion perception or the laws of perceptual grouping. Here we investigate whether such a relationship can be expected in the entire tactile modality, by starting with amplitude estimation of simple broadband signals.

A few studies investigate tactile intensity perception, but the literature is dominated by studies regarding detection thresholds [76] and, on the other hand of the scale, by the effect of strong, unpleasant and potentially noxious vibrations, e.g. [78]. The relationship between frequency and perceived intensity was investigated by Verrillo [256] who showed that it obeys a power law function. However, to the best of our knowledge, there has been no work on the relationship between duration and perceived intensity of a tactile stimulus. Since human tactile discrimination is more sensitive to duration than to frequency [73, 81, 158], thedependency of perceived intensity of a tactile stimulus on its duration has the potential to be stronger than that found by Verrillo on its frequency.

Because the somatosensory system has longer integration time constants than the auditory system, transients presented to the skin must last 5 to 10 times longer than those presented to the ear to obtain comparable effects [14]. In the same study, von Békésy reports that the growth of sensation intensity on the finger tip is much like the growth of loudness in hearing. Therefore, a power law relationship should also hold for the tactile modality. We expect, however, the relation between duration and perceived intensity to be less steep than for audition since the auditory system is considerably more sensitive than the somatosensory system at amplitude discrimination.

We report here the results of a study on equal perceived intensity tests using a two alternative, forced choice staircase procedure. Ten observers were asked to compare the intensity of two consequently presented pink noise Gabor wavelets, varied in amplitude and duration. Pink noise was used to keep consistent with studies in other sensory modalities [2, 172]. It reduced the discomfort experienced with 'monochromatic' stimuli [205], since natural tactile stimuli are broadband and tend to conserve the same signal energy per frequency band [273]. Additionally, pink noise has no strict spectral localisation and thus can be assumed to be stimulating all the somatosensory sub-modalities.

3.2 Methods

3.2.1 Apparatus.

The setup comprised of a generic laptop computer with an audio channel linked to an audio amplifier which drove a motor (Haptuator, Tactile Labs, Saint-Bruno, Quebec, Canada). The motor was bonded to an aluminium plate (10 x 10 x 3 mm), under which four hard rubber

cylinders were placed perpendicularly to the vibrotactile transducer to allow free vibration-induced movements (see Fig. 3.1a), impeded only by rolling friction. The lightness of the plate and the strength of the motor allowed for a vivid sensation of vibration when the finger was placed on the plate.

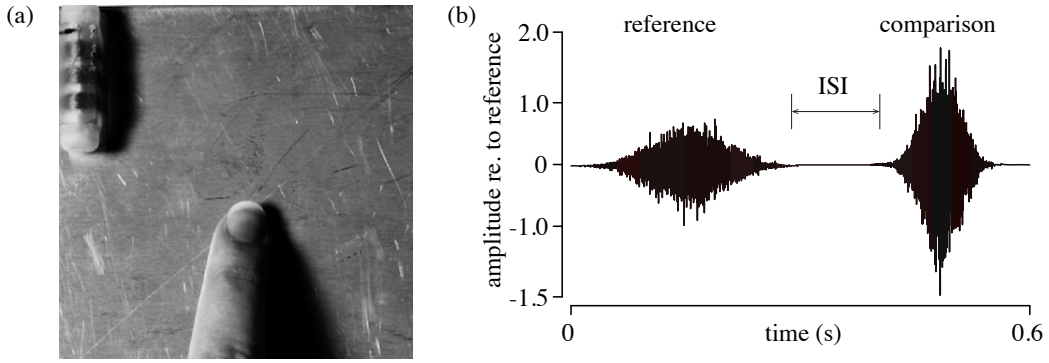

Figure 3.1 – (a) Apparatus. The right index was placed on an aluminium plate supported by four rubber cylinders, controlled by a vibrotactile transducer. (b) Example of the signal in one test: two consecutive pink noise Gabor enveloppes, with ISI the inter-stimulus interval. The amplitude is normalised in relation to the reference $A = 1.5\ 10^{-3}$ m/s^2.

3.2.2 Stimuli.

Pink noise signal was generated in Matlab (R2011a, Mathworks) at a 44100 Hz sampling frequency. It was generated by applying an inverse Fourier transformation to amplitude coefficients proportional to the frequency and to random phase coefficients. In order to fit the bandwidth of the amplifier to that of the motor, the signal was subsequently filtered using a high-pass 4^{th} order Butterworth filter with a 70 Hz cut-off frequency. The filter served to compensate for the natural frequency of the transducer, flattening the response in the low frequencies. The stimulus,

$$\psi_{\delta t}(t) = A \exp\left(\frac{-\pi\,(t-t_0)^2}{2\delta t^2}\right) I(t)\ , \tag{3.1}$$

was the product of a Gabor envelope of characteristic time, δt, with a pink noise signal, $I(t)$, of amplitude, A. The system was calibrated using an accelerometer bonded onto the plate and oriented in the direction of the vibrotactile motion. Test were made in the presence of the finger for several stimuli with different durations and amplitudes.

3.2.3 Observers.

Ten right-handed volunteers (two female and eight male), 22 to 36 years old, with no history of neurological disorders or manual sensorimotor function disorders, participated in the study. The observers were naive to the aims of the study. They all gave their informed consent for

the experimental procedure, which was approved by the 'Comité de protection des personnes en Ile-de-France II'.

3.2.4 Protocol.

The observers sat in a chair, wore passive noise-cancelling headphones and a blindfold. They put their hands on the table, with the right elbow resting on the table top, and gently placed the right index finger on the plate. The left hand was on the computer keyboard.

They were presented with a sequence of two stimuli, one of them being the reference and the other one being a comparison. The order of the stimuli was random. The inter-stimulus pause was also random; it ranged between 0.3 and 0.8 s. They were asked to report 'which of the two consequent stimuli felt overall stronger' by pressing one of two keyboard keys denoting the first and the second stimulus respectively. The reference signal had an amplitude $A = 1.5\ 10^{-3}$ m/s^2 and a duration $\delta t = 400$ ms. The comparison stimuli had amplitudes ranging between 0.3 and 3.0 10^{-3} m/s^2 and δt could be 0.1, 0.2, 0.3, 0.5, 0.6 or 0.7 s. Examples of these stimuli are presented in Fig. 1b.

The experiment was organised into six sub-sessions corresponding to different durations δt of the comparison stimulus. The order of the sub-sessions was balanced among observers. Within each sub-session the amplitude of the comparison stimulus was selected using two interleaving staircases, one starting at 2.0 of the reference amplitude and the other starting at 0.2 of the reference amplitude. The order in which the two staircases were presented was always random. The staircase step size was fixed at 0.2. Each trial started with the stimulus presentation and ended with the observer pressing the key reporting the subjectively stronger stimulus. The duration of each trial never exceeded 5 seconds; the overall experiment took about 20 minutes.

3.2.5 Data analysis.

The responses of each observer for two staircases were pooled together and a single psychometric curve was determined by fitting it with the cumulative normal distribution function. The point of subjective equivalence, μ, between the reference and comparison stimuli is the amplitude at which the psychometric curve crosses a probability of 0.5. Psychometric curves were discarded if the left boundary values exceeded 0.1 or if the right boundary values were smaller than 0.9. The μ values determined from the retained curves were then used for further analysis. The regression coefficient between stimulus duration and perceived equivalence amplitude was computed. It was justified using non-parametric Durbin test ('durbin.test' function, 'agricolae' package, R statistical software) with observers as judges and the duration δt as treatment. In order to have a balanced experimental design, the data of the observers who had at least one discarded psychometric curve were excluded from the statistical analysis.

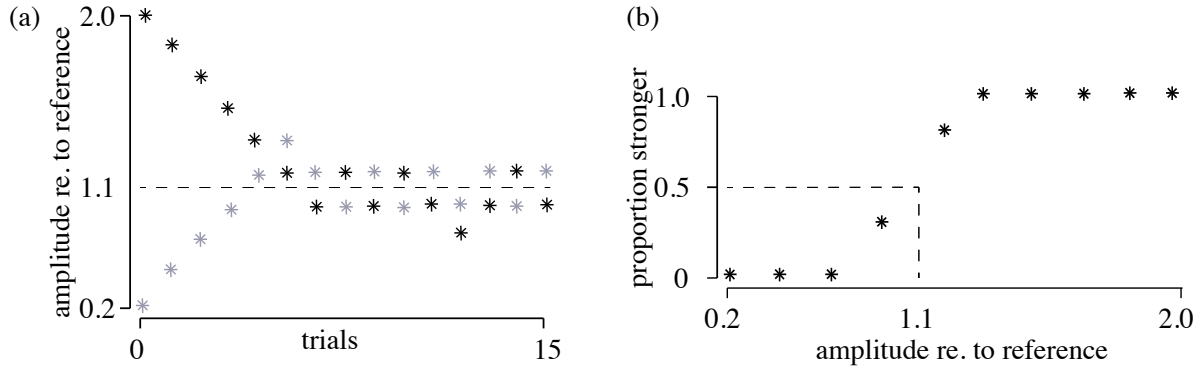

Figure 3.2 – (a) Staircase for one participant at δt = 0.5 s. The test converges to the amplitude at which the two signals feel identical, called the point of subjective equivalence. Here, $\mu \approx 1.1$. (b) Psychometric curve fitted to the points for the same test. μ is found at proportion stronger = 0.5.

Table 3.1 – Amplitude of subjective equivalence for all participants.

δt [s]	0.7	0.6	0.5	0.3	0.2	0.1
P1	0.67	0.95	0.80	1.11	1.27	0.99
P2	0.86	1.17	1.01	1.27	1.13	1.19
P3	1.10	0.90	0.92	0.87	0.79	1.75
P4	1.22	0.99	0.84	1.17	1.09	1.58
P5	0.63	0.77	0.86	1.00	1.28	1.50
P6	0.80	0.76	0.99	1.13	1.44	1.24
P7	0.78	0.88	0.91	0.97	0.99	2.17
P8	0.82	1.07	0.88	1.08	0.98	1.07
P9	0.83	0.92	1.07	1.08	1.15	1.56
P10	0.77	0.86	0.95	1.11	1.19	1.75

The highlighted μ values correspond to those discarded from the analysis.

3.3 Results

For each observer two staircases, one rising and the other descending, usually converged to value of the bias, justifying the pooling of their data (see example in Fig. 3.2a). The observers' responses could usually be fitted rather well with a psychometric curve (see example in Fig. 3.2b and all subjective equivalence values in Table 3.1). In some cases, however, the slope of the curve was too shallow, suggesting a low quality estimate of the point of subjective equivalence. Overall, five psychometric curves in four observers, which corresponds to less than 10%, have been discarded on this basis. The discarded curves mostly corresponded to the shortest stimulus duration (0.1 s; three curves). The staircases for higher δt values usually had points of subjective equivalence closer to zero (see Fig. 3.3), suggesting an inverse relationship between the stimulus exposure time and its perceived intensity. This trend, visible from the average data in Fig. 3.4, was also confirmed by the Durbin test: the effect of the duration on perceived intensity is highly significant ($p < .001$).

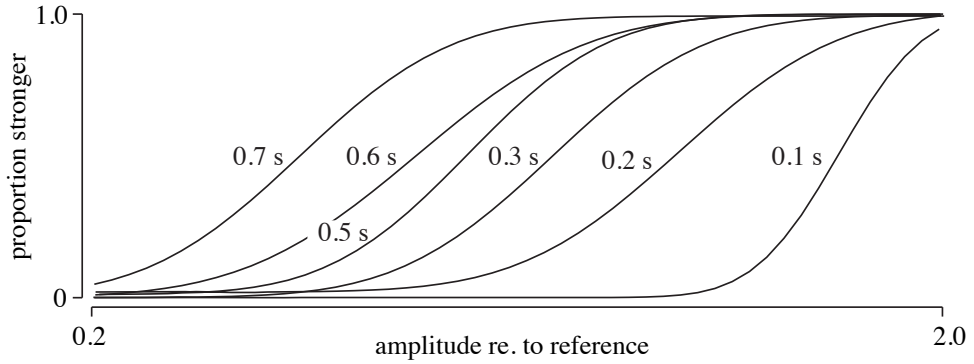

Figure 3.3 – General trend of the psychometric curves with stimulus time.

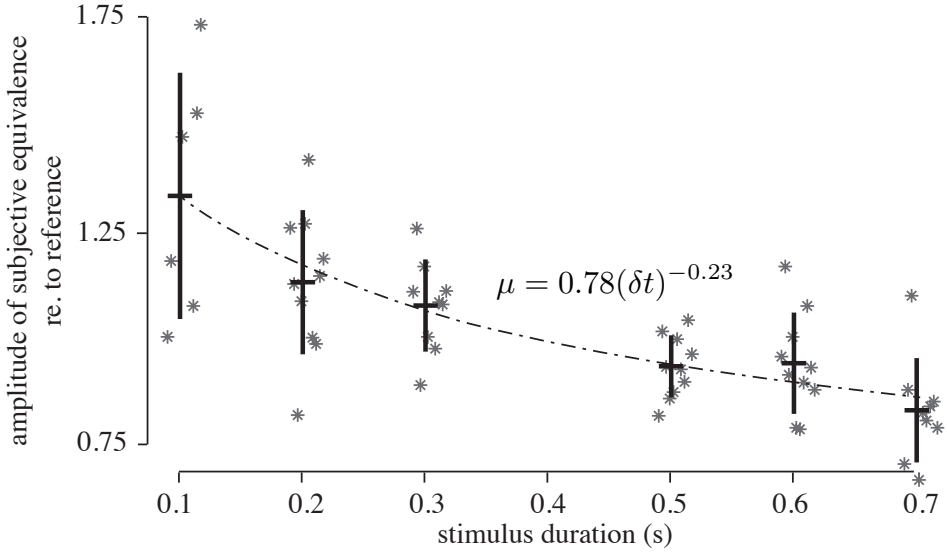

Figure 3.4 – The amplitude of subjective equivalence as a function of the stimulus exposure time δt, showing a negative power law relationship with a regression coefficient of -0.23.

3.4 Discussion

The current study explored the relationship between the duration of a tactile stimulus and its perceived intensity. Our results show that in the case of a Gabor vibratory skin stimulation, the perceived intensity is negatively correlated with the temporal dimension of the envelope.

This temporal dependency could be related to the biotribology of the skin. Indeed, the characteristic time of the skin deformation could prevent the vibrations from propagating within the given time. We could for example think that at short times, it is the lack of skin response, not the stimulus duration perception, that creates the necessity for an increase in amplitude. However, the characteristic time of the bulk fingerpad skin is just of the order of a few milliseconds [194, 259, 269] and thus would unlikely cause any noticeable difference in

perception.

One could surmise the existence of a mechanism to ensure the constancy of tactile perception when a finger swipes over an asperity. One perceives an asperity by and large in the same way independently of the velocity at which one explores it. This could be explained by an adjustement mechanism in the brain. When one swipes an asperity more rapidly, the skin oscillations are stronger and hence yield a more intense sensory stimulus. However, the intensity of the received sensations are felt less strongly to match the expected spatial dimension of the asperity, and hence the temporal window of the vibrations it creates. With such a mechanism, a temporally longer stimulus would need to have a lower amplitude than a temporally shorter simulus for the same spatial asperity to be felt with the same coarseness.

The pink noise stimulus used here can be seen as the input of a finger sliding over an uneven surface. In this case, the duration of the stimulus corresponds to the spatial extent of the asperity or to the velocity of the finger motion. The inverse relationship between the intensity of the perceived stimulus and its temporal duration, may thus correspond to the same constancy. This suggests that, unlike the auditory system, the tactile system might not be tuned to the discrimination of duration.

Since the majority of the skin receptors are sensitive to both the skin deformation and its temporal derivative, it can be assumed that the same asperity explored at a different speed creates the same deformation, but at different velocity. Thus, for the same surface asperity, instantaneous output of the skin receptors will be stronger if the exploration speed is higher.

Pink noise being a broadband signal, all the submodalities of mechanoreceptors (slowly and rapidly adapting) are likely to be excited. For the tactile modality, it takes time for the sensation magnitude to develop to its full power, about one second according to von Békésy [14]. In our study, the signals (0.1 to 0.7 s) and the inter-stimulus pause (0.4 s) do not allow the stimulus to fully develop into a conscious percept. However, we did not observe a steepening of the regression at smaller stimulus times, where we would have expected an overcompensation. This could suggest that the rapidly adapting afferents are predominantly recruted instead of the slowly adapting ones. It could also imply that the slowly adapting afferents are also recruted but that the coding of the incoming stimulus is much faster than previously reported and that it is the decay of the signal which takes time.

These observed particularities of the tactile modality offer explanations for why the perceived intensity is negatively correlated with the temporal dimension of the stimulus. However, while these explanations are all specific to the tactile modality, this relationship was also observed in audition [134, 234], vision [13, 64] and pain [222] perception. The result herein therefore strongly suggest that this negative correlation between amplitude and duration might be viewed as a non modal-specific law of perception.

3.5 Acknowledgments.

This study was funded by the FP7 Marie Curie Initial Training Network PROTOTOUCH, grant agreement No. 317100. It was also sup- ported by the European Research Council (FP7) ERC Advanced Grant (patch) to V.H. (No. 247300). The authors would like to thank

Stephen Sinclair for helpful discussions, as well as Amir Berrezag and Ramakanth Singal for excellent technical assistance.

Chapter 4

Physical invariants in the Mechanical Response of a Tactually Scanned Braille Dot

Contents

This work was published in S. Bochereau, S. Sinclair, and V. Hayward. Looking for Physical Invariants in the Mechanical Response of a Tactually Scanned Braille Dot. In *Proceedings of IEEE World Haptics Conference 2015*, Chicago, IL, pp. 119-12, 2015.

Preface to Chapter 4

The recording task was aimed at characterising the interdependence found in Chapter 3 in terms of the mechanical response of a real situation: a finger sliding over an asperity with different velocities. The intent was to find a constant physical quantity, commonly referred to as an "invariant", that could explain the reason for the wavelets of different combinations of amplitude and duration to be judged equal in intensity.

Abstract

One human finger explored plastic Braille dots using a variety of velocity and force profiles. The fingertip friction forces were measured. Characteristics of the interaction were studied to explore the manifestation of the amplitude/duration interdependence of signals across velocity, normal force and dot height. Both amplitude, defined here as maximum tangential force, and duration, were seen to vary with velocity and normal force, however the integral of the tangential force over time was found not to have a strong dependence on either variable. When three consecutive dots of varying height were examined, the tangential force integral was not constant, but increased in proportion to height. We propose that the nervous system may use the tangential force integral as an invariant to recognise the same spatial asperity explored under different velocity and force conditions.

4.1 Introduction

A tactual texture is never explored in exactly the same mechanical conditions. In addition, the frictional interactions of a fingertip with surfaces frequently exhibit chaotic characteristics. This complexity can clearly be attributed to multi-scale, nonlinear physics that are at play during sliding [273]. Physiological and environmental factors such as fingertip hydration, applied pressure, contaminants, and exploration velocity are also constantly fluctuating during sliding and influence the frictional mechanics [4]. The fingertip itself is a bi-phasic, multi-material, multilayer composite structure which has different dynamic behaviors at the different length and time scales involved in frictional interactions.

Yet, the perceptual quantity of a texture is experienced similarly despite exploring it in a variety of ways [127, 141, 142, 282]. This independence to sensing conditions could appeal to a mechanism in the brain able to extract certain physical invariants. Since textures may be considered as a collection of asperities, the study of a single asperity, such as a Braille dot, may help clarify what these invariants might be.

The objective of the current study is to explore the physics underpinning the tactile perceptual invariant responsible for the constancy observed when a finger swipes over an asperity. Several groups studied skin deformation over small asperities [150, 230] but only quasi-statically. Among the considerable number of perceptual studies employing surfaces made of isolated asperities, Lamb found that subjects could correctly distinguish 75% of surfaces in which the period of the dots differed by only 2 percent [136]. Performance was virtually independent of the method of movement used, despite large differences in the velocity profiles. Conversely, Dépeault et al. found that average dot spacing affected the perception of sliding speed [52]. These results support the notion that whether swiping over an asperity quickly or slowly, asperities are perceived similarly. We propose that this constancy takes its roots in a physical effect where the same asperity scanned at different speeds preserves the time integral of the friction force over the traversal of the asperity.

It was previously shown that in the tactile modality the perceived intensity of a stimulus tends to depend on the time of exposure to the stimulus [14], [76]. This was also shown in the case of a Gabor-windowed pink noise vibratory skin stimulus [27], which could model the sensory experience of a finger sliding over an asperity. Since the duration of a stimulus is determined by the scanning velocity, we hypothesized that a larger instantaneous mechanical effect for a faster scanning velocity of the same asperity could be equivalent to a slower velocity with a smaller mechanical effect. A purely elastic finger would preclude the occurrence of this dependency. We investigated this possibility by studying the friction mechanics of a finger exploring a Braille dot of different heights at different velocities and normal forces. The prediction power of these three variables (normal force, velocity and dot height) on the tangential force time integral of several braille dots was examined.

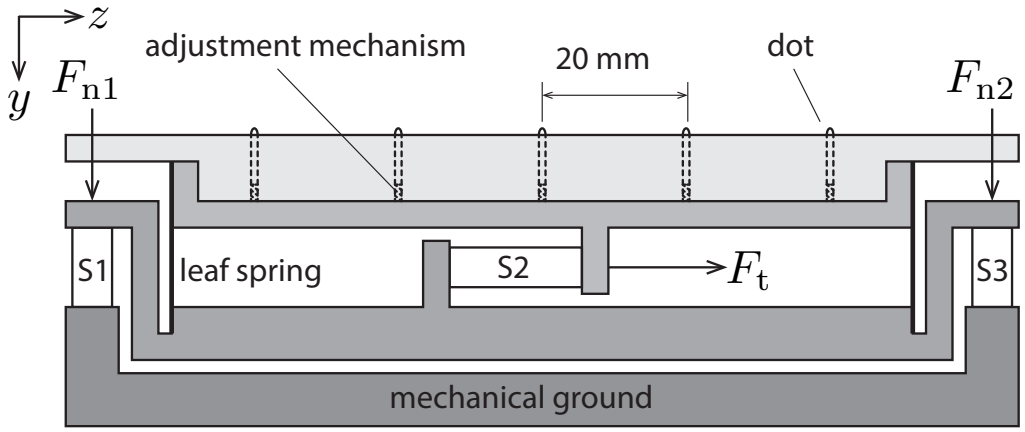

Figure 4.1 – The apparatus. The transducer measures the interaction forces of the finger exploring the Braille dot platform with dots of adjustable heights.

4.2 Methods

4.2.1 The Experimental Set-up

The set-up comprised a friction force transducer as seen in Fig. 4.1, able to measure the normal force $F_n = F_{n1} + F_{n2}$ (Kistler 9313AA1) and tangential force F_t (Kistler 9217A) independently, described elsewhere [267]. A Braille dot exploration plate was tightly fixed to the set-up. Displacement $x_1 = (yF_{n2} + zF_t)/F_n$ was computed using the force sensors to determine the displacement of the centre of pressure, which we considered to represent the position of the finger, see Fig. 4.3.

4.2.2 Task

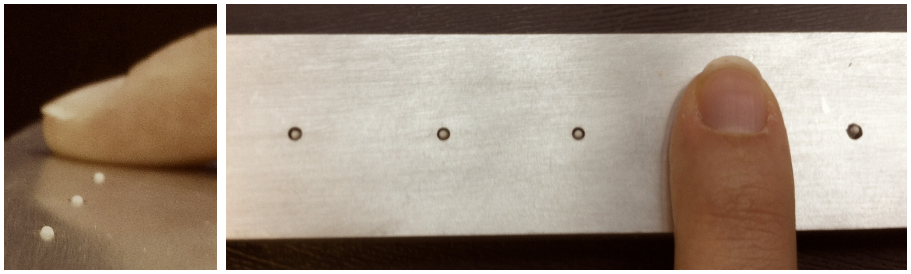

Figure 4.2 – The Braille dot platform consisting of five consecutive dots mounted on an aluminium plate. The finger had no inclination to the platform.

The aluminum plate (1.6×3×20 cm) held equally-spaced plastic Braille dots contributed by Metec Ingenieur AG, see Fig. 4.2. Before the dots were secured, the aluminum surface was polished using fine sanding paper ensuring a smooth background. An adjustment mechanism

allowed control of the Braille dot height around 0.48 mm, as recommended by the Braille Authority [1]. The space between the Braille dots was set at 2 cm to ensure that the finger was exploring one dot at a time. The platform allowed us to make measurements for dots of different heights with similar exploratory conditions.

The participant (female, 22 years old) slid her finger (with no inclination) over the platform at different speeds (79 to 555 mm/s) and normal forces (0.4 to 1 N), see Table 4.1. The participant was instructed to try different speeds but in practice trials tended to be grouped into slow and fast. She presented no history of skin pathology or motor disorders. Only one finger was used in the study owing to very large individual differences in finger mechanics. Futhermore, since such physical invariants are fundamental consequences of the mechanics of touch, the existence of such a quantity for a single participant featuring otherwise uniform properties such as skin condition may suggest that this quantity could have an important role in tactile perception. The finger used in the study had an approximate normalized hydration of 0.6. Generalization to populations of individuals is left for future studies.

Dot 3	Min.	Median	Max.
Velocity (mm/s)	80	151	529
Normal force (N)	0.4	0.57	0.98
Dot 4	Min.	Median	Max.
Velocity (mm/s)	80	166	542
Normal force (N)	0.43	0.6	0.97
Dot 5	Min.	Median	Max.
Velocity (mm/s)	79	180	555
Normal force (N)	0.4	0.59	1

Table 4.1 – The range of normal force and velocities of exploration for dots 3, 4 and 5 (40 samples per dot).

4.2.3 Data Analysis

The tangential force F_{t} was analysed for each dot. To determine the velocity of exploration for each Braille dot, the position data was fitted to a 2^{nd}-order polynomial with appropriate boundary values and differentiated to give a linear fit estimate. The velocity was then sampled at the center of each dot for analysis.

The data was filtered using a 5–50 Hz band-pass 1^{st}-order Butterworth filter applied bidirectionally, thus preserving the shape and phase of the signal while removing the offset and fast oscillations.[1] The five Braille dots were segmented in each recording by zero-crossing analysis. To avoid any effect of the initial skin compression, only the last three dots were analyzed. They also showed a greater range of normal force and velocity. The three dots had increasing physical heights: 0.42, 0.48 and 0.61 mm respectively.

For each Braille dot recording (40 swipes in total = 120 dots), features were extracted as shown in Fig. 4.3. We analyzed both the duration and the amplitude of the swipe, where the amplitude is defined as the maximal tangential force, $\max_{t_1 \ldots t_2} F_t$, over the time interval of the dot. Since the finger is almost purely dissipative, the force samples collected over the course

[1] Hereafter F_t shall refer to the filtered tangential force.

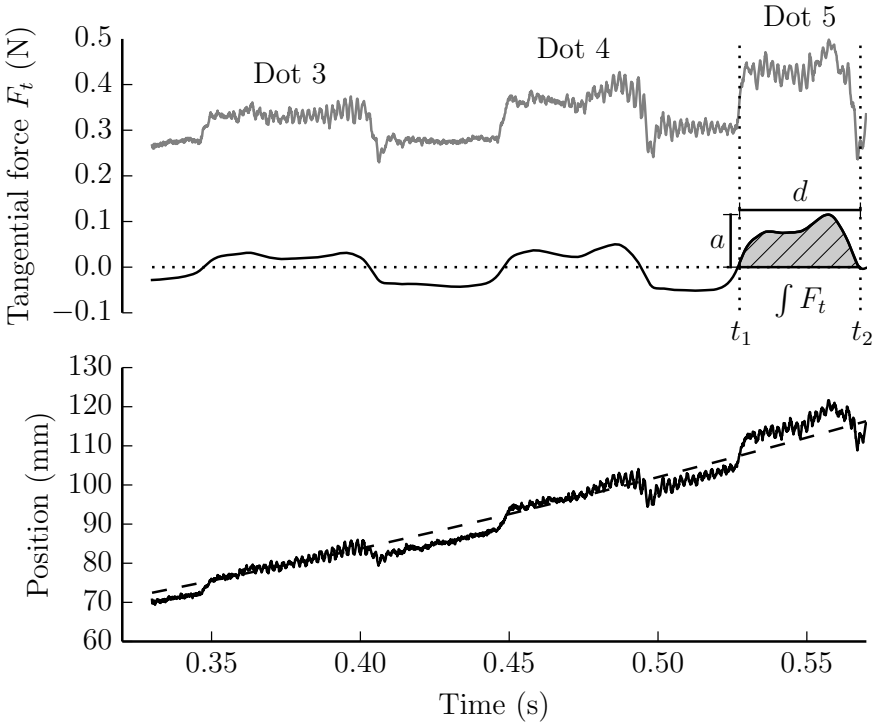

Figure 4.3 – Recording of a finger exploring three consecutive Braille dots. The raw recording of the tangential force is shown above as well as its filtering with a 5-50Hz bandpass. On the filtered recording, the duration d and amplitude a, defined as $\max_{t_1 \dots t_2} F_t$, of the interaction to measure the friction force integral are shown. The position of the finger was computed using the force sensors, as $x_1 = (yF_{\mathrm{n2}} + zF_{\mathrm{t}})/F_{\mathrm{n}}$.

of the contact with a dot is related to the work exchanged with the finger as follows: the work exchanged between the finger and the scanned dot is $W_{\mathrm{e}} = \int_{t_1}^{t_2} \vec{F}(t) \cdot \mathrm{d}\vec{x}(t) = \int_{t_1}^{t_2} \vec{F}(t) \cdot \vec{v}(t)\mathrm{d}t$, where t_1 and t_2 are the times at which the finger meets the dot and leaves it, respectively, $\vec{F}$ is the force of interaction and $\vec{v}$ the average velocity of the particles in contact with the dot, which we approximate by the velocity of the point of action of the measured force on the plate. Because the force of interaction did no work in the direction perpendicular to the plate, $\vec{v}$ could be substituted by a constant, $\bar{v}$, during the traversal of a dot. Hence, the work exchanged by the finger was approximatively proportional to $\bar{v} \int_{t_1}^{t_2} F_t$ since the forces were sampled at regular time intervals. As a result, the summed measurements $\int_{t_1}^{t_2} F_t$ represent the work exchanged by the finger normalized by scanning velocity up to a constant. Thereafter, this value is described as tangential force integral.

Tangential force integral	The area of the tangential force signal, $\int F_t$, for the duration of the time interval of the dot exploration, as defined by *duration*, below. Estimated as $h \sum_{i=k_1}^{k_2} F_t[i]$, where $k_i = \lfloor t_i/h \rfloor$, h is the sampling period (10 kHz), and $F_t[i]$ is a discrete-time sampling of F_t.
Amplitude	The maximum tangential force over the time interval of the dot exploration, defined as $\max_{t_1 \ldots t_2} F_t$.
Duration	The time of the swipe over the braille dot, measured as $t_2 - t_1$, where t_i are identified as the zero-crossing times of F_t surrounding the peak of each finger–dot collision.
Height	The distance from the platform to the top of the Braille dot, as measured using a high-quality height gauge providing sub-millimeter precision.

Table 4.2 – Features of the mechanical response to scanning a dot.

4.3 Results

In contrast to most studies, we investigated features of the data with the aim of identifying physical quantities that have *low* correlation with exploratory conditions. These values are known as physical invariants. We found that W_e was somewhat correlated with velocity ($r = 0.47$, see Fig. 4.7) while $\int_{t_2}^{t_1} F_t$ (equivalent to $W_\mathrm{e}/\bar{v}$) remained independent ($r = -0.13$), Fig. 4.4a). The influences of the three variables (velocity, normal force and height) were plotted for each feature (tangential force integral, amplitude and duration, as defined in Table 4.2). Dotted lines showed the recordings for dots within the same swipe, with the black line as the regression across dots. Pearson's correlation is given for each diagram with a p value indicating 95% confidence.

Both amplitude and duration were well predicted by velocity, despite the fact that velocity did not well-predict the tangential force integral, see Fig. 4.4. The increase in amplitude with velocity was in line with the hypothesis proposed in [27]; that amplitude and duration have a multiplicative relationship to perceived intensity. This is analogous to their product being approximately constant for the same asperity explored at different velocities. In other words, we expected the amplitude of the signal to increase with velocity v when exploring the same Braille dot of width w since the duration d of the measurement is shorter ($v = w/d$), which was confirmed in our analysis, see Fig. 4.4c.

For the normal force, the same relationship was seen, as shown in Fig. 4.5. The increase in amplitude with normal force could be logically explained by a stronger impact if the pressure is high. The increase in duration as the normal force increases resulted from the observation that during a faster swipe, the participant tended to press harder, see Fig. 4.8. These results showed that velocity and normal force don't predict the tangential force integral even though they influence the amplitude and the duration of the signals.

Examining the interaction of the finger with three dots of increasing physical height, we found that both the amplitude and the tangential force integral increased correspondingly, see Fig. 4.6. A dependent Student's t-test was used to determine whether distributions were significantly different. It was found that both friction force integral and amplitude scaled significantly with dot height, while the duration remained essentially constant: although a small significant difference was found for dots 4 and 5, the Pearson's correlation $r = 0.09$ was quite low for Fig. 4.6c. Indeed, the diameter of the dot studs was consistently 1.6 mm and

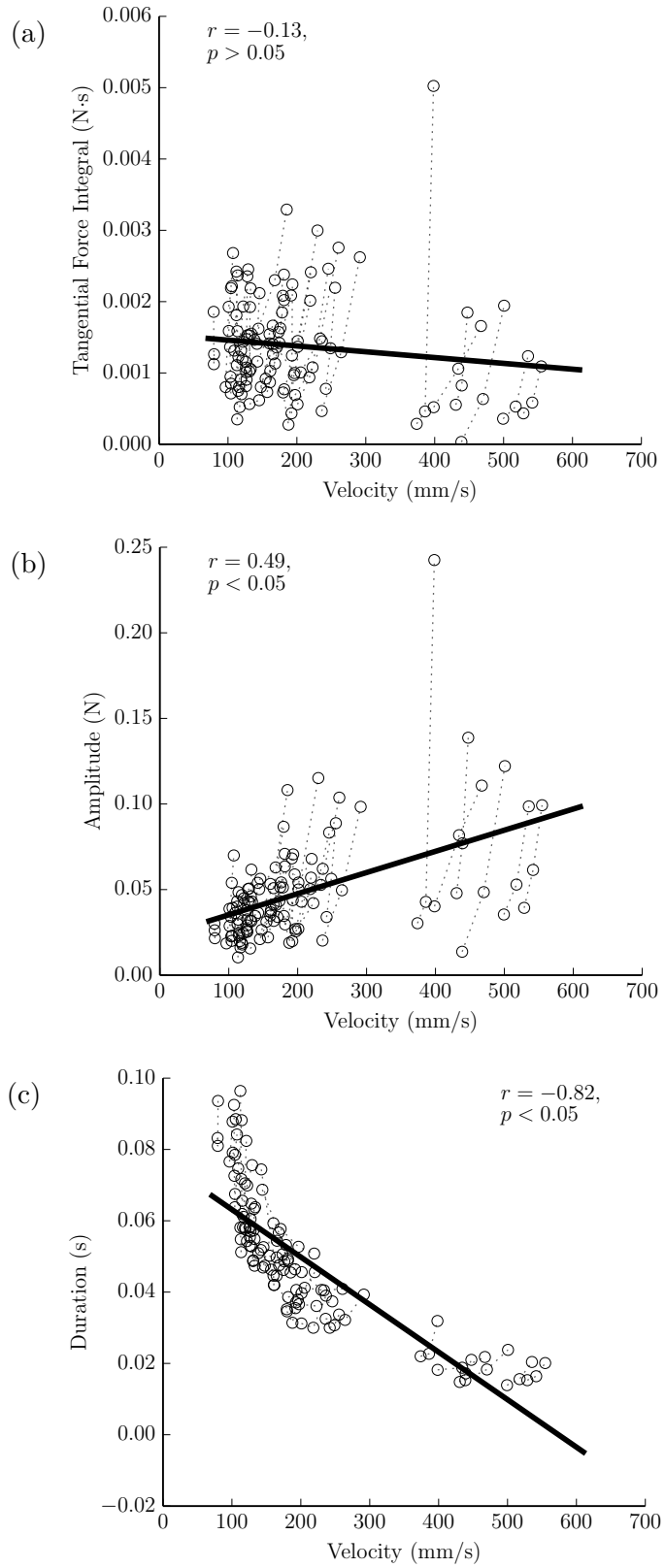

Figure 4.4 – Tangential force integral, amplitude and duration of the recording as a function of velocity for all three dots. The amplitude consistently increases with velocity, while the duration decreases. However, the friction force integral remains relatively constant, or invariant (low correlation).

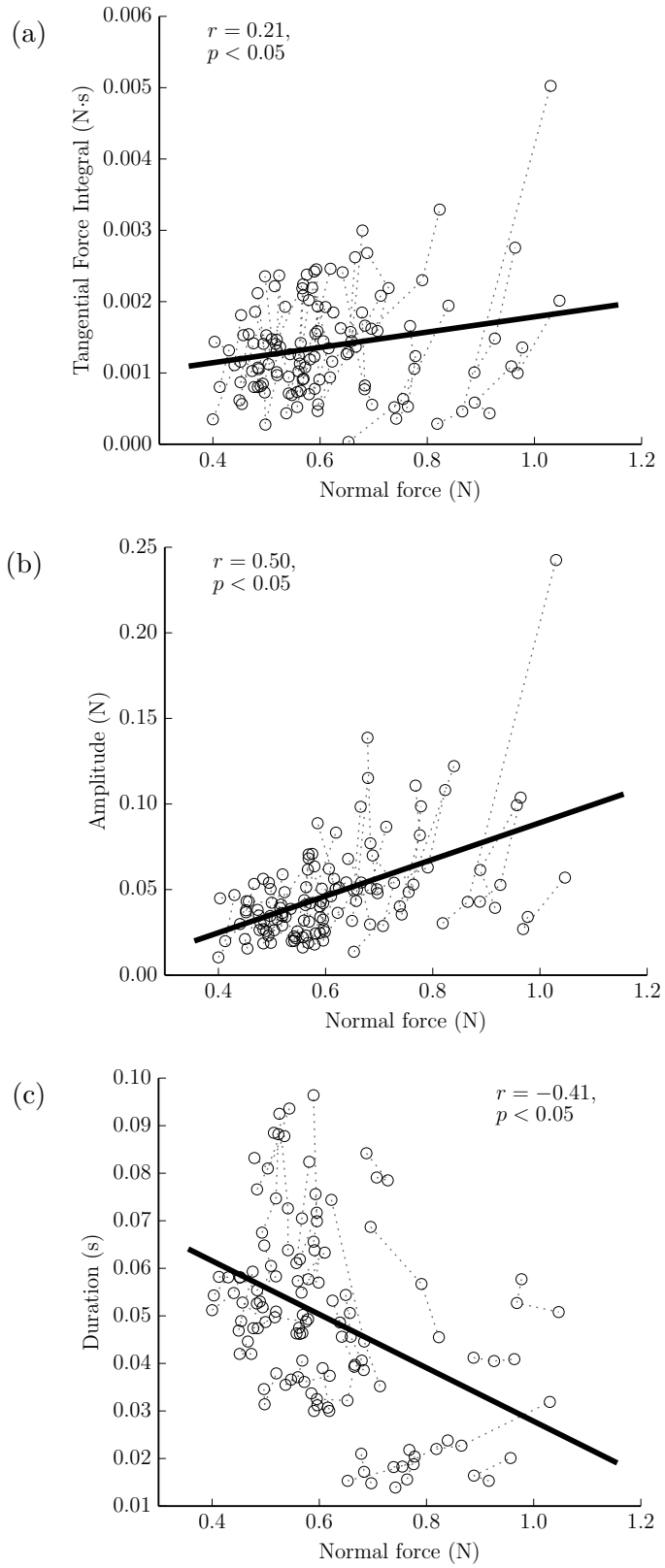

Figure 4.5 – Tangential force integral, amplitude and duration of the recording as a function of normal force for all three dots. The duration consistently decreases with normal force, while the amplitude increases. However, the friction force integral remains relatively constant, or invariant (low correlation).

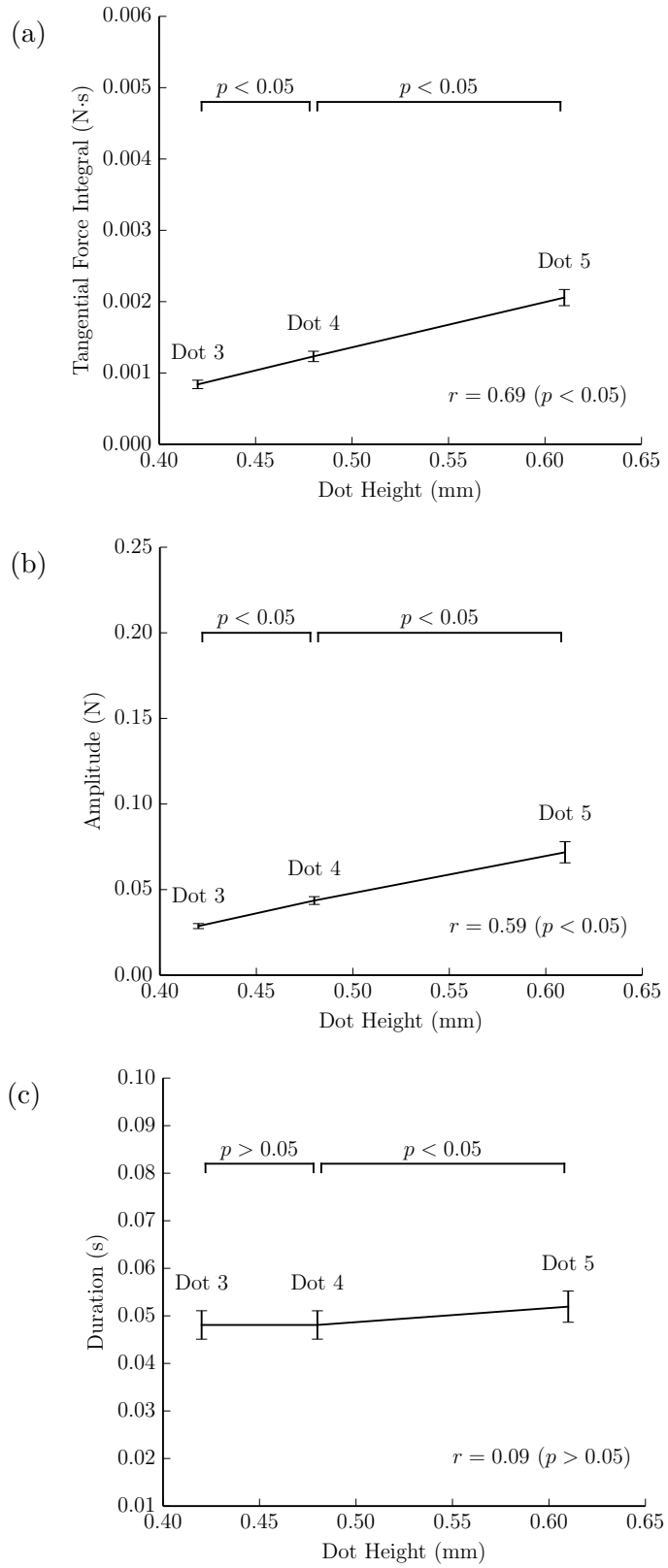

Figure 4.6 – Tangential force integral, amplitude and duration of the recordings as a function of dot height. Using 40 samples per dot, a dependent Student's t-test was computed to determine whether distributions were significantly different. It was found that both friction force integral and amplitude scaled with the physical height of the dot, while the duration remained essentially constant.

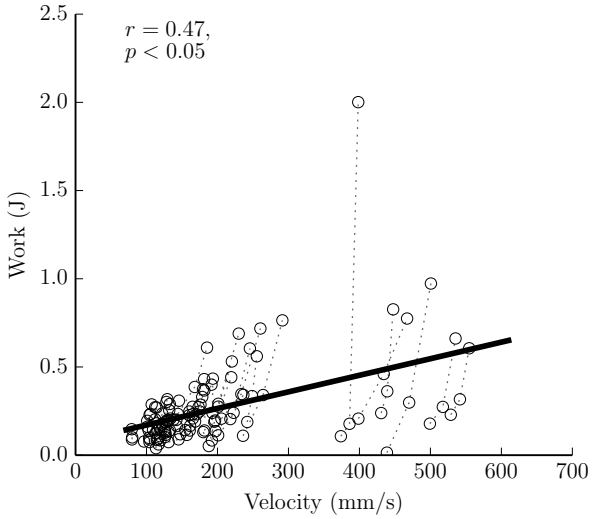

Figure 4.7 – Work exchanged between the finger and the Braille dot against velocity of exploration.

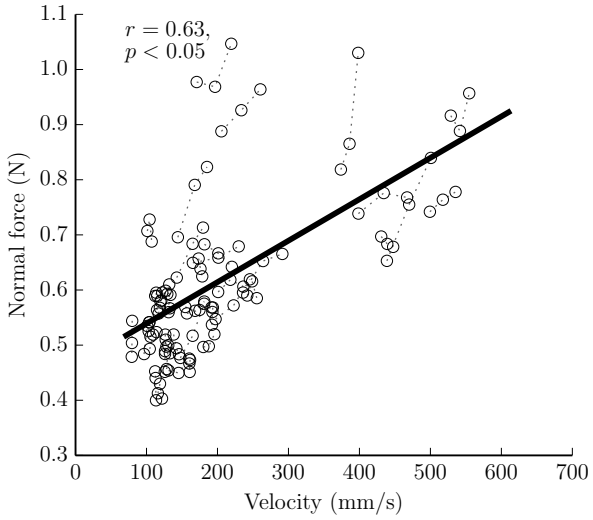

Figure 4.8 – The normal force increases with velocity during the exploration of different Braille dots.

the increase in height very minimally affected the trajectory of the finger.

4.4 Discussion

In this experiment the influence of velocity and normal force over the mechanical response of three dot heights was investigated. The aim was to find correspondences with a physical constant in the tactile modality, which we propose as a basis for perceptual constancy during asperity exploration.

Both amplitude and the tangential force integral scale with dot height, see Fig 4.6a,b. However, the observation that the amplitude is well correlated with the dot height (Fig 4.6b) is misleading because the amplitude is also seen to increase with velocity, see Fig 4.4b, and therefore can not be considered an invariant. In fact, the tangential force integral improved on the predictive power of the amplitude ($r = 0.69$ vs. 0.59)[2], and it was not confounded with exploration parameters. That the tangential force integral appeared to be the best predictor agrees well with our previous observation that both the amplitude and the duration of the interaction contribute to the perceived intensity [14, 76, 27], since it is the product of both parameters.

The third variable, the physical height of the dots, also allowed us to show that even when the movement is complex and many variables are at play, the tangential force integral systematically scaled with the dot height. This reinforces the low predictive power of the velocity and normal force on the tangential force integral and proposes this value as the invariant used by the somato-sensory system. It also shows that the major source of variance within a single dot is probably contaminants or sweat, since it is minimal compared to the variation caused by height increase. The heights of the dots in this experiment varied by 0.2 mm, however the change in the tangential force integral was very significant (regression coefficient of 0.69, Fig. 4.6a). This leads us to wonder whether such changes in the tangential force integral can be seen in discrimination tasks at the nanometer scale [226]. Conversely, it questions whether the inability to discriminate asperity height could be predicted by the tangential force integral. On the other hand, such a discrimination difficulty might be explained by the Weber fraction: the ability to perceive intensity likely worsens as features decrease in size. We plan to consider such possibilities in future research.

We can surmise that the reason why the physical constancy was represented by the tangential force integral is because it best reflects the overall strain delivered to the finger. During lateral motion, a single bump on the surface can yield a skin stretch larger than 30% [150]. Since the finger may be compared to an elastic membrane filled with an incompressible fluid [230], we can imagine that at each impact, the skin deforms toward the bone. The same overall deformation occured for each dot, however the details of the deformation at a given time are probably different when the velocity or the normal force change. If the overall deformation is the same, how can we explain our use of different exploration techniques [239] to discriminate different objects?

These observations further suggest that regardless of the scanning kinematic and tonic characteristics, the same dot is perceived, in line with what was observed perceptually [282, 105]. We have investigated the effect of two important exploration conditions, however there exist other parameters during a single swipe which influence the mechanics of the impact, which we have not accounted for in this work. For example, it is known that the occlusion mechanism (sweat accumulation between the ridges during sliding) affects the friction mechanics [192, 60]. We can infer that these variables will show a similarly poor relationship to

[2]Correlations were significantly different with $p < 0.05$ [233]

the tangential force integral. We found however that a lot of these variables are inter-related, see Fig. 4.8, meaning they will most likely already be included in the bulk strain measurement.

4.5 Conclusion

Both amplitude and duration were well predicted by velocity and normal force, despite the fact that the various experimental conditions did not correlate with the tangential force integral over a single asperity. However, when studying the tangential force integral for the exploration of three consecutive dots of different heights, the integral increased with dot height. These findings showed that the integral is a good predictor of asperity characteristics since it remained constant regardless of exploration conditions, but varied with dot height.

4.6 Future Work

The existence of a mechanical invariant quantity, the tangential force integral, which is robust to changes in velocity and pressing force when scanning Braille dots is the main contribution of the present article. We intend to expand the present study with a view to clarify whether this invariant is found in an intra-subject condition for several participants and whether it further correlates with psychophysical experiments on asperity discrimination

4.7 Acknowledgements

This study was funded by the FP7 Marie Curie Initial Training Network PROTOTOUCH, grant agreement No. 317100. It was further supported by the European Research Council (FP7) ERC Advanced Grant (patch) to V.H. (No. 247300). The authors would like to thank Camille Fradet for her help with the numerical analysis as well as Ramakanth Singal, Rafal Pijewski and Bernard Javot for their excellent technical advice.

Chapter 5

Mutability of Amplitude and Duration in Touch

Contents

This work is being prepared as a part of a submission by S. Bochereau, M. Amante, S. Sinclair, R. Watkins, A. Terekhov, J. Wessberg, and V. Hayward entitled "Mutability of Amplitude and Duration in Touch" to be submitted to the Journal of Neurophysiology. An important result that will be reported in this article is that for brief tactile stimuli frequently encountered in everyday life such as when a

finger comes into contact with a surface or when a fingertip slips over an asperity, which are events lasting a fraction of second, there are strong connections between three quantities, one in the cognitive domain, one in the mechanical domain, and the third in the neural domain. In these three domains, a signal wavelet representation of a brief event is adopted because it parsimoniously captures the key aspects of brief tactile events with just two parameters. In the cognitive domain, the quantity is the perceived intensity. In the mechanical domain, the quantity is the integral of the interaction force magnitude over the duration of the event which can equivalently be viewed as the mechanical work exchanged with the finger normalised by the finger velocity, or else, as the overall strain experienced by the finger. In the neural domain, the quantity is the total number of spikes. Using measurements of the afferent fibres activity in humans stimulated by such brief events, and adopting the paradigm of considering a pool of neurons as an ideal observer, we demonstrate that the total number of spikes sent to the brain is an excellent predictor of stimulus intensity while the firing rate fails predicting the character of the stimulus.

Preface to Chapter 5

Chapter 5 lays out the grounds for the strong connection between the tangential force integral in the mechanical domain and the perceived intensity in the cognitive domain in the case of short events in which amplitude and duration play an central role. It comprises first an overview of the previous two chapters and then proceeds with verifying the robustness of the tangential force integral as an invariant by investigating whether it trumps over the details of the mechanical deformation profile at different velocities. For that, a comparison task using the recordings from Chapter 4 was carried out to investigate the discrimination threshold of the height of Braille dot.

Abstract

In all sensory modalities, when trying to capture a scene in order to recreate it, it is of great interest to understand how to extract the relevant cues of an real interaction in order to generate virtual interactions most simply and effectively. Here, we've focussed on seeing whether we can find such a cue to inform on the height of an asperity in virtual interaction. We've investigated whether the tangential force integral could be an invariant responsible for asperities to be experienced the same way regardless of differences in the speed with which it is encountered by the skin. In the first experiment, wavelets of varying duration and amplitude were presented to participants in a staircase procedure. We found a negative power law relationship between amplitude and duration in terms of the perceived intensity. We then studied whether such a phenomenon held for ecological stimuli. Looking at measurements of one finger sliding on a braille platform at different speeds, the tangential force of a finger sliding over a braille dot at different speeds was found to remain constant while the amplitude and duration varies significantly and increased for a higher dot. These recordings were then used in a comparison task, in which participants explored virtual dots at different speeds and successfully identified which of the two interactions was the higher dot. The profile of the dot changed correspondingly with the exploration speed. We conclude that the integral of the tangential force characterises the overall mechanical response of a finger sliding over a dot independently of exploration speed and differs between the dots. It is an excellent candidate quantity for informing perceptual constancy and one of the major cues that needs to be rightly rendered if the height of the asperity is to be correctly sensed.

5.1 Introduction

5.1.1 Natural Scenes.

It has long been assumed that sensory neurons adapt to the signals to which they are exposed and therefore should be best at processing the signals that occur most frequently. This was shown in vision [224] and audition [151] where efficient coding mechanism in terms of frequency, time, spectral power, colour etc. used by our sensory organs can successfully explain the properties of their receptive fields. The knowledge of how the statistics of natural classes of stimuli are efficiently captured has allowed us to engineer simple devices that generate the information that will be effectively picked up by the receptors.

The reason for the existence of such cues comes from the active nature of sensory interactions. For example, in the haptic modality, different factors vary constantly during the exploration of an object because of the complexity of the parameters involved in the sliding event [271]: stimulus parameters, environmental conditions, interaction differences, humidity, etc. [4]. The brain tries to extract information to achieve the task at hand (recognise a texture, eat a fruit, move the arm with adequate pressure, etc.) in the most efficient manner (i.e. by searching for these cues).

In touch, Merkel cells and Pacinian corpuscles [263] are both involved in texture perception. In terms of asperities, which is the subject of the current paper, Blake et al. [23] found that varying the height and width of small dots had more effect on the SAI firing rates than on the RA firing rates. Several of these receptor cells characteristics are known but the functional benefits of these characteristics are not understood. Measuring perceptual constancies or invariance at the peripheral level can bring forward theories on their computational functions.

Vibrotaction plays a key role in our discrimination of fine textures [99], with spatial cues becoming predominant for coarse textures (elements above 100 μm) [103]. If vibrotaction is primarily responsible for our ability to distinguish fine textures, it is reasonable to expect that we should be able to exploit the richness of the complex vibrations. Barlow [10] analyzed the properties of texture-elicited vibrations to determine the extent to which they convey information about surface microgeometry and examine the implications for the neural basis of texture perception. Since then, it was shown that vibrotaction provides a rich array of highly specific sensory messages that convey information about the frequency and amplitude of a temporal stimulus, and even its waveform [17, 160]. In particular, Bensmaia and Hollins [18] found that the roughness of fine textures is a function of the power of the vibrations they elicit in the skin.

5.1.2 Measuring and Recreating Virtual Tactile Scenes.

By contrast to vision and audition, in touch, one has to take into account the interaction between the physical world (i.e. surface topology) and the observer (i.e. friction between a surface and a finger pad, fingertip mechanics, exploration parameters). There are multiple methods to measure the interaction forces and accelerations created from the relative movement between a finger and different surface features. Biomimetic finger which contain an array of sensor can be scanned over textures [104]. Sensors can be used to measure the friction fluctuations due to the moving contact between a texture and a human fingerpad. Such methods include gluing an accelerometer on the fingertip nail [19, 108, 238, 220] or remotely measuring signals from microphones [67] or vibrometers [161]. Force sensors can also be incorporated into a tribometer for more precise measurements [192, 53, 3, 273, 69, 201]. Regardless of the method used, the aim is the same: capture the relevant information that could be sensed by

the mechanoreceptors making sure it is contained in the virtual stimulation.

Few groups have analysed these texture vibratory signals thoroughly to separate the noise from the salient features. Usually the recreation is done by directly using the recorded vibrations to recreate the sensation or only the large spatial features of a periodic texture [21, 272].

5.1.3 How Can we Detect the Relevant Cues for Virtual Interactions?

As pointed out by Platkiewicz et al. [200], several mechanical parameters have been proposed to be tactually relevant (surface deformation, normal strain or stress, shear strain or stress, principal strains or axial strains, or a combination of these parameters) but there is no consensus as to which ones are the most pertinent. To answer that, they formally studied haptic edge detection looking at different types of contacts and concluded that the shear component of strain is the most informative cue for rendering shape-related sensations. Monnoyer et al. [170] followed a similar approach to render the sensation of a keystroke using an ultrasonic haptic display. They found that the robust cue to a mechanical indent is a release of skin stretch after a high friction level state. They are however not the first to look at ways at rendering relevant cues. Such examples include devices which display cues for fingerpad contacts [280, 211], slip [106] and shape [212].

5.1.4 Mechanical Basis to Perceptual Invariants between Amplitude and Duration in Asperity Exploration.

Our work has also focussed on decoding what cues are important when it comes to recreating a single short tactile event. More specifically, we investigated the presence of a mechanical invariant experienced when a finger is sliding over an asperity, such as a braille dot. The aim was to elucidate what the speed signal may be in different exploration conditions. We investigated the mechanism by which an asperity is experienced the same way, which we deem 'perceptually constant', regardless of the speed or force with which the asperity was encountered by the skin. Since the amplitude of deformation in the skin and duration of the encounter are important variables that vary with exploration speed, we first investigated if one of these could be exchanged for the other by presenting wavelets of pink noise of varying duration and amplitude, to a finger gently resting on a plate. In a second experiment, the mechanical response of a finger sliding over a braille dot was investigated, by recording force and velocity using a tribometer. Physical quantities in these recordings were analysed by correlation with the known variants to isolate a physical invariant, the integral of the tangential force, which we propose could be responsible for the perceptual constancy. Finally, the recordings were used as stimuli in another psychophysical task in which participants explored virtual dots at different speeds. They had to identify the two stimuli, a smaller and a larger dot, by reporting which one was stronger, a task which they could successfully accomplish despite being forced to explore them at different velocities. Similarly to the previous experiment, the integral of the tangentially displayed forces was independent of exploration speed, but differed between the dots, and therefore remained an excellent candidate quantity for informing on perceptual constancy.

5.2 Materials and Methods

5.2.1 Experimental Apparatus

The device we used was described in more detail elsewhere [25]. It is a transducer capable of measuring the interaction between a bare finger and different surfaces (1, Fig. 5.1) by decoupling the tangential and normal forces. It can also be used in stimulation mode (2, Fig. 5.1), where a suspended glass plate vibrates to reproduce some elements of the recorded texture when a finger slides on the plate.

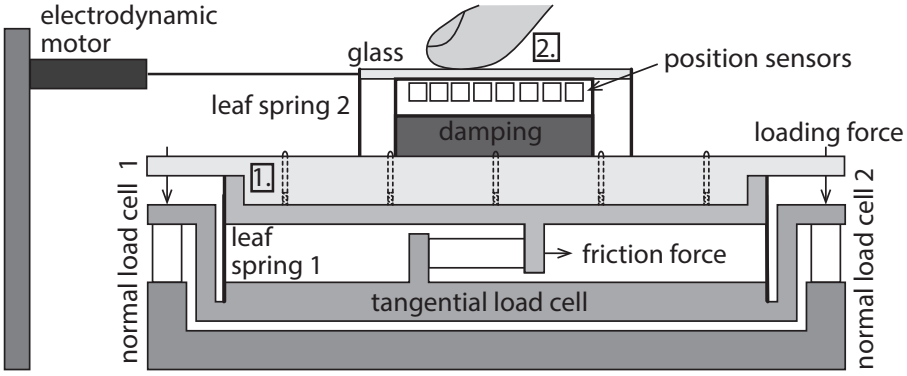

Figure 5.1 – The apparatus. 1) The tribometer measures the interaction forces of the finger exploring the braille dot platform. 2) The same transducer is then used in stimulation mode. An electrodynamic motor is grounded and in contact with a vibrating glass plate attached to the transducer through a mass-damper system. The tangential force and normal force sensors can be measured as in mode 1. In addition, 8 photocell sensors measure the velocity of exploration.

5.2.2 Cognitive Equivalence between Amplitude and Duration in Tactile Signals

5.2.2.1 Synthetic Stimuli

The stimuli consisted of pink noise vibrations I(t) enveloped in a Gabor wavelet (see equation) with characteristic durations ranging between 0.1 and 0.7 s, and intensities of acceleration ranging from 300 to 3000 m/s^2.

$$\psi_{\delta t}(t) = A \exp\left(\frac{-\pi\,(t-t_0)^2}{2\delta t^2}\right) I(t)\ , \tag{5.1}$$

5.2.2.2 Psychophysical Method

In the preliminary experiment, [27], a simplified version of the stimulator in 2, Fig. 5.1 was used. It consisted of an electrodynamic motor glued onto an aluminium plate. 10 naive observers (22 to 36 years old) were presented two pink noise vibrations at their dominant hand index fingertip which was gently resting on the plate. They wore noise cancelling headphones and were blind folded. Their task was to spontaneous report which of the two stimuli felt overall stronger. Using a two alternative forced choice staircase procedure, the points of subjective equivalence were estimated for the 0.4 s long reference stimulus.

5.2.3 Comparison between Braille Dot Recordings at Different Speeds

5.2.3.1 Mechanical Stimuli

To prepare more ecological stimuli for a perceptual study in active touch, a recording task [26] was elaborated to measure fingertip friction forces using the transducer in mode 1, Fig. 5.1. One human finger (22 years old female) explored plastic Braille dots using a variety of velocity (79 to 555 mm/s) and force (0.4 to 1 N) profiles. The tangential force of each recording was filtered using a 5-50 Hz band-pass first order Butterworth filter, to eliminate DC bias and ignore high-frequency vibrations while keeping the overall shape of the interaction force profile. Physical quantities characterising the finger-dot interactions were derived from these filtered signals and correlation analysis was applied to estimate dependencies between these quantities. Finally, the recordings from the two dots that differed the most in height (0.42 mm and 0.61 mm) were classified by their velocity of exploration in a dataset for use in the following experiment. The velocity was obtained by fitting the position data to a 2nd order polynomial across the recording, and taking the value of the derivative at the center of each dot.

5.2.3.2 Psychophysical Method

The verification task involved a binary forced-choice procedure in which 17 participants (19 to 32 years old) were asked to compare two stimuli presented during active exploration of a flat glass surface. The stimuli consisted of the force signals recorded during the braille dot interaction, reconstructed using an electrodynamic motor oriented tangentially to the plane. They were asked to report which of the two interactions felt stronger. Each participant was presented with 96 trials of randomly-ordered but equal combinations of slow (below 100 mm/s) or fast (100 to 400 mm/s) movement and the two dots of different height (0.4 and 0.6 mm), totalling 12 repetitions of each of the 8 conditions (4 speed combinations $\times$ 2 dot combinations, i.e., dot 1 then dot 2, dot 2 then dot 1). Another 24 trials asked participant to compare dots of the same height explored at different speeds (6 repetitions of the 2 speed combinations x 2 same dot combinations) to check for perceptual biases. Before each trial, an indication of the speed at which the participant should go was given by the experimenter, such as 'two slow swipes' , 'two fast swipes', 'one slow swipe, one fast swipe' or 'one fast swipe, one slow swipe'. At each swipe, the finger velocity was measured using the time it took the finger to go from one edge of a photocell sensors to the next (mode 2, Fig. 5.1). The data acquisition was at 5000 Hz sampling frequency so the velocity measure was accurate in time provided the participant's speed was constant, which was the assumption used. The braille dot recording closest to that velocity was chosen and its shape was adjusted to its measured velocity by mutliplying the stimuli by *target velocity/source velocity*. If the speed was out of bounds, they were asked to repeat the swipe until it was in the desired range.

5.2.4 Participants

In all experiments, the participants had no history of neurological disorders or manual sensorimotor function disorders. They were asked to use their dominant hand. In all but the recording task, the participants were naive to the aims of the study.

5.3 Results

5.3.1 Interdependence of Amplitude and Duration

In the preliminary experiment, the amplitude of subjective equivalence as a function of the stimulus exposure time *dt* showed a negative power law relationship with a regression coefficient of -0.23, see Fig. 5.2.

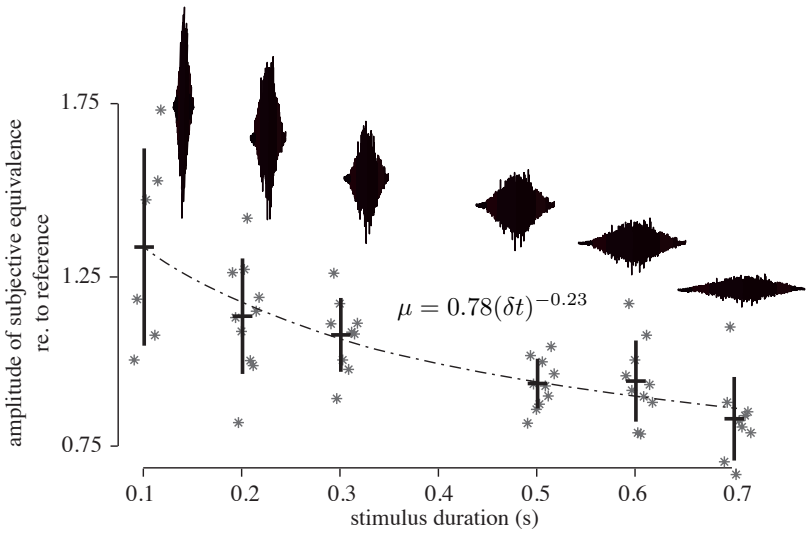

Figure 5.2 – A negative power law relationship between amplitude and duration is found in the intensity perception of complex tactile stimuli. The wavelet signals perceived by the participants as points of subjective equivalence vary in shape but are overall felt equal in intensity.

5.3.2 Braille Dots of Different Heights Recordings at Different Speeds

In the recording task, characteristics of the interaction were studied to explore the manifestation of the amplitude/duration interdependence of signals across velocity, normal force and dot height. While the amplitude and duration varied significantly with the velocity of exploration (regression coefficients of 0.49 and -0.82 respectively), the tangential force over time remained relatively constant (regression coefficient of -0.13), see Fig. 5.3.

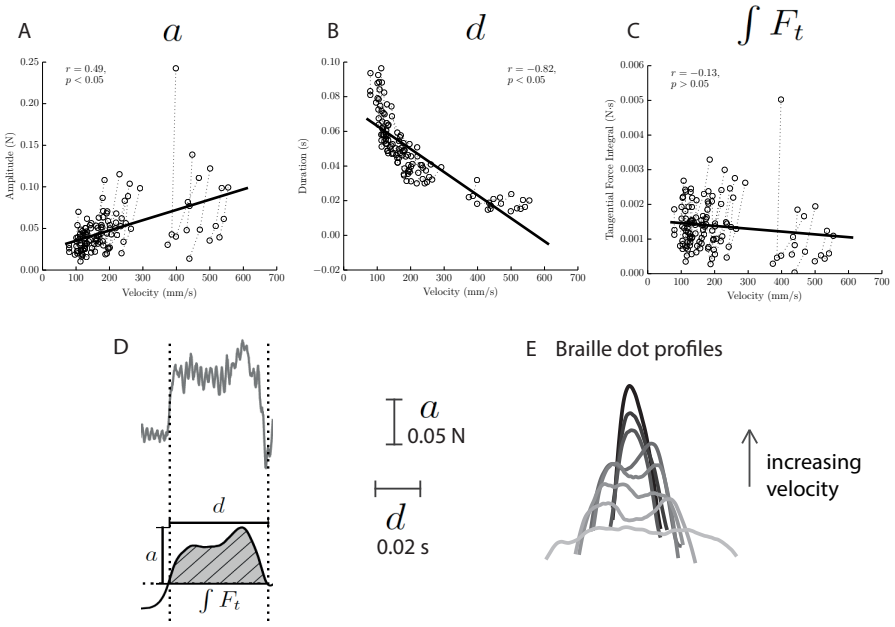

Figure 5.3 – The mechanical response of a finger exploring a braille dot at different speeds shows that while the amplitude increases and the duration decreases with velocity, the tangential force integral remains relatively constant. The different filtered dot profiles shown here are classified by velocity and used in a psychophysical task.

5.3.3 Perceptual Evaluation of Virtual Braille Dots of Different Heights

Across two dots of varying height, the tangential force integral was not found to be constant but increased in proportion to height (regression coefficient of 0.69), see Fig. 5.4a. Two clearly separate distributions were found for the perceptual discrimination ability of subjects to correctly differentiate these two dots, see Fig. 5.4b, indicating that there were two distinct categories of participants. 12 participants were able to distinguish (mean of 71.8%) which dot was more intense, even though the signals systematically varied in duration and amplitude depending on the exploration velocity, see Fig 5.4b. However, 5 participants were at chance level (50%). These subjects reported not always feeling the stimuli or not understanding the stimuli, which could be confused with a stick-to-slip transition typical of finger-glass interaction [4], the material of the experimental platform. We removed these from the analysis as we were not able to fairly measure their percept to the different stimuli. There were no perceptual biases; on average, 48.4% of participants selected the second dot in all conditions and 45.5% of participants selected the slower dot in different speed conditions. Henceforth we therefore restrict our discussion to the former group, which successfully differentiated the conditions.

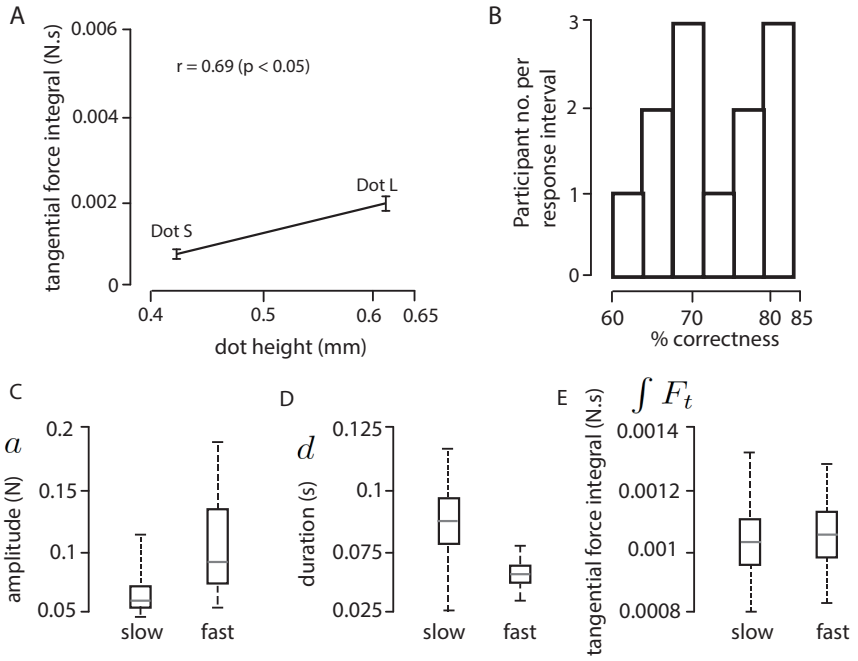

Figure 5.4 – Two synthesised braille dots (Dot Small and Dot Large) differing in height by 0.2 mm can be distinguished in intensity by most participants based on a constant difference in the tangential force integral, while the amplitude and duration vary significantly when the finger explored them at different velocities. The distribution of the correctness response has a mean of approximately 72%.

5.4 Discussion

5.4.1 Evidence of the Tangential Force Integral as an Invariant

In the preliminary experiment, two parameters were manipulated to see if they could affect the intensity perception. It showed that when a stimulus is temporally larger but has a smaller amplitude, it can be felt as intense as a stimulus that is temporally shorter and that has a larger amplitude. Next, the recording task was aimed at characterising the invariance itself in terms of the mechanical response of a real situation: a finger sliding over an asperity with different velocities. It was found that it is the tangential force integral which best reflects a specific dot height regardless of the exploration profile. This confirmed our hypothesis that although the instantaneous mechanical perturbation is different under various exploration conditions, meaning that it persists for different durations while being compensated by different amplitudes of force at a given moment, the overall deformation is nonetheless the same. This suggests that the nervous system may be acute to the tangential force integral, in the form of total skin deformation throughout the event, as one physical invariant quantity that could play a role in the recognition of the same spatial asperity explored under different velocity and force conditions. Finally, in the verification task, participants were able to distinguish between different dot heights in virtual dots displayed using a tangential motion platform, in which tangential force integral was the only constant quantity in the synthesized signals. We can infer from these results that if we generate two recordings of the same dot at different velocities when the finger is exploring a surface at those exact velocities, the participant should feel them similarly.

5.4.2 Stretching the Dot Recordings to Maintain Speed Specificities

We recorded the interaction with the dot, and noticed that the duration and amplitude scale with exploration conditions. However, the force integral over the duration of the impact event remained constant. In order to maintain this constancy during virtual, synthesized interaction, it is necessary to maintain this scaling, so that durations and amplitudes vary as expected with the exploration conditions. We play back a recording that is close to the detected exploration conditions, but about 10% slower than the recording. Therefore, we slow down the playback by 10%, and diminish the amplitude by 10%. This is to correspond with what we presume would be felt under normal circumstances.
By selecting a sample taken when exploration conditions were close to the sensed conditions, we are trying to minimize the amount of 'stretching' that we need, trying to be as ecological as possible. However, some stretching can still make the synthesized signal closer to 'reality'. Importantly, the stretching we are applying to the sample does not change the integral, since we change duration and amplitude proportionally.

5.4.3 Variations in Amplitude and Durations During Swipes

This study shows that when exploring an asperity, neither amplitude A of friction force, nor D duration of the event can independently help us identify the dot –however, their product, proportional to the friction force integral, provides a constant that may do so. The integral of friction force F over the duration D is

$$\int F = \mu AD, \tag{5.2}$$

such that μ may reflect the details of impact. This suggests that, for the same asperity, different amplitudes for the same duration will produce different integrals, and similarly different durations for the same amplitude will also produce different integrals. Therefore, while amplitudes and durations of the event may change, only the shape of the dot, in this case its height, reflects changes in the integral.

5.4.4 Encoding of the Tangential Force Integral

We propose therefore that this information is made available to the brain when deciding whether it is touching the same dot or a different one. Whether the integral is computed by some neural circuit, or sensed by some mechanical phenomenon such as skin plasticity, is not determined by these experiments, and may be considered in future work. The paper shows that mechanical invariant are important in perception. We however don't know at what level it is evaluated but we know it's present. Is it in the skin deformation? Deformation contains proportional force integral.

5.4.5 Extending the Phenomenon to Different Types of Dots

This study only investigated height differences since we used the same dots and kept other things equivalent. Therefore, while here the force integral was used to distinguish heights of

dots, it does not suffice to explain how we identify their material, the shape of their corners, or their radius. Rather, it is known that for a given cue, multiple invariants must be recruited [89]. Maybe this is where the other variable comes in. In fact, behind each cue, it has been stated that several different invariants are recruited [89]. We can infer from these results that if we generate two recordings of the same dot at different velocities when the finger is exploring a surface at those exact velocities, the participant should feel them equal. If they had felt differently, it could have been due to the fact that their own state is making them feel different, i.e. the speed of the interaction. It would be interesting to extend the study to dots with different shapes but which have the same overall tangential force integral. Would they also feel the same based on the integral? Information about slip and texture is contained in the variation of the tangential force over time. Therefore it is likely that these interaction may not be comparable. Aside from mechanical differences in shape and size, chemical properties (temperature and moisture absorption) can vary considerably between different types of materials.

5.5 Conclusion

This work suggests that the integral of the local tangential forces is an invariant available to the brain. The tangential force integral remains constant during swipes of the finger at different speeds over an asperity, even though the amplitude and duration of the tangential force signal both vary significantly. We can conclude that it is the integral of the local tangential forces that should be provided to the somatosensory system in asperity height reproduction instead of the set of all the instantaneous values.

5.6 Acknowledgements

This study was funded by the FP7 Marie Curie Initial Training Network PROTOTOUCH, grant agreement No. 317100. It was further supported by the European Research Council (FP7) ERC Advanced Grant (patch) to V.H. (No. 247300).

Chapter 6

Perceptual Constancy With Respect to Speed in the Reproduction of Virtual Textures

Contents

This work was submitted as S. Bochereau, S. Sinclair and V. Hayward. Perceptual Constancy With Respect to Speed in the Reproduction of Virtual Textures to *ACM Transactions on Applied Perception*

Preface to Chapter 6

The previous chapters have shown that the overall experience seems to be more perceptually relevant than the details of the force profile at a given time. This agrees with other findings that we are particularly insensitive to changes in vibration frequency as well as to the detection of the speed of moving objects. Until now in the thesis, we have been looking at reproducing asperities. This chapter investigates design liberties in terms of speed to reproduce textures by drawing hypotheses for how few pre-recorded texture samples can be used and how often and how precisely the signal should be adapted to be matched to the user's exploration speed.

Abstract

For very rough surfaces, friction-induced vibrations contain frequencies that shift multiplicatively with sliding speed. Given the poor capacity of the somatosensory system to discriminate frequencies, this fact raises the question of how accurately finger sliding speed must be known during the reproduction of virtual textures with a tactile display. During active touch, ten observers were asked to discriminate texture recordings corresponding to different speeds. The samples were constructed from a common texture which was resampled at various frequencies to give a set of stimuli of different swiping speeds. In trials, they swiped their finger in rapid succession over a glass plate which vibrated to reproduce three texture recordings. Two of these recordings were identical and the third differed in that the sample represented a texture swiped at a speed different from the other two. Observers identified which of the three samples felt different. Seven observers reported differences when the speed varied by 60, 80 and 100 millimetres per second while the other three did not reach a discrimination threshold. These results show that the need for high-accuracy measurement of swiping speed during texture reproduction may actually be quite limited compared to what is commonly found in the literature.

6.1 Introduction

Perceptual constancy is a singularly important phenomenon and was enshrined by the Gestalt school of psychology as one of the perceptual principles, *e.g.* [46]. There are indeed numerous examples of its existence. But of course, the many counterexamples where perceptual constancy also breaks down may explain why it has been the topic of countless studies, and arguments about the scope of its application, *e.g.* [95]. Perceptual constancy is vitally important for the operation of any display. Television sets would be useless without perceptual constancy because people shown on them would appear to us at their 'veridical' size. Voices and music tunes would vary at infinitum at the whim of each sound reproduction system, each of which produce vastly different acoustic fields for a same source. Fortunately, in all sensory modalities, including olfaction, most perceptual dimensions are subject to constancy since, without it, the world around us would appear to us like an undecipherable mess.

6.1.1 Constancy in Touch

In touch, constancy operates in an apparent manner for some perceptual dimensions. For instance a book, by-and-large, is felt to have the same heaviness whether it is held between two fingers or whether it rests on the palm of a hand supported by a table. These conditions nevertheless correspond to utterly different haptic inputs. It is also easy to render it inoperative, for instance, under the effect of the size-weight illusion [177]. Similarly, force feedback devices often exhibit widely different characteristics [214]. Yet, once a certain level of performance is achieved different models can provide similar sensations. In the haptic domain, constancy, like in vision, is known to break down for certain sensations and under certain conditions [265, 87, 174], but can be robust for other conditions [283].

It is known that the tactile perception of texture is relatively insensitive to changes in exploration speed [142] and exploration method [135, 282], which may be viewed as an instance of perceptual constancy. Textural perceptual constancy is astonishing given the dramatic changes in the proximal stimulus as a function of changing scanning speeds [52, 273, 50, 161]. The brain is thus capable of extracting the invariant characteristics of a surface, even during passive touch, when there is no direct information about the sliding speed. Therefore, the brain must have developed powerful constancy mechanisms since the inter-spike intervals of peripheral afferent responses dilate or contract multiplicatively according to speed [263].

6.1.2 Sensing Requirements In Tactile Displays

With the recent development of numerous approaches to realise tactile displays able to provide sensations of texture [262, 181, 276, 21, 275, 5, 166, 80, 272, 272, 9], comes the need to specify their actuation and sensing performance. Sensing requirements can be quantified by relating spatial resolution, temporal resolution, and scanning velocity [34]. To this end, it is possible to invoke the so-called Courant-Friedrichs-Lewy (CFL) condition, $v_C < \delta/T$, that specifies the conditions under which spatio-temporal signals can be represented (and by way of consequence enable the convergence of the associated computational problems) if δ is the spatial resolution, T the temporal resolution, and v_C a not-to-be-exceeded slip velocity. Thus, a brute force approach to realise exact texture reproduction imposes exacting sensing requirements that are such that a desired temporal sampling frequencies would be of the order of 10^4 Hz and a spatial sampling frequency of the order of 10^6 m^{-1}. These figures would inflict drastic requirements on the finger position detection systems of any tactile display.

6.1.3 Human Factors

Seen from another perspective, it is wholly unlikely that our haptic sensory system be capable of such performance. Clearly it must employ a tradeoff, the simplest of which is to ignore the actual velocity at which a finger slides on a texture and to replace it with a standard value. It is what neuroscientists call the temporal coding of tactile textures [83, 36, 99, 123, 109].

Our own work has shown the existence of a mechanical invariant that could be extracted by the brain during the exploration of isolated asperities at different speeds [26]. This finding suggests that the cumulative skin deformation elicited by a scanned asperity could represent such an invariant physical quantity whereas the previously considered instantaneous mechanical loading on the finger skin would not. This quantity is insensitive to speed but varies with other exploration conditions and surface properties such as the height of an asperity.

This and other mechanisms led us to put forward the hypothesis that significant liberties with respect to the actual finger sliding velocity could be taken during virtual texture reproduction that would remain undetectable. In keeping with the previous reasoning, this hypothesis is equivalent to assuming the poor capacity of the tactile system to discriminate temporal frequencies, a fact that is born out empirically [81].

6.1.4 How Much Resolution is Really Needed?

We investigated the aforementioned hypothesis by measuring the perceptual ability of twelve observers to become aware of the differences in the textures corresponding to different scanning speeds during active sliding on a vibrating glass plate that reproduced a signal closely resembling that which is elicited by scanning the actual texture. Even with a texture having a strong character of periodicity — hence giving a signal that is highly sensitive to scanning speed — we found that reproduction speed could vary by $\pm$ 60% around a nominal velocity of 0.16 m/s before observers could notice a difference. In other words, this result implies that a desirable velocity quantum for a tactile display system, i.e. the smallest detectable velocity difference, can be of the order of 0.1 m/s. Thus for a display operating in open loop having a temporal resolution of 1.0 ms, the requirement for sensing would be on the order of 0.1 mm and not 1.0 μm as the naive application of the CFL condition could lead one to conclude. Please observe that in closed operation the application of the CFL condition to tactile displays would still be needed because of the possibility of noise re-injection [34].

6.2 Materials and Methods

6.2.1 Apparatus

We used a tribometer apparatus to make recordings of a reference stimulus. This apparatus, described in greater detail elsewhere [25], combines a finger stimulation system with a highly sensitive transducer able to measure the interfacial force components between a bare finger and natural surfaces. The transducer uses leaf springs to separate out the normal contact loading component from the friction component, and does so in a wide range of frequencies, owing to its high rigidity. The stimulator system also uses a suspension made of cantilever leaf springs, Fig. 6.1, but arranged to be highly compliant in the tangential direction in order to ensure a robust causality between the signal that drives the motor and the stimulus applied to the skin.

To compensate for the highly undamped response of the system, the stimulator included a Foucault-current damper that introduced, without contact, a viscous force and which was

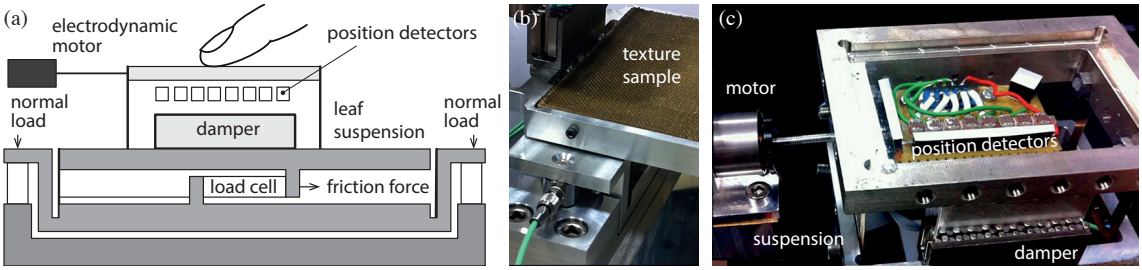

Figure 6.1 – Apparatus. (a) Schematic representation. (b) Texture sample mounted to the tribometer. (c) View of the stimulator.

linear in a wide range of velocities. The stimulator was actuated by an electrodynamic voice-coil motor which was also very linear. This arrangement ensured an accurate reproduction of the measured friction force signal on the skin without the need for causality inversion [274], because in a dominantly inertial system, forces and accelerations are equivalent. The stimulator also included a set of eight optical sensors that could detect the instant when a scanning finger would come into coincidence with their positions.

6.2.2 Stimulus

The reference stimulus was a 500 ms recording of a finger sliding over a metal mesh (texture No. 42 from [243], see Fig. 6.1(b)) which corresponded to an exploration speed of 180 mm/s. The original sample was pre-filtered by spectral truncation in the 60 – 500 Hz range in order to remove the high-frequency modal imperfections introduced by the recording device. The samples were edited to conserve the central, steady-state portion, minimising the variations due to changes in normal force and exploration movement. The reference sample was then resampled using linear interpolation and windowed to equalise the duration, in order to prevent the observers from using the stimulus duration as a cue. Fig. 6.2a shows the stretch stimuli for speeds 180 (the reference), 120 and 100 mm/s. The spectral centroid of all stimuli shifted regularly as they were resampled to create stimuli of decreasing speeds, see Fig. 6.2. The centroids were determined by taking the product of the magnitude, $A_i(f_i)$ $i = 1, \ldots, 5000$, with each frequency, f_i, in the fast Fourier transform (FFT) of the signal and normalising it by the sum of all magnitudes, $\sum f_i A_i / \sum A_i$. The stimuli were convolved with a 500 ms Gaussian window to eliminate sharp discontinuities and minimise the spurious introduction of unwanted frequencies.

Below the glass plate was an array of photocell light detectors 5 mm apart from each other, used to compute the speed over each interval. The data acquisition had a 5 kHz sampling frequency. This configuration allowed us to measure average speed between two photocells precisely since by the inverse-time method the velocity estimation error was of the order $1/(\delta/\mathrm{T}) \approx 1^{-3}$ mm/s [110]. The first photocell detector was used as a flag to indicate that the participant was sliding on the platform. The assumption that the finger was sliding at a relatively constant speed during the duration of the stimulation could thus be easily verified.

6.2.3 Procedure

The twelve observers were given the task of detecting which one of a set of three consecutive stimuli was different from the other two. In an three-alternative force choice paradigm (3-AFC), chance level is 33% of correct answers. Thus, we considered that above 33% of correct responses, an observer would begin to detect the difference between stimuli. A forced-choice

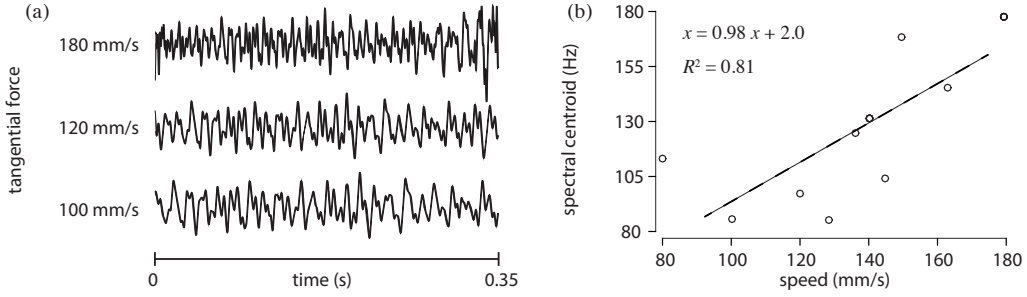

Figure 6.2 – The time-warped filtered stimuli at 180, 120 and 100 mm/s. (b) The spectral centroid increased with speed, with a 0.98 slope and a 0.81 regression.

task with three alternatives has several advantages in same/different judgements. The most important is that observers, being provided with three pairs of stimuli, have the opportunity to compare pairs that are perceived to be the same to pairs that are perceived to be different, thus reducing reliance on an internal criterion of sameness. In other words, this method offers more alternatives in a set of choices that includes a status quo option [209]. The stimuli were selected from a set of speed differences comprising 5, 10, 20, 40, 60, 80 and 100 mm/s with respect to the 180 mm/s standard.

Observers were informed that they would experience three simulated textures when sliding the index of their dominant hand on the stimulator's glass plate and that they had to look out for differences between them. During training, they were instructed to slide at a constant speed which felt comfortable for them while no texture was reproduced. After a few trials of practice they were blindfolded and pink noise was played in the noise cancelling headsets that they wore. They continued to practice exploring at a constant speed but could experience the stimuli. During this period the experimenter could adjust the oscillation amplitude to ensure that observers could feel the simulated textures at a level that was natural to them. The experimenter also adjusted the sound level such that the acoustic emissions arising from the stimulator were not heard by the observer. Once the preparation phase was completed, each observer experienced eight repetitions of triads of stimuli including one of the six speed differences with additional twelve control trials where the triads had the same stimuli, totalling 60 trials. The order of presentation was randomised within trials and across trials for all participants. The trials were not rejected on the basis of constant velocity, although this was informally enforced by the experimenter by trial repetition. They could take an optional rest half way through the blocks of trial but frequently opted out. The procedure lasted approximately 45 minutes.

Because the perceptual task was difficult, which is a problem to contend with for same/different judgements with no sharp boundaries, the results were expected to be noisy and sensitive to individual differences. To address this problem, observers also rated on a scale of weak, medium, and high (converted to numerical values of 2, 5, and 8) the confidence that they had of their own judgements. Recently, confidence ratings have been argued to be an effective probe into one's own perceptual states because confidence ratings relate directly to our second-order ability to monitor the value of first-order perceptual judgements [279, 55]. Here, it might be argued that a judgment of sameness relates more to a second-order judgement than to a first-order judgement such as ordinal ratings, for instance intensity. In fact, it would be hard with our textures to come up with ordinal perceptual dimensions that could be ranked since the textures were artificially constructed to have the same roughness, the same implicit periodicity, and other similarities in all their aspects.

6.3 Results

As was anticipated, the performance of the observers increased as the difference in speed between the reference and the comparison stimuli also increased, see Fig. 6.3(a). Data dispersion, however, remained by-and-large independent from performance. The speed discrimination threshold was defined to be the speed difference at which the percentage of correct answers exceeded 67% and the 'just noticeable difference' (JND) was defined to be the speed difference at the mid-point location between 33 % and 67% correct answers. On average, the rate of 72% of correct answers was attained only for a speed difference of 100 mm/s, suggesting that the threshold of 67%was not systematically reached in a range of speed exploration from 80 to 180 mm/s. Two observers were discarded from the analysis because their performance was at chance level. This correction had no effect on the conclusions.

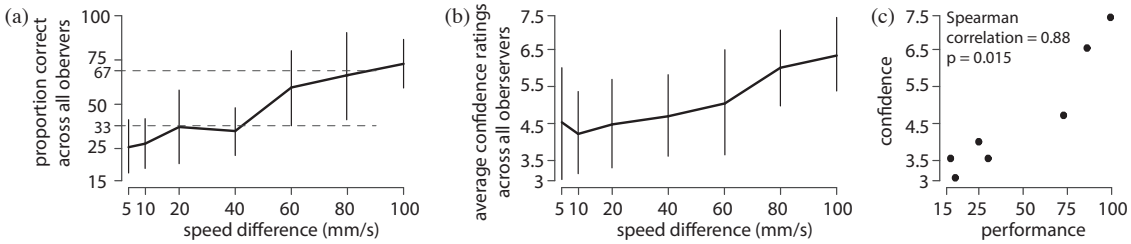

Figure 6.3 – (a) Fraction of correct answers across all observers. (b) Averaged confidence ratings for all observers and trials. In the two plots, error bars show standard deviation. (c) Correlation between performance and confidence.

Interestingly, the confidence ratings of the observers, Fig. 6.3(b), tracked their performance. Figure 6.3(c) presents the same data but with confidence ratings plotted against performance, showing a high degree of correlation between the two measures. There is, however, a noticeable difference in that performance remained almost constant until a threshold of 60 mm/s and then started rising whereas confidence ratings rose gradually, even when the difference in stimulus was not consciously detectable. Because this study aimed at suggesting design guidelines for tactile displays, detection threshold values that would be useful for engineering purposes should be aligned with the results of the most sensitive observers, rather than on average. Of the ten observers that could do the task, one was particular sensitive. The corresponding result is shown on Fig. 6.4.

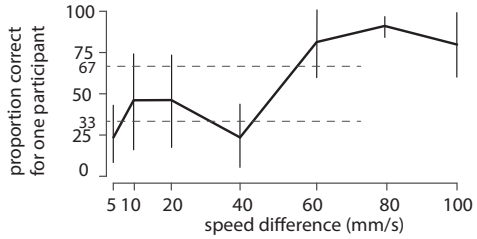

participant	67 % threshold (mm/s)	participant	67 % threshold (mm/s)
S01	>100 (>60)	S06	60 (55)
S02	100 (80)	S07	100 (90)
S03	80 (40)	S08	60 (50)
S04	100 (90)	S09	>100 (>60)
S05	>100 (>80)	S10	60 (50)

Figure 6.4 – Performance for one participant and individual results for the others. The JND (mm/s) is specified in parenthesis after the 67 % threshold. Error bars show standard deviation of this observer's answers.

In the range of speed variations used, seven observers met a perceptual threshold (60, 80 and 100 mm/s), but the other three were unable to detect differences between the recordings (success rate lower than 67% for all speed differences). The lowest JND was at 40 mm/s

amongst our pool of observers. For the three least sensitive observers, we could not measure the JND since their speed discrimination threshold exceeded 100 mm/s.

We conducted further analysis to better analyse the relation between performance and confidence ratings, and to evaluate possible biases introduced by the method. Figure 6.5(a) shows that when an answer was correct, it was more likely to be rated with high confidence. Conversely, when an answer was incorrect, it was more likely to be of low confidence albeit less strictly than in the other case.

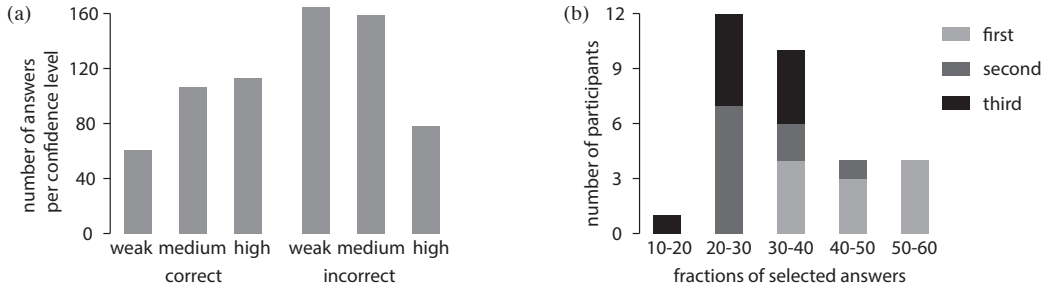

Figure 6.5 – (a) Distribution of confidence estimates per correct and incorrect answers. (b) Biases towards answering the first, second, or third sample in a triad.

On the whole, observers chose the first sample more often than the second or the third, see Fig. 6.5(b). Overall the average was around 30-35% which is roughly one third of all answers. This slight imbalance would not change our conclusions since the stimuli were randomised.

6.4 Discussion and Implications

A few observers spontaneously reported that they felt that the temporal frequencies were different across samples while, interestingly, others felt that the temporal extent of the stimuli was changing when, in fact, the stimuli all had the same duration. This observation suggests that a perceived change of duration could have the interpretation that textures explored at a faster speed also led to a shorter temporal exposure, confirming that speed was the cue which most observers used to distinguish between stimuli. Similar interactions between speed, duration, and spatial extent have been reported in the past, see [58] and references therein.

The mechanisms underlying textural constancy in touch are still debated [105, 282, 50, 152, 263]. Our results show that textural perceptual constancy operates powerfully even under the conditions of stimuli produced by a display system which, by necessity, are impoverished compared to natural stimuli. It is therefore worth considering which aspect of the natural stimuli are missing in the artificially generated stimuli. In natural stimuli, there is normally a strong correlation between the position of the temporal spectrum on the frequency scale and speed, a property that was notable in the case of the texture that we selected for our experiments. The artificial stimuli, however, abolished this correlation completely, yet constancy was still operating. This finding thus undermines models of texture perception based on temporal coding since, in our experiments, the temporal aspects of the stimuli changed dramatically without being noticed. It is also argued that texture perception instead arises from a dual coding process, one in the temporal domain and the other in the spatial domain [103]. Our results do not support well this view either, since the artificial stimuli that we employed did not contain any spatial components. We thus may conclude the texture constancy must rely in great part on top-down processes where the predictions of pre-internalised models of textures are matched against raw sensory inputs.

On the whole, a robust threshold (above 67 % of speed variation was not reached by all the observers in the speed exploration range from 80 to 180 mm/s, but when looking at individual performance, some observers could detect differences. Still, considerable liberties can be taken in the reproduction of texture when it comes to scanning speed. More specifically, the results suggest that it is pertinent to reproduce texture up to a 40 mm/s difference compared to a reference exploration speed. Our results were obtained for only one texture, a metal mesh of medium coarseness, which was selected to provide a clear sensation of periodicity; they can be expected to apply as well to other textures having a lesser character of periodicity.

In future work, we would like to use more diverse texture recordings and conduct identification tasks with recorded texture stimuli that are perfectly matched with the exploration speed on one hand and with samples recorded with a ±40 mm/s discrepancy on the other. If the texture recognition ability is comparable, it would gives us a speed matching threshold necessary for texture reproduction that will allow us to engineer devices that have very low speed sensing requirements.

6.5 Acknowledgements

This study was funded by the FP7 Marie Curie Initial Training Network PROTOTOUCH (No. 317100) and by the European Research Council (FP7) ERC Advanced Grant (patch) to V.H. (No. 247300).

Conclusions & Perspectives

The aim of this thesis was to investigate an approach to simplify the rendering of asperities and textures using haptic displays. We have shown that an invariant exists in the mechanical interaction between a bare finger and an asperity. This invariant, the tangential force integral, reflects the intensity of the interaction regardless of the speed at which the finger impacts the asperity. As we have seen, what feels natural to humans and helps them achieve the best discrimination performance is the use of a variety of exploratory movements and speeds. Our findings suggest that these explorations can be encouraged when interacting with a device because the speed can be accounted for with much more leniencies as we expected. This thesis presents such a hypothesis. Interestingly, different types of textures or surfaces, especially the very gross textures with a clear spatial frequency, will probably have different (potentially stricter) requirements than the finer metal mesh texture or a single bump I studied which did not require much speed scaling. The necessity to match for speed could also vary with device specifications. Similar experiments as that done in Chapter 6 could be carried out for a few textures from fine to coarse spanning the range of everyday textures. This would give a good idea of the variation in speed matching necessity across most of the textures users would be interested in exploring virtually.

The device developed in this thesis allows for stimulation in only one direction, and this will have to be changed to allow for a non-restrictive experience. Its bandwidth is quite satisfactory but would ideally reach 1000 Hz or even 800 Hz in the recording mode, allowing for all of the mechanical information sensed by the four mechanoreceptor channels to be included in the raw measurements on which the synthesis is based. Our results have shown that lateral vibrations are successful in recreating bumps, even if some participants required high amplitude for the tangential vibration to be felt comfortably. Simply replaying lateral vibrations worked with this device for bump synthesis however it did not seem to be sufficient to synthesize fine textures. Future work could involve more thorough transformations on the raw texture signal to extract or exaggerate the salient features while still keeping the vibration noise, which contains the texture information and adds realism. Another approach could be to add a method of vibrating the plate normally, allowing to inform cues on the compliance or softness of the explored surface and to provide an additional stimulation channel.

A new line of research that results from this thesis relates to the extensive possibilities of experiments that can be carried out with the new device. Unfortunately, I did not have the time to exploit it to its full capability. One can imagine that any texture or topography can be recorded, replayed and imaged by taking advantage of all of the functionalities of the device. Some illusions could be recreated with the current stimulator or with another stimulator attached to the platform. Visualizing the skin deformation occurring during an illusory percept could help elucidate the foundations of that illusion. More simply, by capturing how

the finger vibrates, occludes and maintains its contact area at different speeds and frequencies, we could understand further what makes certain stimulation conditions more realistic or sensitive than others. These are just examples and suggestions of the many possibilities on how to grow the knowledge of the somatosensory system further in order to optimize the design of new generations of haptic displays.

Bibliography

[1] Braille authority of north america. (Cited on page 59.)

[2] M. Abe and S. Ando. Computational auditory scene analysis based on loudness/pitch/timbre decomposition. In *Proceedings of the IJCAI Workshop on Computational Auditory Scene Analysis*, pages 2646–2649, 1997. (Cited on page 47.)

[3] M. J. Adams, B. J. Briscoe, and S. A. Johnson. Friction and lubrication of the human skin. *Tribology Letters*, 26(3):239–253, 2007. (Cited on pages 10, 11, 23, 31, and 72.)

[4] M. J. Adams, S. A. Johnson, P. Lefèvre, V. Levesque, V. Hayward, T. André, and J.-L. Thonnard. Finger pad friction and its role in grip and touch. *Journal of the Royal Society Interface*, 10(80):467, 2013. (Cited on pages xi, 7, 9, 10, 11, 30, 39, 41, 57, 72, and 77.)

[5] M. Altinsoy and S. Merchel. Electrotactile feedback for handheld devices with touch screen and simulation of roughness. *IEEE Transactions on Haptics*, 5(1):6–13, 2012. (Cited on pages 24 and 83.)

[6] T. Amemiya and H. Gomi. Distinct pseudo-attraction force sensation by a thumb-sized vibrator that oscillates asymmetrically., 2014. (Cited on page 25.)

[7] T. André, V. Lévesque, V. Hayward, P. Lefèvre, and J-L. Thonnard. Effect of skin hydration on the dynamics of fingertip gripping contact. *The Journal of the Royal Society Interface*, 8(64):1574–1583, 2011. (Cited on pages 10, 11, 29, 30, and 42.)

[8] J. F. Archard. Elastic deformation and the laws of friction. *Proceedings of the royal society A*, 1233(243):214, 1957. (Cited on page 8.)

[9] S. Asano, S. Okamoto, and Y. Yamada. Vibrotactile stimulation to increase and decrease texture roughness. *IEEE Transactions on Human-Machine Systems*, 45(3):393–398, 2015. (Cited on page 83.)

[10] H. Barlow. The exploitation of regularities in the environment by the brain. *Behavioral and Brain Sciences*, 24(4):602–607, 2001. (Cited on page 72.)

[11] M. Barquins. Sliding friction of rubber and schallamach waves – a review. *Materials Science and Engineering*, 73:45–63, 1985. (Cited on page 11.)

[12] O. Bau, I. Poupyrev, A. Israr, and C. Harrison. Teslatouch: electrovibration for touch surfaces., 2010. (Cited on page 24.)

[13] E. Baumgardt and B. Hillmann. Duration and size as determinants of peripheral retinal response. *Journal of the Optical Society of America*, 51(3):340–344, 1961. (Cited on pages 47 and 52.)

[14] G. Von Békésy. Similarities between hearing and skin sensations. *Psychological Review*, 66(1):1–22, 1959. (Cited on pages 47, 52, 57, and 66.)

[15] G. Von Békésy. *Experiments in Hearing*. New York, 1960. (Cited on page 17.)

[16] J. Bell, S. Bolanowski, and M. H. Holmes. The structure and function of pacinian corpuscles: a review. *Progress in Neurobiology*, 42(1):79–128. (Cited on page 13.)

[17] S. Bensmaïa and M. Hollins. Complex tactile waveform discrimination. *The Journal of the Acoustical Society of America*, 108(3):1236–1245, 2000. (Cited on pages 16 and 72.)

[18] S. J. Bensmaïa and M. Hollins. The vibrations of texture. *Somatosensory & Motor Research*, 20(1):33–43, 2003. (Cited on page 72.)

[19] S. J. Bensmaïa and M. Hollins. Pacinian representation of fine surface texture. *Perception & Psychophysics*, 67(5):842–854, 2005. (Cited on pages 19, 23, and 72.)

[20] S. J. Bensmaïa, Y. Y. Leung, S. S. Hsiao, and K. O. Johnson. Vibratory adaptation of cutaneous mechanoreceptive afferents. *Journal of Neurophysiology*, 94(5):3023–3036, 2005. (Cited on page 15.)

[21] M. Biet, F. Giraud, and B. Lemaire-Semail. Squeeze film effect for the design of an ultrasonic tactile plate. *IEEE Transactions on Ultrasonics, Ferroelectrics and Frequency Control*, 54(12):2678–2688, 2007. (Cited on pages 24, 73, and 83.)

[22] I. Birznieks, V. G. Macefield, G. Westling, and R. S. Johansson. Slowly adapting mechanoreceptors in the borders of the human fingernail encode fingertip forces. *Journal of Neuroscience*, 29(29):9370–9379, 2009. (Cited on page 12.)

[23] D. T. Blake, K. O. Johnson, and S. S. Hsiao. Monkey cutaneous SAI and RA responses to raised and depressed scanned patterns: effects of width, height, orientation, and a raised surround. *Journal of Neurophysiology*, 78(5):2503–2517, 1997. (Cited on pages 12, 13, and 72.)

[24] F. Blankenburg, C. C. Ruff, R. Deichmann, G. Rees, and J. Driver. The cutaneous rabbit illusion affects human primary sensory cortex somatotopically. *PLoS Biology*, 4(3):69–527, 2006. (Cited on page 17.)

[25] S. Bochereau, B. Dzidek, M. Adams, and V. Hayward. Characterizing and imaging gross and real finger contacts under dynamic loading. *Submitted*, 2016. (Cited on pages 74 and 84.)

[26] S. Bochereau, S. Sinclair, and V. Hayward. Looking for physical invariants in the mechanical response of a tactually scanned braille dot. In *Proceedings of the IEEE World Haptics Conference*, pages 119–124, 2015. (Cited on pages 75 and 84.)

[27] S. Bochereau, A. V. Terekhov, and V. Hayward. Amplitude and duration interdependence in the perceived intensity of complex tactile signals. In *Haptics: Neuroscience, Devices, Modeling, and Applications, Part-I*, pages 93–100, 2014. (Cited on pages 57, 61, 66, and 74.)

[28] F. P. Bowden and D. Tabor. The area of contact between stationery and moving surfaces. *Proceedings of the royal society, series A*, 169(938):391–413, 1939. (Cited on page 9.)

[29] A. J. Brisben, S.S. Hsiao, and K. O. Johnson. Detection of vibration transmitted through an object grasped in the hand. *Journal of Neurophysiology*, 81(4):1548–1558, 1999. (Cited on page 14.)

[30] B. J. Briscoe, A. Arvanitaki, M. J. Adams, and S. A. Johnson. The friction and adhesion of elastomers. *Tribology Series*, 39:661–672, 2001. (Cited on page 11.)

[31] W. H. Briscoe, S. Titmuss, F. Tiberg, R. K. Thomas, D. J. McGillivray, and J. Klein. Boundary lubrication under water. *Nature*, 444(7116):191–194, 2006. (Cited on page 29.)

[32] M. F. Bruce. The relation of tactile thresholds to histology in the fingers of elderly people. *Journal of Neurology, Neurosurgery and Psychiatry*, 43(8):730–734, 1980. (Cited on page 14.)

[33] D. B. Calne and C. A. Pallis. Vibratory sense: a critical review. *Brain: a Journal of Neurology*, 89(4):723–746, 1966. (Cited on page 13.)

[34] G. Campion and V. Hayward. Fundamental limits in the rendering of virtual haptic textures. In *Proceedings of the First Joint Eurohaptics Conference and Symposium on Haptic Interfaces for Virtual Environment and Teleoperator Systems*, pages 263–270, 2005. (Cited on pages 33, 83, and 84.)

[35] M. Cartmill. The volar skin of primates: it's frictional characteristics and their functional significance. *American Journal of Physical Anthropology*, 50(4):497–509, 1979. (Cited on page 8.)

[36] C. J. Cascio and K. Sathian. Temporal cues contribute to tactile perception of roughness. *Journal of Neuroscience*, 21(14):5289–5296, 2001. (Cited on page 84.)

[37] N. Cauna. Nature and functions of the papillary ridges of the digital skin. *The Anatomical Record*, 119(4):449–468, 1954. (Cited on page 7.)

[38] M. R. Chambers, K. H. Andres, M. von Duering, and A. Iggo. The structure and function of the slowly adapting type ii mechanoreceptor in hairy skin. *Quaterly Journal of Experimental Psychology*, 57(4):417–445, 1972. (Cited on page 12.)

[39] A. Charpentier. Analyse experimentale de quelques elements de la sensation de poids. *Archives de Physiologie Normale et Pathologique*, 2:122–135, 1891. (Cited on page 17.)

[40] E. C. Chubb, J. E. Colgate, and M. A. Peshkin. Shiverpad: A glass haptic surface that produces shear force on a bare finger. *IEEE Transactions on Haptics*, 3(3):189–198, 2010. (Cited on page 24.)

[41] E. C. Chubb, J. E. Colgate, and M. A. Peshkin. Physical and perceptual independence of ultrasonic vibration and electrovibration for friction modulation. *IEEE Transactions on Haptics*, 8(2):235–239, 2015. (Cited on page 24.)

[42] W. B. Saunders Co., editor. *Bloom & Fawcett: A textbook of Histology.* D. W. Fawcett, 1991. (Cited on page 6.)

[43] J. C. Cohen, J. C. Makous, and S. J. Bolanowski. Under which conditions do the skin and probe decouple during sinusoidal vibrations? *Experimental Brain Research*, 129(2):211–217, 1999. (Cited on page 7.)

[44] C. E. Connor, S. S. Hsiao, J. R. Phillips, and K. O. Johnson. Tactile roughness: neural codes that account for psychophysical magnitude estimates. *Journal of Neuroscience*, 10(12):3823–3836, 1990. (Cited on page 12.)

[45] C. E. Connor and K. O. Johnson. Neural coding of tactile texture: Comparison of spatial temporal mechanisms for roughness perception. *The Journal of Neuroscience*, 12(9):3414–3426, 1992. (Cited on page 17.)

[46] S. Coren and J. S. Girgus. Principles of perceptual organization and spatial distortion: The gestalt illusions. *Journal of Experimental Psychology: Human Perception and Performance*, 6(3):404–412, 1980. (Cited on page 83.)

[47] C. H. Daly. Biomechanical properties of dermis. *Journal of Investigative Dermatology*, 79:17–20, 1982. (Cited on page 7.)

[48] P. W. Davidson, S. Abbott, and J. Gershenfeld. Influence of exploration time on haptic and visual matching of complex shape. *Perception & Psychophysics*, 15(3):539–543, 1974. (Cited on page 21.)

[49] B. Delhaye, A. Barrea, B. B. Edin, P. Lefèvre, and J.-L. Thonnard. Surface strain measurements of fingertip skin under shearing. *Journal of the Royal Society Interface*, 13(115):874, 2016. (Cited on page 8.)

[50] B. Delhaye, V. Hayward, P. Lefèvre, and J.-L. Thonnard. Texture-induced vibrations in the forearm during tactile exploration. *Frontiers in Behavioural Neuroscience*, 6(37), 2012. (Cited on pages 19, 83, and 88.)

[51] B. Delhaye, P. Lefèvre, and J.-L. Thonnard. Dynamics of fingertip contact during the onset of tangential slip. *Journal of the Royal Society Interface*, 11(100):698, 2014. (Cited on pages 8, 9, 10, and 30.)

[52] A. Dépeault, E.-M. Meftah, and C. E. Chapman. Tactile speed scaling: contributions of time and space. *Journal of Neurophysiology*, 99(3):1422–1434, 2008. (Cited on pages 16, 57, and 83.)

[53] S. Derler and L.-C. Gerhardt. Tribology of skin: Review and analysis of experimental results for the friction coefficient of human skin. *Tribology Letters*, 45(1):1–27, 2012. (Cited on pages 23, 31, and 72.)

[54] S. Derler, R. M. Rossi, and G.-M. Rotaru. Understanding the variation of friction coefficients of human skin as a function of skin hydration and interfacial water films. volume 229, pages 285–293, 2014. (Cited on page 10.)

[55] O. Deroy, C. Spence, and U. Noppeney. Metacognition in multisensory perception. *Trends in Cognitive Sciences*, 20(10):736–747, 2016. (Cited on page 86.)

[56] O. S. Dinç, C. M. Ettles, S. J. Calabrese, and H. A. Scarton. Some parameters affecting tactile friction. *Journal of Tribology*, 113(3):512–517, 1990. (Cited on page 10.)

[57] F. B. Dresslar. Studies in the psychology of touch. *The American Journal of Psychology*, 6(3):313–368, 1894. (Cited on page 17.)

[58] L. Dupin, V. Hayward, and M. Wexler. Direct coupling of haptic signals between hands. *Proceedings of the National Academy of Sciences*, 112(2):619–624, 2015. (Cited on page 88.)

[59] N. I. Durlach, L. A. Delhorne, A. Wong, W. Y. Ko, W. M. Rabinowitz, and J. Hollerbach. Manual discrimination and identification of length by the finger-span method. *Perception & Psychophysics*, 46(1):29–38, 1989. (Cited on page 15.)

[60] B. Dzidek, M. Adams, Z. Zhang, S. Johnson, S. Bochereau, and V. Hayward. Role of occlusion in non-coulombic slip of the finger pad. In *Haptics: Neuroscience, Devices, Modeling, and Applications, Part-I*, pages 109–116, 2014. (Cited on pages 23, 31, 39, and 66.)

[61] B. Dzidek, S. Bochereau, M. Adams, V. Hayward, and S. Johnson. Frictional dynamics of finger pads are governed by four length-scales and two time-scales. In *Proceedings of the Haptic Symposium*, pages 161–166, 2016. (Cited on pages 7, 9, 40, 41, and 43.)

[62] B. B. Edin, G. K. Essick, M. Trulsson, and K. O. Olsson. Receptor encoding of moving tactile stimuli in humans. I. temporal pattern of discharge of individual low-threshold mechanoreceptors. *The Journal of neuroscience*, 15(1):830–847, 1995. (Cited on page 12.)

[63] R. Ehrlich. *Why toast lands jelly-side down: Zen and the art of physics demonstrations.* Princeton University Press, 1997. (Cited on page 30.)

[64] G. Ekman. Temporal integration of brightness. *Vision Research*, 6(12):683–688, 1966. (Cited on pages 47 and 52.)

[65] G. Ekman, J. Hosman, and B. Lindstrom. Roughness, smoothness, and preference: A study of quantitative relations in individual subjects. *Journal of Experimental Psychology*, 70(1):18–26, 1965. (Cited on page 18.)

[66] G. K. Essick, O. Franzen, and B. L. Whitsel. Discrimination and scaling of velocity of stimulus motion across the skin. *Somatosensory & Motor Research*, 6(1):21–40, 1988. (Cited on pages 15 and 16.)

[67] F. F. Martinot, P. Plenacoste, and C. Chaillou. Haptic sounds and vibrations of human fingerprints. In *International Conference on Sensing Technology*, pages 615–620, 2005. (Cited on pages 23, 29, and 72.)

[68] L. Farren, S. Shayler, and A. R. Ennos. The fracture properties and mechanical design of human fingernails. *Journal of Experimental Biology*, 207(5):735–741, 2004. (Cited on page 6.)

[69] J. A. Fishel and G. E. Loeb. Bayesian exploration for intelligent identification of textures. *Frontiers in Neurorobotics*, 6(4):17603–17611, 2012. (Cited on pages 23, 31, and 72.)

[70] J. R. Flanagan and M. A. Beltzner. Independence of perceptual and sensorimotor predictions in the size-weight illusion. *Nature Neuroscience*, 3(7):737–741, 2000. (Cited on page 16.)

[71] J. R. Flanagan and S. J. Lederman. Neurobiology: Feeling bumps and holes. *Nature*, 412:389–391, 2001. (Cited on page 22.)

[72] M. Fukumoto and T. Sugimura. Activeclick: Tactile feedback for touch panels. In *CHI Extended Abstracts on Human Factors in Computing Systems*, pages 121–122, 2001. (Cited on page 25.)

[73] E. Gamzu and E. Ahissar. Importance of temporal cues for tactile spatial-frequency discrimination. *Journal of Neuroscience*, 21(18):7416–7427, 2001. (Cited on pages 15 and 47.)

[74] R. Gault. Progress in experiments on tactual interpretation of oral speech. *Journal of Abnormal Psychology and Social Psychology*, 19(2):155–159, 1924. (Cited on page 22.)

[75] F. Gemperle, D. Ota, and D. Siewiorek. Design of the wearable tactile display. In *Proceedings of the 5th IEEE International Symposium on Wearable Computers*, pages 5–12, 2001. (Cited on page 25.)

[76] G. A. Gescheider, M. A. Berryhill, R. T. Verrillo, and S. J. Bolanowski. Vibrotactile temporal summation: probability summation or neural integration? *Somatosensory & Motor Research*, 16(3):229–242, 1999. (Cited on pages 14, 47, 57, and 66.)

[77] G. A. Gescheider, S. J. Bolanowski, T. C. Greenfield, and K. E. Brunette. Perception of the tactile texture of raised-dot patterns: a multidimensional analysis. *Somatosensory & Motor Research*, 22(3):127–140, 2005. (Cited on page 13.)

[78] J. Giacomin, M. S. Shayaa, E. Dormegnie, and L. Richard. Frequency weighting for the evaluation of steering wheel rotational vibration. *International Journal of Industrial Ergonomics*, 33(6):527–541, 2004. (Cited on page 47.)

[79] J. J. Gibson. Observations on active touch. *Psychological Review*, 69:477–491, 1962. (Cited on pages 20 and 29.)

[80] F. Giraud, M. Amberg, and B. Lemaire-Semail. Merging two tactile stimulation principles: electrovibration and squeeze film effect. In *World Haptics Conference*, pages 199–203. IEEE, 2013. (Cited on pages 24 and 83.)

[81] G. D. Goff. Differential discrimination of frequency of cutaneous mechanical vibration. *Journal of Experimental Psychology*, 74(2):294–299, 1967. (Cited on pages 15, 47, and 84.)

[82] A. W. Goodwin and J. W. Morley. Sinusoidal movement of a grating across the monkey's fingerpad: effect of contact angle and force of the grating on afferent fiber responses. *Journal of Neuroscience*, 7(7):2192–2202, 1987. (Cited on page 33.)

[83] A. W. Goodwin, K. Sathian, K. T. John, and I. Darian-Smith. Spatial and temporal factors determining afferent fiber responses to a grating moving sinusoidally over the monkey's fingerpad. *Journal of Neuroscience*, 9(4):1280–1293, 1989. (Cited on page 84.)

[84] D. Gueorguiev, S. Bochereau, A. Mouraux, V. Hayward, and J.-L. Thonnard. Touch uses frictional cues to discriminate flat materials. *Scientific reports*, 6:25553, 2016. (Cited on pages 10, 29, and 34.)

[85] Z. Halata, M. Grim, and K. I. Bauman. Friedrich sigmund merkel and his "merkel cell", morphology, development, and physiology: review and new results. *The Anatomical Record Part A: Discoveries in Molecular, Cellular, and Evolutionary Biology*, 271(1):225–239, 2003. (Cited on page 12.)

[86] Z. Halata and B. L. Munger. Indentification of the ruffini corpuscle in the human hairy skin. *Cell Tissue Research*, 219(2):437–440, 1981. (Cited on page 12.)

[87] J. Hartcher-O'Brien, A. Terekhov, M. Auvray, and V. Hayward. Haptic shape constancy across distance. In *Haptics: Neuroscience, Devices, Modeling, and Applications*, pages 77–84. Springer, 2014. (Cited on page 83.)

[88] V. Hayward. A brief taxonomy of tactile illusions and demonstrations that can be done in a hardware store. *Brain Research Bulletin*, 75(6):742–752, 2008. (Cited on pages 17, 18, and 20.)

[89] V. Hayward. *Haptic Shape Cues, Invariants, Priors, and Interface Design.* 2008. (Cited on pages 16 and 80.)

[90] V. Hayward. Is there a plenhaptic function? *Philosophical Transactions of the Royal Society B*, 366(1581):3115–3122, 2011. (Cited on page 29.)

[91] V. Hayward, O. R. Astley, M. Cruz-Hernandez, D. Grant, and G. Robles-De-La-Torre. Haptic interfaces and devices. *Sensor Review*, 24(1):16–29, 2004. (Cited on page 22.)

[92] V. Hayward and K. E. MacLean. Do it yourself haptics, part-I. *IEEE Robotics & Automation Magazine*, 14(4):88–104, 2007. (Cited on page 23.)

[93] M. A. Heller. Active and passive touch: the influence of exploration time on form recognitions. *Journal of General Psychology.*, 110(2):243–249, 1984. (Cited on page 21.)

[94] K. Hirota and M. Hirose. Development of surface display. In *Virtual Reality Annual International Symposium*, pages 256–262, 1993. (Cited on page 24.)

[95] J. E. Hochberg. Effects of the Gestalt revolution: the Cornell symposium on perception. *The Psychological Review*, 64(2):73–84, 1957. (Cited on page 83.)

[96] K. A. Holbrook and G. F. Odland. Regional differences in the thickness (cell layers) of the human stratum corneum: an ultrastructural analysis. *Journal of Investigative Dermatology*, 62(4):415–422, 1974. (Cited on page 6.)

[97] M. Hollins and S. J. Bensmaïa. The coding of roughness. *Canadian Journal of Experimental Psychology*, 61(3):184–195, 2007. (Cited on pages 19, 20, and 29.)

[98] M. Hollins, S. J. Bensmaïa, K. Karlof, and F. Young. Individual differences in perceptual space for tactile textures: Evidence from multidimensional scaling. *Perception & Psychophysics*, 62(8):1534–1544, 2000. (Cited on page 18.)

[99] M. Hollins, S. J. Bensmaïa, and E. A. Roy. Vibrotaction and texture perception. *Behavioural Brain Research*, 135(1):51–56, 2002. (Cited on pages 19, 72, and 84.)

[100] M. Hollins, S. J. Bensmaïa, and S. Washburn. Vibrotactile adaptation impairs discrimination of fine, but not coarse, textures. *Somatosensory & Motor Research*, 18(4):253–262, 2001. (Cited on page 13.)

[101] M. Hollins, R. Faldowski, S. Rao, and F. Young. Perceptual dimensions of tactile surface texture: A multidimensional scaling analysis. *Perception & Psychophysics*, 54(6):697–705, 1993. (Cited on pages 18, 20, and 29.)

[102] M. Hollins and A. K. Goble. Perception of the length of voluntary movements. *Somatosensory & Motor Research*, 5(4):335–348, 1988. (Cited on page 15.)

[103] M. Hollins and S. R. Risner. Evidence for the duplex theory of tactile texture perception. *Perception & Psychophysics*, 62(4):695–705, 2000. (Cited on pages 19, 72, and 88.)

[104] R. D. Howe and M. R. Cutkosky. Sensing skin acceleration for slip and texture perception. In *IEEE International Conference on robotics and automation*, number 1, pages 145–150, 1989. (Cited on pages 23 and 72.)

[105] B. Hughes, J. Wang, D. Rosic, and K. Palmer. Texture gradients and perceptual constancy under haptic exploration. In *Proceedings of the Second Joint EuroHaptics Conference and Symposium on Haptic Interfaces for Virtual Environment and Teleoperator Systems*, pages 66–71, 2007. (Cited on pages 66 and 88.)

[106] R. J. Webester III, T. E. Murphy, L. N. Verner, and A. M. Okamura. A novel two-dimensional tactile slip display: design, kinematics and perceptual experiments. *ACM Transactions on Applied Perception*, 2(2):150–165, 2005. (Cited on page 73.)

[107] A. Israr, S. Choi, and H. Z. Tan. Detection threshold and mechanical impedance of the hand in a pen-hold posture. pages 427–477, 2006. (Cited on pages 7 and 14.)

[108] T. Iwamoto and H. Shinoda. Finger ring tactile interface based on propagating elastic waves on human fingers. In *Proceedings of World Haptics*, pages 145–150, 2007. (Cited on pages 23, 29, and 72.)

[109] S. P. Jadhav, J. Wolfe, and D. E. Feldman. Sparse temporal coding of elementary tactile features during active whisker sensation. *Nature Neuroscience*, 12(6):792–800, 2009. (Cited on page 84.)

[110] F. Janabi-Sharifi, V. Hayward, and C.-S. J. Chen. Discrete-time adaptive windowing for velocity estimation. *IEEE Transactions On Control Systems Technology*, 8(6):1003–1009, 2000. (Cited on page 85.)

[111] M. Janko, R. Primerano, and Y. Visell. On frictional forces between the finger and a textured surface during active touch. *IEEE Transactions on Haptics*, 9(2):221–232, 2015. (Cited on page 31.)

[112] D. L. Jindrich, Y. Zhou, T. Becker, and J. T. Dennerlein. Non-linear viscoelastic models predict fingertip pulp force-displacement characteristics during voluntary tapping. *Journal of Biomechanics*, 36(4):497–503, 2003. (Cited on page 7.)

[113] R. S. Johansson and R. H. LaMotte. Tactile detection thresholds for a single asperity on an otherwise smooth surface. *Somatosensory & Motor Research*, 1(1):21–31, 1983. (Cited on page 15.)

[114] R. S. Johansson, U. Landström, and R. Lundström. Responses of mechanoreceptive afferent units in the glabrous skin of the human hand to sinusoidal skin displacements. *Brain Research*, 244(1):17–25. (Cited on pages 12 and 13.)

[115] R. S. Johansson and A. B. Vallbo. Tactile sensibility in the human hand: relative and absolute densities of four types of mechanoreceptive units in glabrous skin. *Journal of Physiology*, 286:283–300, 1979. (Cited on pages 6 and 12.)

[116] K. L. Johnson. *Contact Mechanics.* 1987. (Cited on page 9.)

[117] K. O. Johnson. The roles and functions of cutaneous mechanoreceptors. *Current Opinion in Neurobiology*, 11(4):455–461, 2001. (Cited on pages 11 and 12.)

[118] K. O. Johnson and S. S. Hsiao. Neural mechanisms of tactual form and texture perception. *Annual Review of Neuroscience*, 15:227–250, 1992. (Cited on pages 12, 13, and 19.)

[119] K. O. Johnson and G. D. Lamb. Neural mechanisms of spatial tactile discrimination: neural patterns evoked by braille-like dot patterns in the monkey. *The Journal of Physiology*, 310:117–144, 1981. (Cited on page 19.)

[120] K. O. Johnson and J. R. Phillips. Tactile spatial resolution. I. two-point discrimination, gap detection, grating resolution, and letter recognition. *Journal of Neurophysiology*, 46(6):1177–1192, 1981. (Cited on pages 12 and 15.)

[121] K. O. Johnson, T. Yoshioka, and F. Vega-Bermudez. Tactile functions of mechanoreceptive afferents innervating the hand. *Journal of Clinical Neurophysiology*, 17(6):539–558, 2000. (Cited on pages 12 and 13.)

[122] L. A. Jones and I. W. Hunter. Changes in pinch force with bidirectional loads. *Journal of Motor Behaviour*, 24(2):157–164, 1992. (Cited on page 8.)

[123] L. M. Jones, D. A. Depireux, D. J. Simons, and A. Keller. Robust temporal coding in the trigeminal system. *Science*, 304(5679):1986–1989, 2004. (Cited on page 84.)

[124] S. J. Bolanowski Jr., G. A. Gescheider, R. T. Verrillo, and C. M. Checkosky. Four channels mediate the mechanical aspects of touch. *Journal of Acoustical Society of America*, 84(5):1680–1694, 1988. (Cited on pages 11 and 12.)

[125] D. Kahneman and J. Norman. The time-intensity relation in visual perception as a function of observer's task. *Journal of Experimental Psychology*, 68(3):215–220, 1964. (Cited on page 47.)

[126] M. Kahrimanovic, W. M. Tiest, and A. M. Kappers. Haptic perception of volume and surface area of 3-d objects. *Attention, Perception & Psychophysics*, 72(2):517–527, 2010. (Cited on page 17.)

[127] D. Katz. *The world of touch.* Leipzig, 1925. (Cited on pages 19, 20, 23, and 57.)

[128] M. Keetels and J. Vroomen. Temporal recalibration to tactile-visual asynchronous. *Neuroscience Letters*, 430(2):130–134, 2008. (Cited on page 22.)

[129] R. Kikuuwe, A. Sano, H. Mochiyama, N. Takasue, and H. Fujimoto. Enhancing haptic detection of surface undulation. *ACM Transactions on Applied Perception*, 2(1):46–67, 2005. (Cited on page 17.)

[130] R. L. Klatzky and S. J. Lederman. Tactile roughness perception with a rigid link interposed between skin and surface. *Perception & Psychophysics*, 61(4):591–607, 1999. (Cited on page 21.)

[131] R. L. Klatzky, S. J. Lederman, C. Hamilton, M. Grindley, and R. H. Swendsen. Feeling textures through a probe: Effects of probe and surface geometry and exploratory factors. *Perception & Psychophysics*, 65(4):613–631, 2003. (Cited on page 21.)

[132] A. A. Koudine, M. Barquins, P. H. Anthoine, L. Aubert, and P. Léveque. Frictional properties of skin: proposal of a new approach. *International Journal of Cosmetic Science*, 22(1):11–20, 2000. (Cited on page 9.)

[133] L. E. Krueger. Tactual perception in historical perspective: David Katz's world of touch. In W. Schiff and E. Foulke, editors, *Tactual Perception; A Sourcebook*, pages 1–55. Cambridge University Press, 1982. (Cited on pages 20 and 29.)

[134] K. D. Kryter and K. S. Pearsons. Some effects of spectral content and duration on perceived noise level. *Journal of the Acoustical Society of America*, 35(6):866, 1963. (Cited on pages 47 and 52.)

[135] G. D. Lamb. Tactile discrimination of textured surfaces: psychophysical performance measurements in humans. *The Journal of Physiology*, 338(1):551–565, 1983. (Cited on pages 9, 18, and 83.)

[136] G. D. Lamb. Tactile discrimination of textured surfaces: psychophysical performance measurements in humans. *The Journal of Physiology*, 338(1):551–565, 1983. (Cited on pages 16, 17, and 57.)

[137] R. H. LaMotte and V.B. Mountcastle. Capacities of humans and monkeys to discriminate vibratory stimuli of different frequency and amplitude: a correlation between neural events and psychological measurements. *Journal of Neurophysiology*, 38(3):539–559, 1975. (Cited on pages 13 and 14.)

[138] R. H. Lamotte and M. A. Srinivasan, editors. *Surface micro geometry: Tactile perception and neural encoding.* London: Macmillan. (Cited on page 19.)

[139] R. H. LaMotte and M. A. Srinivasan. Tactile discrimination of shape: responses of rapidly adapting mechanoreceptive afferents to a step stroked across the monkey fingerpad. *Journal of Neuroscience*, 7(6):1672–1681, 1987. (Cited on page 12.)

[140] R. H. LaMotte and J. Whitehouse. Tactile detection of a dot on a smooth surface: peripheral neural events. *Journal of Neurophysiology*, 56(4):1109–1128, 1986. (Cited on page 14.)

[141] S. J. Lederman. Tactile roughness of grooved surfaces: the touching process and effects of macro– and microsurface structure. *Perception & Psychophysics*, 16(2):385–395, 1974. (Cited on pages 16 and 57.)

[142] S. J. Lederman. Tactual roughness perception: Spatial and temporal determinants. *Canadian Journal of Psychology*, 37(4):498–511, 1983. (Cited on pages 16, 17, 57, and 83.)

[143] S. J. Lederman and L. A. Jones. Tactile and haptic illusions. *IEEE Transaction on Haptics*, 4(4):1939–1412, 2011. (Cited on page 17.)

[144] S. J. Lederman and R. L. Klatzky. Hand movements: A window into haptic object recognition. *Cognitive Psychology*, 19(3):342–368, 1987. (Cited on page 21.)

[145] S. J. Lederman and R. L. Klatzky. Extracting object properties through haptic exploration. *Acta Psychologica*, 84(1):29–40, 1993. (Cited on pages 20 and 29.)

[146] S. J. Lederman, R. L. Klatzky, and P. O. Barber. Spatial and movement-based heuristics for encoding pattern information through touch. *Journal of Experimental Psychology: General*, 114(1):33–49, 1985. (Cited on page 15.)

[147] S. J. Lederman, R. L. Klatzky, C. L. Hamilton, and G. I. Ramsay. Perceiving roughness via a rigid probe: Psychophysical effects of exploration speed and mode of touch. 1999. (Cited on pages 16 and 21.)

[148] S. J. Lederman, J. M. Loomis, and D. A. Williams. The role of vibration in the tactual perception of roughness. *Perception & Psychophysics*, 32(2):109–116, 1982. (Cited on page 19.)

[149] S. J. Lederman and M. M. Taylor. Fingertip force, surface geometry, and the perception of roughness by active touch. *Perception & Psychophysics*, 12(5):401–408, 1972. (Cited on page 19.)

[150] V. Levesque and V. Hayward. Experimental evidence of lateral skin strain during tactile exploration. In *Proceedings of the Eurohaptics Conference*, pages 261–275, 2003. (Cited on pages 8, 30, 57, and 66.)

[151] M. S. Lewicki. Efficient coding of natural sounds. *Nature Neuroscience*, 5(4):356–363, 2002. (Cited on page 72.)

[152] X. Libouton, O. Barbier, Y. Bergera, L. Plaghkia, and J.-L. Thonnard. Tactile roughness discrimination of the finger pad relies primarily on vibration sensitive afferents not necessarily located in the hand. *Behavioural Brain Research*, 229:273—279, 2012. (Cited on page 88.)

[153] W. Liu, L. A. Lipsitz, M. Montero-Odasso, J. Bean, D. C. Kerrigan, and J. J. Collins. Noise-enhanced vibrotactile sensitivity in older adults, patients with stroke, and patients with diabetic neuropathy. *Archives of Physical Medicine and Rehabilitation*, 83(2):171–176, 2002. (Cited on page 14.)

[154] S. Louw, A. M. Kappers, and J. J. Koenderink. Haptic detection thresholds of gaussian profiles over the whole range of spatial scales. *Experimental Brain Research*, 132(3):369–374, 2000. (Cited on pages 14 and 15.)

[155] K. E. MacLean. Haptic interaction design for everyday interfaces. *Reviews of Human Factors and Ergonomics*, 4(1):149–194, 2008. (Cited on pages 20 and 25.)

[156] K. E. MacLean and V. Hayward. Do it yourself haptics, part-II. *IEEE Robotics & Automation Magazine*, 15(1):104–119, 2008. (Cited on pages 22 and 23.)

[157] T. Maeno, K. Kobayashi, and N. Yamazaki. Relationship between the structure of human finger tissue and the location of tactile receptors. *Bulletin of JSME International Journal*, 41(1):94–100, 1998. (Cited on page 11.)

[158] D. A. Mahns, N. M. Perkins, V. Sahai, L. Robinson, and M. J. Rowe. *Journal of Neurophysiology*, (3). (Cited on pages 15 and 47.)

[159] V. Makinen, J. Linjama, and Z. Gulzar. Tactile stimulation apparatus having a composite section comprising a semiconducting material. *Patent US8766933 B2*, 2010. (Cited on page 24.)

[160] J. C. Makous, R. M. Friedman, and C. Jr. Vierck. A critical band filter in touch. *Journal of Neuroscience*, 15:2808–2818, 1995. (Cited on page 72.)

[161] L. H. Manfredi, H. P. Saal, K. J. Brown, M. C. Zielinski, J. F. Dammann, V. S. Polashock, and S. J. Bensmaïa. Natural scenes in tactile texture. *Journal of neurophysiology*, 111(9):1792–1802, 2014. (Cited on pages 19, 23, 29, 72, and 83.)

[162] F. Martinot, A. Houzefa, M. Biet, and C. Chaillou. Mechanical responses of the fingerpad and distal phalanx to friction of a grooved surface: Effect of the contact angle. pages 297–300, 2006. (Cited on pages 23 and 31.)

[163] F. Massi, E. Vittecoq, E. Chatelet, A. Saulot, and Y. Berthier. Design of a tribometer for investigating tactile perception. In *Proceedings of the Institution of Mechanical Engineers, Part J: Journal of Engineering Tribology*, 2014. (Cited on pages 23 and 31.)

[164] M. Meenes and M. Zigler. An experimental study of the perception of roughness and smoothness. *The American Journal of Psychology.*, 34(4):542–549, 1923. (Cited on page 20.)

[165] E.-M. Meftah, L. Belingard, and C.E. Chapman. Relative effects of the spatial and temporal characteristics of scanned surfaces on human perception of tactile roughness using passive touch. *Experimental Brain Research*, 132(3):351–361, 2000. (Cited on pages 17 and 18.)

[166] D. J. Meyer, M. A. Peshkin, and J. E. Colgate. Fingertip friction modulation due to electrostatic attraction. In *World Haptics Conference*, pages 43–48, 2013. (Cited on pages 24 and 83.)

[167] T. Miyaoka, T. Mano, and M. Ohka. Mechanisms of fine-surface-texture discrimination in human tactile sensation. *The Journal of Acoustical Society of America.*, 105(4):2485–2492, 1999. (Cited on pages 15 and 18.)

[168] A. Mohand-Ousaid, G. Millet, S. Regnier, S. Haliyo, and V. Hayward. Haptic interface transparency achieved through viscous coupling. *The International Journal of Robotics Research*, 31(3):319–329, 2012. (Cited on page 34.)

[169] I. Moll and R. Moll. Merkel cells in ontogenesis of human nail. *Archives of Dermatological Research*, 285(6):366–371, 1993. (Cited on page 6.)

[170] J. Monnoyer, E. Diaz, C. Bourdin, and M. Wiertlewski. Ultrasonic friction modulation while pressing induces a tactile feedback. In *Haptics: Perception, Device, Control and Applications*, pages 171–179, 2016. (Cited on pages 25 and 73.)

[171] J. Monzée, Y. Lamarre, and A. M. Smith. The effects of digital anaesthesia on force control using a precision grip. *Journal of Neurophysiology*, 89(2):672–683, 2003. (Cited on page 16.)

[172] B. C. J. Moore, B. R. Glasberg, and T. Baer. A model for the prediction of thresholds, loudness, and partial loudness. *The Journal of the Audio Engineering Society*, 45(4):224–240, 1997. (Cited on page 47.)

[173] J. W. Morley, A. W. Goodwin, and I. Darian-Smith. Tactile discrimination of gratings. *Experimental Brain Research*, 49:291–299, 1983. (Cited on pages 9, 15, and 21.)

[174] A. Moscatelli, V. Hayward, M. Wexler, and M. O. Ernst. Illusory tactile motion perception: An analog of the visual filehne illusion. *Scientific reports*, 5:14584, 2015. (Cited on page 83.)

[175] V. B. Mountcastle, R. H. LaMotte, and G. Carli. Detection thresholds for stimuli in humans and monkeys: comparison with threshold events in mechanoreceptive afferent nerve fibers innervating the monkey hand. *Journal of Neurophysiology*, 35(1):122–136, 1972. (Cited on page 13.)

[176] V. B. Mountcastle, M. A. Steinmetz, and R. Romo. Frequency discrimination in the sense of flutter: psychophysical measurements correlated with postcentral events in behaving monkeys. *Journal of Neuroscience*, 10(9):3032–3044, 1990. (Cited on page 16.)

[177] D. J. Murray, R. R. Ellis, C. A. Bandomir, and H. E. Ross. Charpentier (1891) on the size-weight illusion. *Perception & Psychophysics*, 61(8):1681–1685, 1999. (Cited on pages 17 and 83.)

[178] M. Nakatani, R. D. Howe, and S. Tachi. The fishbone tactile illusion. In *Proceedings of Eurohaptics,*, pages 69–73, 2006. (Cited on page 17.)

[179] M. Nakatani, A. Sato, S. Tachi, and V. Hayward. Tactile illusion caused by tangential skin strain and analysis in terms of skin deformation. In *Proceedings of the 6th international conference on Haptics: Perception, Devices and Scenarios*, pages 229–237, 2008. (Cited on page 17.)

[180] N. Nakazawa, R. Ikeura, and H. Inooka. Characteristics of human fingertips in the shearing direction. *Biological Cybernetics*, 82(3):207–214, 2000. (Cited on page 8.)

[181] T. Nara, M. Takasaki, T. Maeda, T. Higuchi, S. Ando, and S. Tachi. Surface acoustic wave tactile display. *Computer Graphics and Applications*, 21(6):56–63, 2001. (Cited on pages 24 and 83.)

[182] H. T. Nefs, A. M. L. Kappers, and J. J. Koenderink. Amplitude and spatial-period discrimination in sinusoidal gratings by dynamic touch. *Perception*, 30(10):1263–1274, 2001. (Cited on page 14.)

[183] R. S. Ogden, D. Moore, L. Redfern, and F. McGlone. Stroke me for longer this touch feels too short: The effect of pleasant touch on temporal perception. *Consciousness and Cognition*, 36:306–313, 2015. (Cited on page 15.)

[184] S. Okamoto, M. Konyo, S. Saga, and S. Tadokoro. Audiotactile temporal order judgments. *Acta Psychologica*, 118(3):277–291, 2005. (Cited on page 22.)

[185] S. Okamoto, M. Konyo, S. Saga, and S. Tadokoro. Detectability and perceptual consequences of delayed feedback in a vibrotactile texture display. *IEEE Consumer Electronics Society*, 2(2):73–84, 2009. (Cited on page 22.)

[186] S. Okamoto, H. Nagano, and Y. Yamada. Psychophysical dimensions of tactile perception of textures. *IEEE Transaction on Haptics*, 6(1):81–93, 2013. (Cited on page 18.)

[187] A. M. Okamura. Haptic surface exploration. *Experimental Robotics VI, Lecture notes in control and information sciences.*, 250:423–432, 2001. (Cited on page 22.)

[188] M. O. Othaman and A. H. Elkholy. Surface-roughness measurement using dry friction noise. *Experimental Mechanics*, 30(3):309–312, 1990. (Cited on page 10.)

[189] M. Paré, C. Behets, and O. Cornu. Paucity of presumptive ruffini corpuscles in the index finger pad of humans. *Journal of Comparative Neurology*, 456(3):260–266, 2003. (Cited on pages 6 and 12.)

[190] M. Paré, A. M. Smith, and F. L. Rice. Distribution and terminal arborizations of cutaneous mechanoreceptors in the glabrous finger pads of the monkey. *Journal of Comparative Neurology*, 445:347–359, 2002. (Cited on page 12.)

[191] M. A. Pastor, B. L. Day, E. Macaluso, K. J. Friston, and R S. J. Frackowiak. The functional neuroanatomy of temporal discrimination. *The Journal of Neuroscience*, 24(10):2585–2591, 2004. (Cited on page 16.)

[192] S. M. Pasumarty, S. A. Johnson, S. A. Watson, and M. J. Adams. Friction of the human finger pad: Influence of moisture, occlusion and velocity. *Tribology Letters*, 44(2):117–137, 2011. (Cited on pages 10, 11, 23, 31, 66, and 72.)

[193] T. C. Pataky, M. L. Latash, and V. M. Zatsiorsky. Viscoelastic response of the finger pad to incremental tangential displacements. *Journal of Biomechanics*, 38(7):1441–1449, 2005. (Cited on page 7.)

[194] D. T. V. Pawluk and R. D. Howe. Dynamic lumped element response of the human fingerpad. *Journal of Biomechanical Engineering*, 121(2):178–183, 1999. (Cited on pages 7, 29, and 51.)

[195] B. N. J. Persson. Theory of rubber friction and contact mechanics. *Journal of Chemical Physics*, 115(8):3840–3861, 2001. (Cited on page 9.)

[196] B. N. J. Persson, I. M. Sivebaeck, V. N. Samoilov, K. Zhao, A. I. Volokitin, and Z. Zhang. On the origin of amontonÕs friction law. *Journal of Physics: Condensed Matter*, 20(39):5006, 2008. (Cited on page 10.)

[197] J. R. Phillips, R. S. Johansson, and K. O. Johnson. Responses of human mechanoreceptive afferents to embossed dot arrays scanned across fingerpad skin. *Journal of Neuroscience*, 12(3):827–839, 1992. (Cited on page 9.)

[198] J. R. Phillips and K. O. Johnson. Tactile spatial resolution. ii. neural representation of bars, edges, and gratings in monkey primary afferents. *Journal of Neurophysiology*, 46(6):1192–1203, 1981. (Cited on page 12.)

[199] D. Picard, C. Dacremont, D. Valentin, and A. Giboreau. Perceptual dimensions of tactile textures. *Acta Psychologica*, 114(2):165–184, 2003. (Cited on page 18.)

[200] J. Platkiewicz, J. Lipson, and V. Hayward. Haptic edge detection through shear. *Scientific Reports*, 6:23551, 2015. (Cited on page 73.)

[201] J. Platkiewicz, J. Mansutti, A. Bordegoni, and V. Hayward. Recording device for natural haptic textures felt with the bare fingertip. In *Haptics: Neuroscience, Devices, Modeling, and Applications, Part-I*, pages 521–528, 2014. (Cited on pages 23, 31, and 72.)

[202] R. O. Potts, E. M. Buras, and D. A. Chrisman. Changes with age in the moisture content of human skin. *Journal of investigative dermatology*, 82(1):97–100, 1984. (Cited on page 29.)

[203] I. Poupyrev, D. S. Tan, M. Billinghurst, H. Kato, H. Regenbrecht, and N. Tetsutani. Developing a generic augmented-reality interface. *Computer*, 35(3):44–50, 2002. (Cited on page 24.)

[204] A. Prévost, J. Scheibert, and G. Debrégeas. Effect of fingerprints orientation on skin vibrations during tactile exploration of textures surfaces. *Communicative & Integrative Biology*, 2(5):422–424, 2009. (Cited on page 7.)

[205] G. H. Recanzone and M. L. Sutter. The biological basis of audition. *Annual Review of Psychology*, 59:119–142, 2008. (Cited on page 47.)

[206] R. L. Reid. An illusion of movement complementary to the horizontal-vertical illusion. *Quaterly Journal of Experimental Psychology*, 6(3):107–111, 1954. (Cited on page 17.)

[207] S. C. Richards and A. D. Roberts. Boundary lubrication of rubber by aqueous surfactant. *Journal of Physics D: Applied Physics*, 25(1A):A76, 1992. (Cited on page 29.)

[208] G. Robles-De-La-Torre and V. Hayward. Force can overcome object geometry in the perception of shape through active touch. *Nature*, 412:445–448, 2001. (Cited on page 22.)

[209] J. Rolfe and J. Bennett. The impact of offering two versus three alternatives in choice modelling experiments. *Ecological Economics*, 68:1140–1148, 2009. (Cited on page 86.)

[210] L. M. Russell, S. Wiedersberg, and M. B. Delgo *n*a Charro. The determination of stratum corneum thickness - an alternative approach. *European Journal of Pharmaceutics and Biopharmaceutics*, 69(3):861–870, 2008. (Cited on page 6.)

[211] M. A. Salada, J. E. Colgate, M. V. Lee, and P. M. Vishton. Validating a novel approach to rendering fingertip contact sensations. In *Proceedings of the Haptic Symposium*, pages 217–224, 2002. (Cited on page 73.)

[212] M. Salazzi, A. Frisoli, F. Salsedo, and M. Bergamasco. A fingertip haptic display for improving local perception of shape cues. In *Proceedings of the joint Eurohaptics Conference and Symposium*, pages 409–414, 2007. (Cited on page 73.)

[213] K. Salisbury, F. Conti, and F. Barbagli. Haptic rendering: Introductory concepts. *IEEE Computer Graphics and Applications*, 24(2):24–32, 2004. (Cited on pages 21 and 22.)

[214] E. Samur. *Performance Evaluation Based on Physical Measurements*, pages 43–65. 2012. (Cited on page 83.)

[215] J. Scheibert, S. Leurent, A. Prévost, and G. Debrégeas. The role of fingerprints in the coding of tactile information probed with a biomimetic sensor. *Science*, 323(5920):1503–1506, 2009. (Cited on page 7.)

[216] B. Z. Seah, C. C. Wu, S. J. Sebastin, and A. Lahiri. Tactile sensibility on the fingernail. *The Journal of Hand Surger*, 38(11):2159–2163, 2013. (Cited on page 6.)

[217] H. Seifi, K. Zhang, and K. E. MacLean. Vibviz: Organizing, visualizing and navigating vibration libraries. In *World Haptics Conference IEEE*, pages 254–259, 2015. (Cited on page 23.)

[218] E. R. Serina, E. Mockensturm, C.D. Mote Jr., and D. Rempel. A structural model of the forced compression of the fingertip pulp. *Journal of Biomechanics*, 31(7):639–646, 1998. (Cited on pages 8 and 9.)

[219] E.R. Serina, C.D. Mote Jr., and D. Rempel. Force response of the fingertip pulp to repeated compressionÑeffects of loading rate, loading angle and anthropometry. *Journal of Biomechanics*, 30(10):1035–1040, 1997. (Cited on pages 7 and 29.)

[220] Y. Shao, V. Hayward, and Y. Visell. Spatial patterns of cutaneous vibration during whole-hand haptic interactions. *Proceedings of the National Academy of Sciences*, 113(15):4188–4193, 2016. (Cited on pages 23, 29, and 72.)

[221] C. A. Sherrick and R. W. Cholewiak. *Cutaneous sensitivity.* (Cited on page 17.)

[222] T. Shimizu. Tooth pre-pain sensation elicited by electrical stimulation. *Journal of Dental Research*, 43:467–475, 1964. (Cited on pages 47 and 52.)

[223] M. M. Shrewsbury and R. K. Johnson. The fascia of the distal phalanx. *The Journal of Bone Joint Surgery*, 57(6):784–788, 1975. (Cited on page 6.)

[224] E. P. Simoncelli and B. A. Olshausen. Natual image statistics and neural representation. *Annual Review of Neuroscience*, 24:1193–1216, 2001. (Cited on page 72.)

[225] R. K. Sivamani, J. Goodman, N. V. Gitis, and H. I. Maibach. Friction coefficient of skin in real-time. *Skin Research and Technology*, 9(3):235–239, 2003. (Cited on page 9.)

[226] L. Skedung, M. Arvidsson, J. Y. Chung, C. M. Stafford, B. Berglund, and M. W. Rutland. Feeling small : Exploring the tactile perception limits. *Scientific reports*, 3, 2013. (Cited on pages 15 and 66.)

[227] A. M. Smith, G. Basile, J. Theriault-Groom, P. Fortier-Poisson, G. Campion, and V. Hayward. Roughness of simulated surfaces examined with a haptic tool: effects of spatial period, friction, and resistance amplitude. *Experimental Brain Research*, 202(1):33–43, 2010. (Cited on page 18.)

[228] A. M. Smith, C. E. Chapman, M. Deslandes, J. S. Langlais, and M. P. Thibodeau. Role of friction and tangential force variation in the subjective scaling of tactile roughness. *Experimental Brain Research*, 144(2):211–223, 2002. (Cited on pages 19 and 29.)

[229] A. M. Smith and S. H. Scott. Subjective scaling of smooth surface friction. *Journal of Neurophysiology*, 75(5):1957–1962, 1996. (Cited on page 19.)

[230] M. A. Srinivasan. Surface deflection of primate fingertip under line load. *Journal of Biomechanics*, 22(4):343–349, 1989. (Cited on pages 57 and 66.)

[231] M. A. Srinivasan, J. M. Whitehouse, and R. H. LaMotte. Tactile detection of slip: Surface microgeometry and peripheral neural codes. *Journal of Neurophysiology*, 63(6):1323–1332, 1990. (Cited on pages 12, 13, and 16.)

[232] B. Stark, T. Carlstedt, R. G. Hallin, and M. Risling. Distribution of human pacinian corpuscule in the hand. *Journal of Hand Surgery*, 23b(3):370–372, 1998. (Cited on page 13.)

[233] J. H. Steiger. Tests for comparing elements of a correlation matrix. *Psychological Bulletin*, 87(2):245, 1980. (Cited on page 66.)

[234] J. C. Stévens and J. W. Hall. Brightness and loudness as functions of stimulus duration. *Perception & Psychophysics*, 1(9):319–327, 1966. (Cited on pages 47 and 52.)

[235] S. S. Stevens and J. R. Harris. The scaling of subjective roughness and smoothness. *Journal of Experimental Psychology*, 64(5):489–494, 1962. (Cited on page 18.)

[236] M. Tada. How does a fingertip slip? visualising partial slippage for modelling of contact mechanics. In *Proceedings of Eurohaptics*, pages 2045–2048, 2006. (Cited on page 11.)

[237] M. Tada and T. Kanade. An imaging system of incipient slip for modelling how human perceives slip of a fingertip. In *Annual International Conference of the IEEE Engineering in Medicine and Biology Society*, volume 3, pages 2045–2048, 2004. (Cited on page 31.)

[238] Y. Tanaka, Y. Horita, A. Sano, and H. Fujimoto. Tactile sensing utilizing human tactile perception. In *World Haptics Conference*, pages 621–626, 2011. (Cited on pages 23, 29, and 72.)

[239] Y. Tanaka, W. M. Bergmann Tiest, A. M. L. Kappers, and A. Sano. Contact force and scanning velocity during active roughness perception. *PloS One*, 9(3):363, 2014. (Cited on page 66.)

[240] H. Tang and D.J. Beebe. A microfabricated electrostatic haptic display for persons with visual impairments. *IEEE Transactions on Rehabilitation Engineering*, 6(3):241–248, 1998. (Cited on page 24.)

[241] M. M. Taylor and S. J. Lederman. Tactile roughness of grooved surfaces: A model and the effect of friction. *Perception & Psychophysics*, 17(1):23–36, 1975. (Cited on page 19.)

[242] A. Terekhov and V. Hayward. Minimal adhesion surface area in tangentially loaded digital contacts. *Journal of Biomechanics*, 44(13):2508–2510, 2011. (Cited on pages 10 and 29.)

[243] W. M. Bergmann Tiest and A. M. L. Kappers. Analysis of haptic perception of materials by multidimensional scaling and physical measurements of roughness and compressibility. *Acta Psychologica*, 121(1):1–20, 2006. (Cited on pages 18 and 85.)

[244] A. Tomassini, M. Gori, D. Burr, G. Sandini, and M. C. Morrone. Perceived duration of visual and tactile stimuli depends on perceived speed. *Frontiers in Integrative Neuroscience.*, 5(51), 2011. (Cited on page 15.)

[245] S. E. Tomlinson, M. J. Carré, R. Lewis, and S. E. Franklin. Human finger contact with small, triangular ridged surfaces. In *18th International Conference on Wear of Materials*, pages 2346–2353, 2011. (Cited on page 10.)

[246] S. E. Tomlinson, R. Lewis, and M. J. Carré. The effect of normal force and roughness on friction in human finger contact. volume 267, pages 1311–1318, 2009. (Cited on page 10.)

[247] S. E. Tomlinson, R. Lewis, X. Liu, C. Texier, and M. J. Carré. Understanding the friction mechanisms between the human finger and flat contacting surfaces in moist conditions. *Tribology Letters*, 41(1):283–294, 2011. (Cited on pages 9 and 10.)

[248] R. P. Tuckett, K. W. Horch, and P. R. Burgess. Response of cutaneous hair and field receptors in cat to threshold stimuli. *Journal of Neurophysiology*, 41(1):138–149, 1978. (Cited on page 13.)

[249] U. Tuzun and O. R. Walton. Micro-mechanical modelling of load dependent friction in contacts of elastic spheres. *Journal of Physics D: Applied Physics*, 25(1A):44–52, 1992. (Cited on page 10.)

[250] J. van Kuilenburg, M. A. Masen, and E. van der Heide. The role of the skin micro relief in the contact behavior of human skin: Contact between the human finger and regular surface textures. *Tribology International*, 65:81–90, 2013. (Cited on page 7.)

[251] R. T. Verrillo. Effect of contractor area on the vibrotactile threshold. *The Journal of Acoustical Society of America*, 35(12):1962–1966, 1962. (Cited on pages 13 and 14.)

[252] R. T. Verrillo. Investigation of some parameters of the cutaneous threshold for vibration. *The Journal of Acoustical Society of America*, 34(11):1768, 1962. (Cited on page 15.)

[253] R. T. Verrillo. The effect of number of pulses on vibrotactile thresholds. *Psychonomic Science*, 3(1):73–74, 1965. (Cited on page 14.)

[254] R. T. Verrillo. Temporal summation in vibrotactile sensitivity. *The Journal of Acoustical Society of America*, 37:843–846, 1965. (Cited on page 14.)

[255] R. T. Verrillo and S. J. Bolanowski. The effects of skin temperature on the psychophysical responses to vibration on glabrous and hairy skin. *Journal of Acoustical Society of America*, 80(2):528–532, 1986. (Cited on pages 13 and 16.)

[256] R. T. Verrillo, A. J. Fraioli, and R. L. Smith. Sensation magnitude of vibrotactile stimuli. *Perception & Psychophysics*, 6(6):366–372, 1969. (Cited on pages 14 and 47.)

[257] M. P. Vitello, M. O. Ernst, and M. Fritschi. An instance of tactile suppression: Active exploration impairs tactile sensitivity for the direction of lateral movement. In *Proceedings of Eurohaptics Conference*, pages 351–355, 2006. (Cited on page 16.)

[258] E. Wandersman, R. Candelier, G. Debrégeas, and A. Prévost. Texture-induced modulations of friction force: the fingerprint effect. *Physical Review Letters*, 107(16):64301, 2011. (Cited on pages 8, 19, and 29.)

[259] Q. Wang and V. Hayward. In vivo biomechanics of the fingerpad skin under local tangential traction. *Journal of Biomechanics*, 40(4):851–860, 2007. (Cited on pages 7, 8, and 51.)

[260] Q. Wang and V. Hayward. Biomechanically optimized distributed tactile transducer based on lateral skin deformation. *International Journal of Robotics Research*, 29(4):323–335, 2010. (Cited on page 29.)

[261] P. H. Warman and A. R. Ennos. Fingerprints are unlikely to increase the friction of primate fingerpads. *Journal of Experimental Biology*, 212(13):2016–2022, 2009. (Cited on pages 7 and 8.)

[262] T. Watanabe and S. Fukui. A method for controlling tactile sensation of surface roughness using ultrasonic vibration. In *IEEE International Conference on Robotics and Automation*, volume 1, pages 1134–1139. IEEE, 1995. (Cited on pages 24 and 83.)

[263] A. I. Weber, H. Saal, J. D. Lieberb, J.-W. Cheng, L. R. Manfredi, J. F. Dammann III, and S. J. Bensmaïa. Spatial and temporal codes mediate the tactile perception of natural textures. *Proceedings of the National Academy of Sciences*, 110(42):17107–17112, 2013. (Cited on pages 12, 72, 83, and 88.)

[264] G. Westling and R. S. Johansson. Factors influencing the force control during precision grip. *Experimental Brain Research*, 53(2):277–284, 1984. (Cited on page 16.)

[265] M. Wexler and V. Hayward. Weak spatial constancy in touch. In *World Haptics Conference*, pages 605–607. IEEE, 2011. (Cited on page 83.)

[266] B. L. Whitsel, O. Franzen, D. A. Dreyer, M. Hollins, M. Young, G. K. Essick, and C. Wong. Dependence of subjective traverse length on velocity of moving tactile stimuli. *Somatosensory & Motor Research*, 3(3):185–196, 1986. (Cited on page 15.)

[267] M. Wiertlewski, S. Endo, A. M. Wing, and V. Hayward. Slip-induced vibration influences the grip reflex: A pilot study. In *World Haptics Conference*, pages 627–632, 2013. (Cited on pages 31 and 58.)

[268] M. Wiertlewski, R. F. Friesen, and J. E. Colgate. Partial squeeze film levitation modulates fingertip friction. *Proceedings of the National Academy of Sciences*, 113(33):9210–9215, 2016. (Cited on pages 31 and 42.)

[269] M. Wiertlewski and V. Hayward. Mechanical behavior of the fingertip in the range of frequencies and displacements relevant to touch. *Journal of Biomechanics*, 45(11):1869–1874, 2012. (Cited on pages 33, 34, and 51.)

[270] M. Wiertlewski and V. Hayward. Transducer for mechanical impedance testing over a wide frequency range through active feedback. *Review of Scientific Instruments*, 83(2):025001, 2012. (Cited on page 8.)

[271] M. Wiertlewski, C. Hudin, and V. Hayward. On the 1/f noise and non-integer harmonic decay of the interaction of a finger sliding on flat and sinusoidal surfaces. In *World Haptics Conference IEEE*, pages 25–30, 2011. (Cited on pages 7, 19, 29, and 72.)

[272] M. Wiertlewski, D. Leonardis, D. J. Meyer, and J. E. Colgate. A high-fidelity surface-haptic device for texture rendering on bare finger. In *Haptics: Neuroscience, Devices, Modelling and Applications*, pages 241–248, 2014. (Cited on pages 24, 73, and 83.)

[273] M. Wiertlewski, J. Lozada, and V. Hayward. The spatial spectrum of tangential skin displacement can encode tactual texture. *IEEE Transactions on Robotics*, 27(3):461–472, 2011. (Cited on pages 23, 29, 31, 47, 57, 72, and 83.)

[274] M. Wiertlewski, J. Lozada, E. Pissaloux, and V. Hayward. Causality inversion in the reproduction of roughness. In *Proceeding of Eurohaptics Conference*, pages 17–24, 2010. (Cited on pages 24 and 85.)

[275] M. Wiertlewski, J. Lozada, E. Pissaloux, and V. Hayward. Tactile interface for stimulation of fingertip via lateral traction. In *12th International Conference on New Actuators*, pages 520–523, Bremen, 2010. Messe Bremen. (Cited on pages 24 and 83.)

[276] L. Winfield, J. Glassmire, J. E. Colgate, and M. Peshkin. T-pad: Tactile pattern display through variable friction reduction. *Proceedings of Worldhaptics*, pages 421–426, 2007. (Cited on pages 24 and 83.)

[277] A. G. Witney, A. Wing, J.-L. Thonnard, and A. M. Smith. The cutaneous contribution to adaptive precision grip. *Trends in Neuroscience*, 27(10):637–643, 2004. (Cited on page 16.)

[278] H. Y. Yao and V. Hayward. An experiment on length perception with a virtual rolling stone. In *Proceeding of Eurohaptics Conference*, pages 325–330, 2006. (Cited on pages 22 and 25.)

[279] N. Yeung and C. Summerfield. Metacognition in human decision-making: confidence and error monitoring. *Philosophical Transactions of the Royal Society B*, 367(1594):1310–1321, 2012. (Cited on page 86.)

[280] Y. Yokokohji, N. Nuramori, Y. Sato, and T. Yoshikawa. Designing an encountered-type haptic display for multiple fingertip contacts based on the observation of human grasping behaviours. *International Journal of Robotics Research*, 24(9):717–729, 2005. (Cited on page 73.)

[281] T. Yoshioka, S. J. Bensmaïa, J. C. Craig, and S. S. Hsiao. Texture perception through direct and indirect touch: An analysis of perceptual space for tactile textures in two modes of exploration. *Somatosensory & Motor Research*, 24(1–2):53–70, 2007. (Cited on page 21.)

[282] T. Yoshioka, J. C. Craig, G. C. Beck, and S. S. Hsiao. Perceptual constancy of texture roughness in the tactile system. *Journal of Neuroscience*, 31(48):17603–17611, 2011. (Cited on pages 17, 57, 66, 83, and 88.)

[283] M. Ziat, V. Hayward, C. E. Chapman, M. O. Ernst, and C. Lenay. Tactile suppression of displacement. *Experimental Brain Research*, 206(3):299–310, 2010. (Cited on page 83.)

Résumé & Abstract

Résumé

Un nouveau dispositif tactile capable d'enregistrer et de reproduire des scènes tactiles à l'aide de forces tangentielles a été conçu et réalisé sur la base des limites et des exigences du système somatosensoriel humain. Les micro-déformations tangentielles du doigt coulissant sur la texture sont mesurées par le transducteur dans une bande passante de 500Hz et sont reproduites par le déplacement d'une plaque de verre sous l'action contrôlée d'un moteur électrodynamique critiquement amorti. Dans le but d'évaluer la pertinence des signaux sensoriels pour la reproduction d'une scène tactile, les grandeurs physiques qui influent sur la perception tactile humaine ont été étudiées. En utilisant une méthode d'escalier, il a été démontré que des ondelettes avec différentes combinaisons d'amplitude et de durée sont ressenties égales en intensité. Ces résultats suggèrent qu'il existe des quantités physiques communes – des invariants – pour ces signaux auques le cerveau est sensible, ce qui pourrait se rapporter à une constance perceptuelle dans l'exploration d'aspérités. En analysant les forces de frottement créées par un doigt glissant sur une surface dotées de points braille à des vitesses différents, il a été constaté que, bien que la réponse mécanique instantanée varie dans son ensemble, l'intégrale des forces tangentielles locales au cours d'une période de déformation courte reste constante. Ces enregistrements ont ensuite été classés selon leur vitesse et utilisés comme stimuli dans une tâche de comparaison. Les participants devaient glisser leur index sur une plateforme de verre qui vibrait afin de reproduire les points brailles de hauteurs différentes enregistrés à la même vitesse d'exploration. Ceux-ci devaient signaler lequel des deux stimuli était le plus fort (ou 'le plus haut'), une tâche qu'ils pouvaient accomplir avec succès en dépit de devoir les explorer à différentes vitesses. Ces études indiquent que c'est bien l'intégrale des forces tangentielles locales qui devrait être fournie au système somatosensoriel pour mesurer la hauteur d'une aspérité, et non l'ensemble de toutes les valeurs instantanées. Cette approche a ensuite été étendue à des stimuli plus généraux tels qu'une texture étirée dans le temps montrant par quelle mesure la déformation globale est dictée par les caractéristiques du signal liées à la vitesse d'exploration.

Mots-clefs

bio-tribologie, frottement digital, stimulation tactile, haptique, invariants tactiles, textures, corrélats neuronaux

Abstract

A new tactile device able to record and reproduce tactile scenes using tangential forces was designed and realized based on the limits and requirements of our somatosensory system. The tangential micro-deformations of the finger sliding on a textured surface can be measured with 500 Hz-bandwidth and reproduced by vibrating a glass plate under the controlled action of a critically damped electrodynamic actuator. In an effort to identify what sensory cues are relevant to tactile sensations for the reproduction of a scene, the physical quantities that influence tactile perception were studied. Using a staircase method, it was demonstrated that tactile wavelets with different combinations of amplitude and duration could be felt perceptually equal in intensity. These results suggested that there are common physical quantities – invariants – for these signals that the brain is sensitive to, which could relate to a perceptual constancy in asperity exploration. By analyzing the friction forces of a finger exploring braille dots with different pressures and velocities profiles, we found that although the mechanical response at a highly localized stimulus varies as a whole, the integral of the local tangential forces during a short deformation period remained constant. These recordings were then categorized by velocity and used as stimuli in a comparison task in which participants explored virtual dots of different heights at different speeds. While sliding on a glass platform which vibrated tangentially to reproduce a braille dot recorded at the same exploration speed, they were asked to report which of the two stimuli was stronger (or 'higher'), a task that they could successfully accomplish despite being forced to explore them at different velocities. These studies suggested that it is the integral of the local tangential forces that should be provided to the somatosensory system in asperity height reproduction instead of the set of all the instantaneous values. This approach was then extended to more general stimuli such as one texture recording stretched in time showing by what extent the overall deformation of a mechanical interaction dictates over its speed characteristics.

Keywords

bio-tribology, fingertip friction, tactile stimulation, haptics, tactile invariants, textures, neural correlates